RICHARD ANDREW TODEBUSH
FT-IR Detection System for Capillary Electrophoresis & a Novel Deposition Method for ATR
(Under the direction of JAMES A de HASETH)

Research performed in this dissertation is concerned with the separation, identification, and structural determination of complex carbohydrates. To help facilitate this research, capillary electrophoresis (CE), Fourier transform infrared (FT-IR) spectrometry and attenuated total reflection (ATR) were employed.

Fourier transform infrared spectrometric interfaces have been used for over forty years. The primary focus of these interfaces usually falls under the heading of separations, which includes gas chromatography (GC) and high performance liquid chromatography (HPLC). Over the past twenty years capillary electrophoresis has become a popular separation technique, however, the use of a FT-IR spectrometric detection system coupled to CE has not been previously reported. This dissertation focuses on the practicality and performance of an interface between a capillary electrophoresis system with a Fourier transform infrared spectrometric microscope instrument, that is, CE/FT-IR spectrometry. The instrument was then used to study oligosaccharides.

There are a number of factors that must be addressed in the design of the CE/FT-IR spectrometric interface. The most important of these is the creation and maintenance of electrical contact at the end of the capillary column. This was achieved through two different methods. The first method involved the use of a stainless steel tee, which was in contact with the end capillary column. The second, more successful method involved coating the exterior of the capillary column with silver paint, which allowed for more flexibility in the design of the interface.

The next important factor in the design of the interface involved selection of the appropriate CE electrolyte system for the separations, in this case monosaccharides,

oligosaccharides, and carbohydrates. The electrolyte system should not have absorption bands in the mid-infrared region, due to interference with the sugar bands. Borate electrolytes are proven to separate these compounds very well, however they have a strong absorption in the IR and they are not very volatile, which are two definite drawbacks. The use of ammonium electrolyte systems provides the needed volatility, but does not produce sufficient separation of the monosaccharides, oligosaccharides, and carbohydrates. This problem should be solved with the use of capillary electrochromatography (CEC), which will provide both chromatographic and electrophoretic separations.

The final concern with the interface design is the ability to control the deposit size and the amount of sample deposited from the end of the capillary column. The smaller the deposition size of the sample, the greater the sensitivity of the FT-IR analysis.

Future studies related to this project include the use of a capillary electrochromatography (CEC)/FT-IR interface to allow for detection and separation of the underivatized oligosaccharides and carbohydrates.

INDEX WORDS: Capillary Electrophoresis, Fourier Transform Infrared Spectrometry, CE/FT-IR, Interface, Nebulizer, Semi-Automated Sample Depositor, Attenuated Total Reflection, ATR

FT-IR DETECTION SYSTEM FOR CAPILLARY ELECTROPHORESIS & A NOVEL DEPOSITION METHOD FOR ATR

by

RICHARD ANDREW TODEBUSH

B.S., Western Carolina University, 1996

A Dissertation Submitted to the Graduate Faculty
of The University of Georgia in Partial Fulfillment
of the
Requirements for the Degree

DOCTOR OF PHILOSOPHY

ATHENS, GEORGIA
2001

FT-IR DETECTION SYSTEM FOR CAPILLARY ELECTROPHORESIS &

A NOVEL DEPOSITION METHOD FOR ATR

by

RICHARD ANDREW TODEBUSH

Approved:

Major Professor:	James A de Haseth
Committee:	John Stickney
	Ron Orlando
	James Anderson
	Robert Phillips

Electronic Version Approved:

Gordhan L. Patel
Dean of the Graduate School
The University of Georgia
August 2001

DEDICATION

This dissertation is dedicated to my wonderful wife and parents for their support, love and patience.

ACKNOWLEDGMENTS

There are a number of people that deserve thanks for their assistance and advise during my graduate career. First and foremost, I would like to thank Dr. de Haseth for his guidance, patience and faith in me. His enthusiasm for teaching and research has been a great inspiration to me over the past 5 years. I would also like to thank Drs. J.L. Stickney, J.L. Anderson, R. Orlando, and R. Phillips for serving on my committee. Additionally I would like to thank Joel Caughran, Dr. C.H. Atwood, and Dr. B.J. Stanton for their support and advice.

An overwhelming thanks goes out to the current and past research group members that have had to put up with me. I would like to thank Dr. Randy Bishop, Brian Melkowits, Andrew Thomas, Tracey Cash, Jessica Jarman, Yu Cang, and Ushiri Kulatunga. I wish you all well in your future endeavors. I would also like to thank Dr. Chad Leverette and Lindell Ward for their friendship and support.

I would like to thank my parents for their unwavering support over the years. Without their love and guidance (let me not forget financial support), I know that I would not the person that I am today. I only hope that I will be able to raise my children with the same values and morals they have instilled in me.

I also would like to thank my best friend Jonathan Owenby. You once told me that if a person has true friends then he has everything he needs. Well if there were, one person that I could call my true friend and brother it would be you.

Last but in no way least, I would like to thank my wife, Dr. Patricia Todebush. Over the past five years, she has helped me through thick and thin. Her inspiration has taught me to take life's little and big hurdles in stride. There is no way that I can ever truly express my feelings in words but I hope that *"I Love You"* will do.

TABLE OF CONTENTS

LIST OF TABLES

Chapter 4

LIST OF FIGURES

Chapter 1

Chapter 2

CHAPTER 1

INTRODUCTION AND LITERATURE REVIEW

Carbohydrates play a major role in all aspects of life. They are present in most animal species and make up most of the organic matter in plants.[1] Carbohydrates perform a number of diverse functions in nature. They can be found as simple monosaccharides, which provide food and energy for some species, or as complex oligosaccharide sugar chains which when covalently bonded to proteins, perform numerous genetic functions. Carbohydrates control protein charge, solubility, viscosity, folding and conformation stabilization. Most importantly they help to make up the backbone of DNA, which consists of four repeating nucleotides that contain 2-deoxy-D-erythro-pentofuranose. This sequence constitutes the coded information responsible for transcription and replication for the development of new cells in the body.[2]

Carbohydrates also play an important role in a number of different industries. Most important of these has to be the food industry, which uses large quantities of starch in the manufacture of gums, pastas, wine, beer, sweeteners, and baked goods. The textile industry is still very dependent on the use of cellulose even with the introduction of synthetic fibers. The pharmaceutical industry has profited from carbohydrates in the areas of vitamins and antibiotics. Other chemical industries have also benefited from the production and marketing of pure monosaccharides, oligosaccharides and their derivatives.

Groups within the scientific community have concentrated recent research efforts to design methods to easily separate and investigate complex carbohydrates.[3]

The separation of complex carbohydrates has been performed by a number of different methods. These methods include thin-layer chromatography (TLC), gas chromatography (GC), supercritical fluid chromatography (SFC), and high performance liquid chromatography (HPLC).[1,4-6] To gain insight on the structure of any complex carbohydrate it is necessary to analyze the individual monosaccharide units. The major obstacle in the separation and detection of these monosaccharide units is their weak absorbance in the near ultraviolet (UV) and lack of fluorescence. This is due to the fact that when the carbohydrate is in an aqueous solution only a small fraction is in the carbonyl form and thus it is not a good chromophore. The lack of fluorescence is due to the fact that the transition states are too high in energy to be observed at wavelengths above 190 nm. To overcome this problem, derivatization of the carbohydrates prior to separation and detection is used.[7-9]

Mass spectrometry (MS) has been successfully used as a detection method for the determination of oligosaccharide composition after hydrolysis into its base monosaccharide components. This technique however, is problematic when it comes to distinguishing between monosaccharides that have similar molecular weights. Hexoses and mannose illustrate this problem as they differ by only the stereochemistry of one of the hydroxyl groups. Thus mixtures of saccharides can prove to be very difficult to analyze. It is also very difficult to effectively ionize the pure monosaccharides, leading to the use of some sort of sample derivatization to help with the ionization and detection of the monosaccharides.[10]

Nuclear magnetic resonance (NMR) spectrometry has also been used in the determination of the composition and structure of carbohydrates. The use of NMR however, requires a large amount of sample, generally more then 50 μg.[11] It has been shown that certain saccharides have over 500,000 different proton environments. For NMR to achieve a separation of 0.5 ppm, this would require the use of a terahertz instrument to provide the needed 10^{-6} ppm resolution.[12] Also, another drawback to the

use of NMR is the time required to process the sample. It can take well over a day to properly scan the sample depending on the number of scans and separation needed to obtain useful information.

Over the past couple of years, there has increased use of capillary electrophoresis (CE) by a number of research groups to separate and detect a number of different types of saccharides.[10,13-26] CE does suffer from the same detection problems that the other separation techniques have when it comes to saccharides. Capillary electrophoresis frequently uses UV and fluorescence detection. Consequently the saccharides must undergo derivatization. The other problem with CE is the analyte of interest must be ionized (or ionic) for separation to occur. The lack of charge can be addressed by the use of a buffer or electrolyte system that can convert the neutral saccharides *in situ* into a charged species. These buffer or electrolyte systems include the use of borate buffers,[7,8,27] high pH alkaline solutions,[28] and some metal ions.[29]

To solve some of the detection problems associated with monosaccharides, oligosaccharides and carbohydrates when using separation techniques, Fourier transform infrared spectrometry (FT-IR) offers a simple and inexpensive analysis tool. For a number of years, FT-IR spectrometry has been used to investigate monosaccharides and polysaccharides in the paper and food industries.[30] Until recently however, it has not been used regularly for structure analysis of biological saccharides due to the lack of characteristic bands for each saccharide investigated. The monosaccharides, which make up the oligosaccharides, are very similar to each other and their absorption bands tend to overlap. This leads to some spectral similarity in most of the monosaccharide and oligosaccharide spectra. Recent advances in computer technology have allowed this problem to be overcome. Methods such as partial least squares (PLS), principal component analysis (PCA), and least squares regression (LSR) now offers a way to interpret the spectra and obtain useful structural information. With the use of an FT-IR microscope system, small quantities of analytes can be measured

with a high signal to noise ratio. FT-IR mircospectrometry has advantages over NMR with its speed and small sample requirement and over MS with its ability to distinguish between molecules of the same molecular weight and structural isomers.

This dissertation discusses the design of an interface between the separation technique of capillary electrophoresis and the spectrometric detection method of Fourier transform infrared spectrometry. Similar interfaces have been attempted in other laboratories but there have yet to be any successful reports. We have an interest in the development of a CE/FT-IR spectrometric interface because of the difficulties in the current detection methods used to analyze carbohydrates and their monosaccharide components.[7-9,31,32] To make this interface, a useful buffer or electrolyte system has to be found that will separate the carbohydrates and not interfere in the mid-infrared region of the spectrum. Chapters 2 and 3 will discuss the development of a CE/FT-IR spectrometric interface and its feasibility for the analysis of monosaccharides. Figures 1 to 3 show the structures of the seven monosaccharides of interest in one of their ring conformations. The monosaccharides are D-glucose, L-fucose, D-mannose, D-galactose, N-acetyl-D-glucosamine, N-acetyl-D-galactosamine, and N-acetyl-D-neuraminic acid. Chapter 4 will discuss the development of a semi-automated sample deposition method for use with a single bounce attenuated total reflectance (ATR) accessory for an FT-IR spectrometer.

Capillary Electrophoresis

Compared to other separation techniques, such as gas chromatography and high performance liquid chromatography, capillary electrophoresis is a relatively new analytical technique. Tiselius first demonstrated electrophoresis as a separation technique in 1937 with his work on proteins. In the late 1960s, Hjerten performed electrophoresis experiments using a strong electric field on open tube columns. As capillary technology improved Virtanen performed electrophoresis using smaller inner

Figure 1.1 Monosaccharide Structures: D-Glucose & L-Fucose

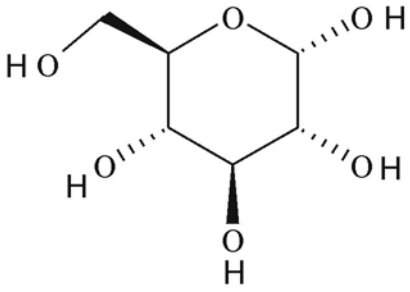

D-Glucose

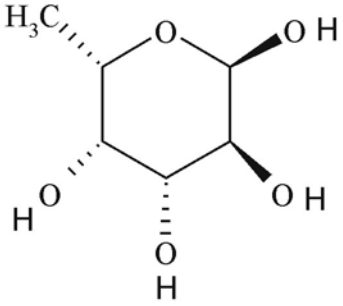

L-Fucose

Figure 1.2 Monosaccharide Structures: N-acetyl-D-glucosamine & N-acetyl-D-galactosamine

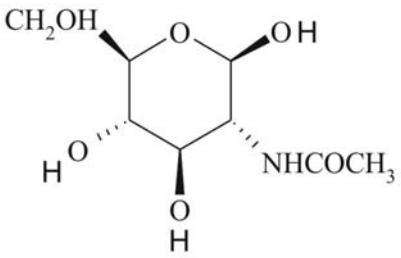

N-Acetyl-D-Glucosamine

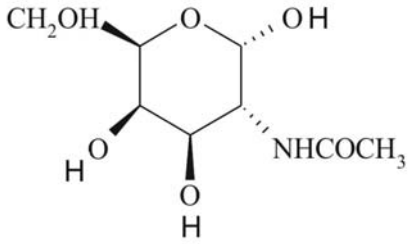

N-Acetyl-D-Galactosamine

Figure 1.3 Monosaccharide Structures: D-Mannose & D-Galactose & N-acetyl-D-Neuraminic Acid

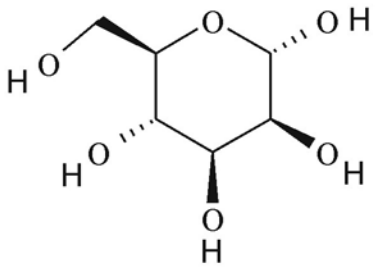

D-Mannose

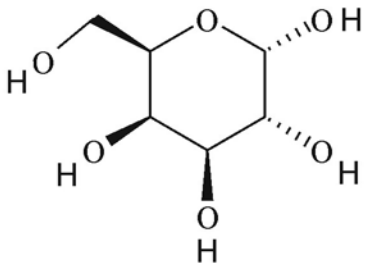

D-Galactose

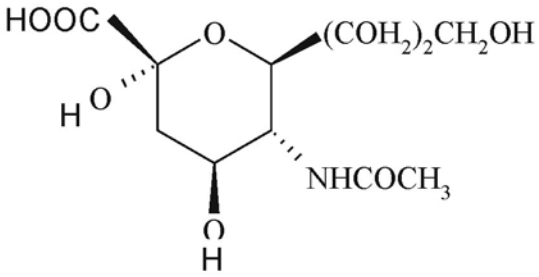

N-Acetyl-D-Neuraminic Acid

diameter columns, ~ 200 μm, made from glass and Teflon.[33] The use of CE was limited, however, because of problems with detection sensitivity and sample overloading. Not until 1981, when Jorgenson and Lukas demonstrated that capillary electrophoresis could provide highly resolved separations, did the method gain credibility.[34,35] Then in the late 1980s the first commercial instruments began to appear on the market and moved the technique into mainstream use.[36,37]

Principles of Capillary Electrophoresis

Capillary electrophoresis involves the movement of analytes within a buffer or electrolyte solution under the influence of an electric charge. These analytes move through a narrow bore capillary column in which both the inlet and outlet are immersed within an electrolytic buffer solution. The capillaries vary in length, typically 10 to 200 cm, and in internal diameter (i.d.) between 2 and 700 μm.[38] The most commonly used capillary is fused silica. These columns have negatively charged silanol groups along the inner wall. The negative groups attract positive ions within the buffer solution. This forms an electric double layer between the wall and the cations. Figure 4 shows a representation of the diffuse double layer. Once an electric current is placed upon the buffer solution this positive layer will move from the inlet (or anode) toward the outlet (or cathode) end of the capillary, thus dragging the bulk solution toward the outlet side of the column. This movement of the positive double layer is known as the electroosmotic flow (EOF). Figure 5 shows the formation of the electroosmotic flow within the CE column. The velocity of the EOF is described by the following equation:

$$\nu_{EOF} = \frac{\varepsilon\zeta}{4\pi\eta} E \qquad (1)$$

where ε is the dielectric constant, ζ is the zeta potential, η is the viscosity of the solution, and E is the applied electric field. The zeta potential is due to the potential

Figure 1.4 Diffuse double layer formation

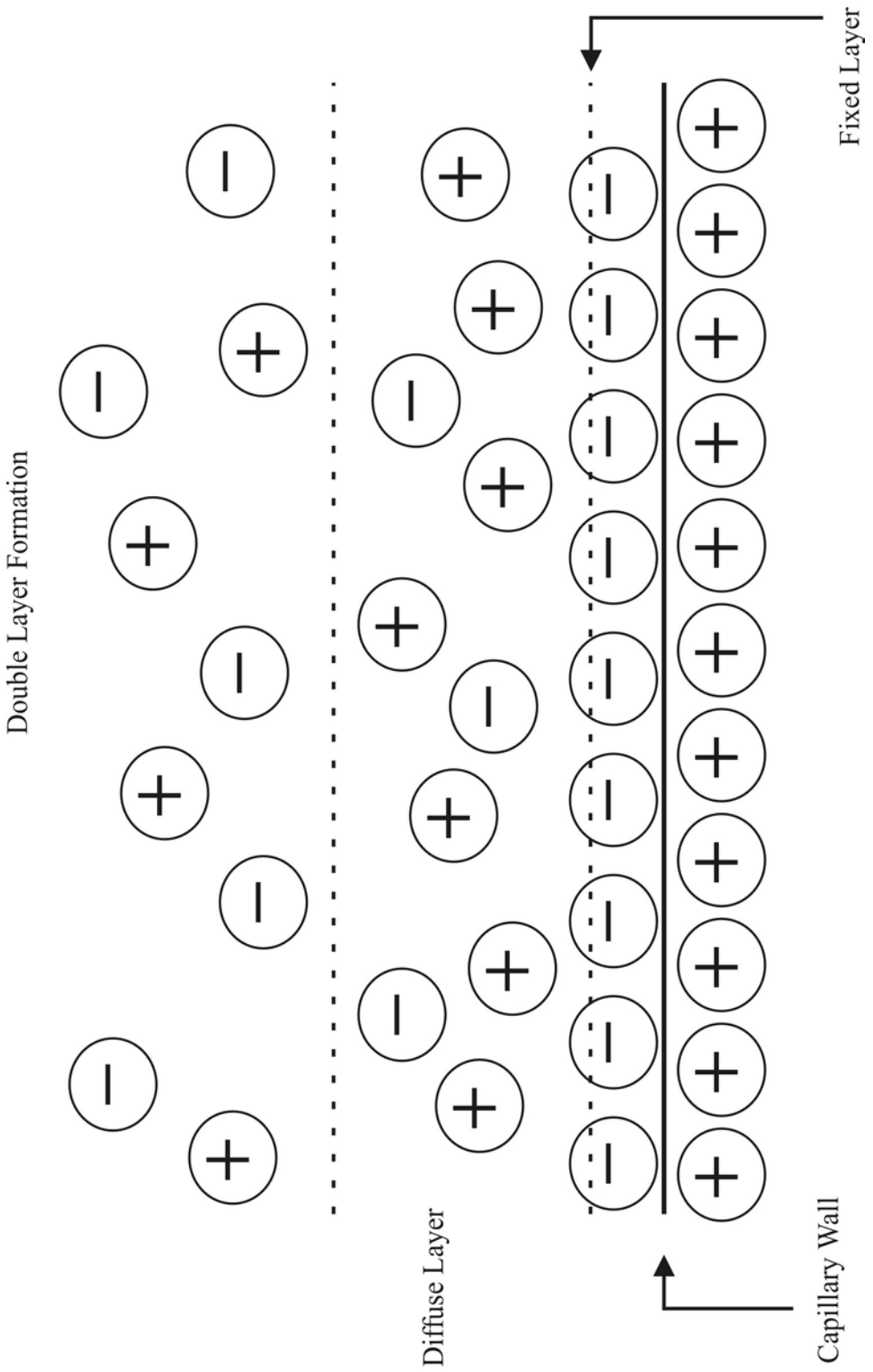
Double Layer Formation
Diffuse Layer
Fixed Layer
Capillary Wall

Figure 1.5 The Si-O groups attract the positively charged ions and form the diffuse double layer close to the wall of the capillary and once the electric field is applied the electroosmotic flow forms

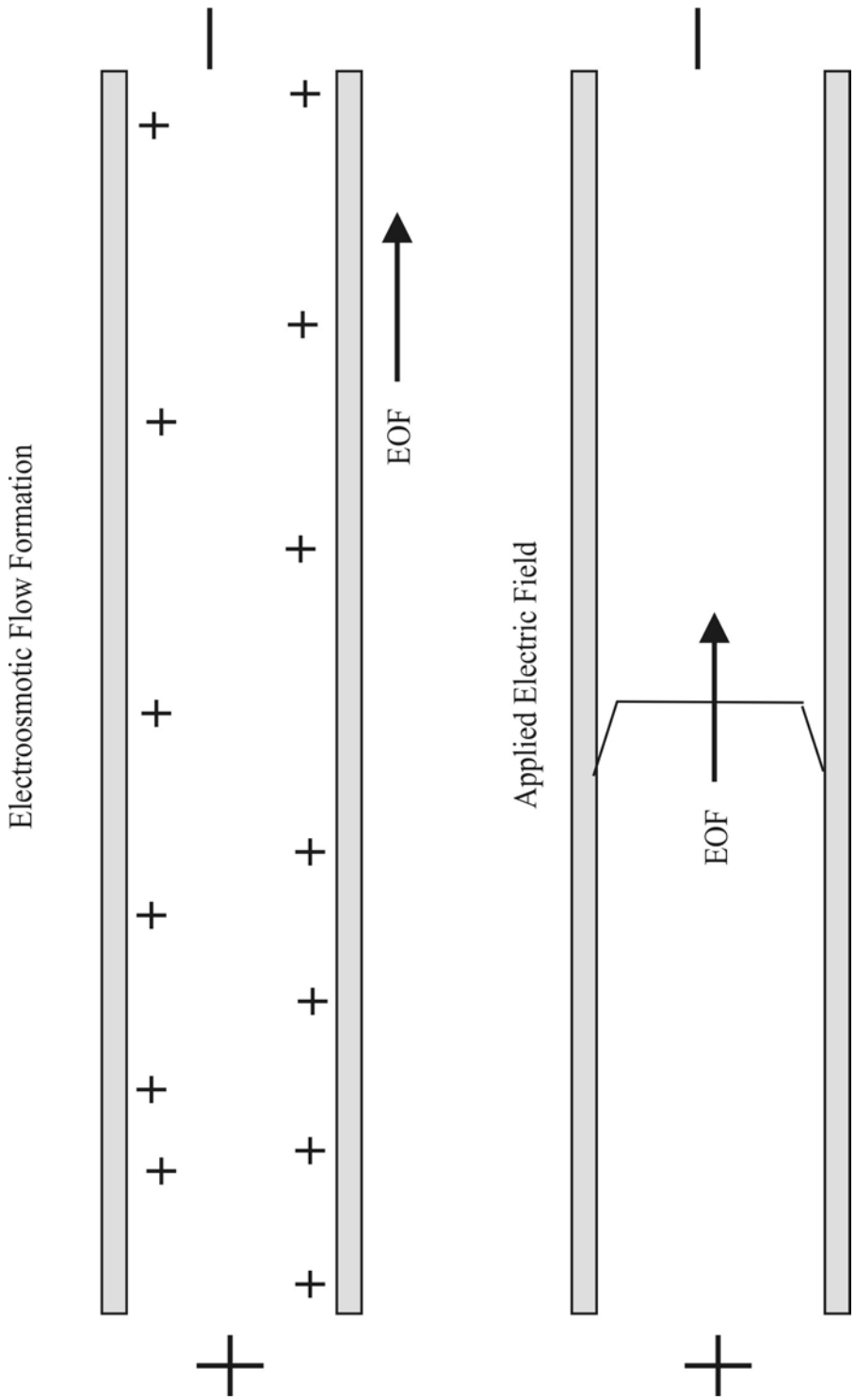
Electroosmotic Flow Formation
EOF
Applied Electric Field
EOF

difference between the wall and the counterions that are close to the wall. ζ is described by the following equation:

$$\zeta = 4\pi\delta e / \varepsilon \quad (2)$$

where δ is the thickness of the double layer, and e is the charge per unit surface area. The thickness of the diffuse double layer is dependent on the concentration of the buffer solution. The higher the electrolyte concentration the more compressed the double layer, thus the lower the zeta potential.

The velocity, volts/cm, of the analytes within the electrolytic buffer solution under the influence of an electric field is given by the following equation:

$$\nu = \mu E \quad (3)$$

where the μ is the electrophoretic mobility (EPM). Species of interest have different electrophoretic mobilities, thus allowing them to be separated once an electric field is applied. This mobility is a function of the size and charge of the species and is defined by the equation:

$$\mu_{ep} = q/(6\pi\eta r) \quad (4)$$

where q is the charge of the ionized species, and r is the species radius. A molecule with a high charge-to-size ratio will have a higher mobility, however there is a number of other factors that will have an effect on the movement of the species. These factors include the hydrophobicity, the functionality and the shape of the molecule.[27,39-41]

The net movement of any species within the capillary column is the composite effect of the electroosmotic flow and electrophoretic mobility. All species will migrate in the same direction, from anode (+) to the cathode (-), under normal operating

conditions. Positively charged ions will migrate faster than the EOF because of the addition of the EPM and thus will pass the detector first. The neutrals will migrate with the EOF and be separated from ions because of the lack of charge or ionization on the compound. This causes little or no separation of the neutral compounds. A method for the separation of neutrals is described later in this introduction. Most anions will migrate toward the cathode more slowly even though their electrophoretic mobility is opposite of the EOF. This is a consequence of the EOF generally being an order of magnitude greater then the EPM. Figure 6 demonstrates the relative order of flow of positive, negative and neutral species through the capillary column under an applied electric field.

By changing the electroosmotic flow, the rate at which the species are separated can be controlled. At high pH, the EOF is very rapid and separations can be very difficult. On the other hand, at low pH's the cations in solution may bind to the negatively charged wall through coulombic interactions. Another way to control the EOF is to increase or decrease the electric field. The concentration of the buffer can have a large effect on the zeta potential which in turn changes the EOF. The higher the concentration of the buffer solution the slower the electroosmotic flow will be. An increase in the capillary temperature can help to increase the EOF and decrease the amount of time it takes for a separation to be performed. The problem with changing most of these parameters can be an increase in Joule heating of the capillary.[27,39-41]

Under normal conditions joule heating is not a problem because it is very easy to dissipate heat from the narrow bore capillary. There are instances when this heating can cause microscopic changes in the viscosity and temperature of the solution, thus leading to broadening of the sample peak. To try to control Joule heating many of the manufacturers have used either air or liquid cooled systems. The liquid cooled systems tend to dissipate heat more efficiently; however, both types are in use today.

Figure 1.6 The movement of ions and neutrals through the CE column

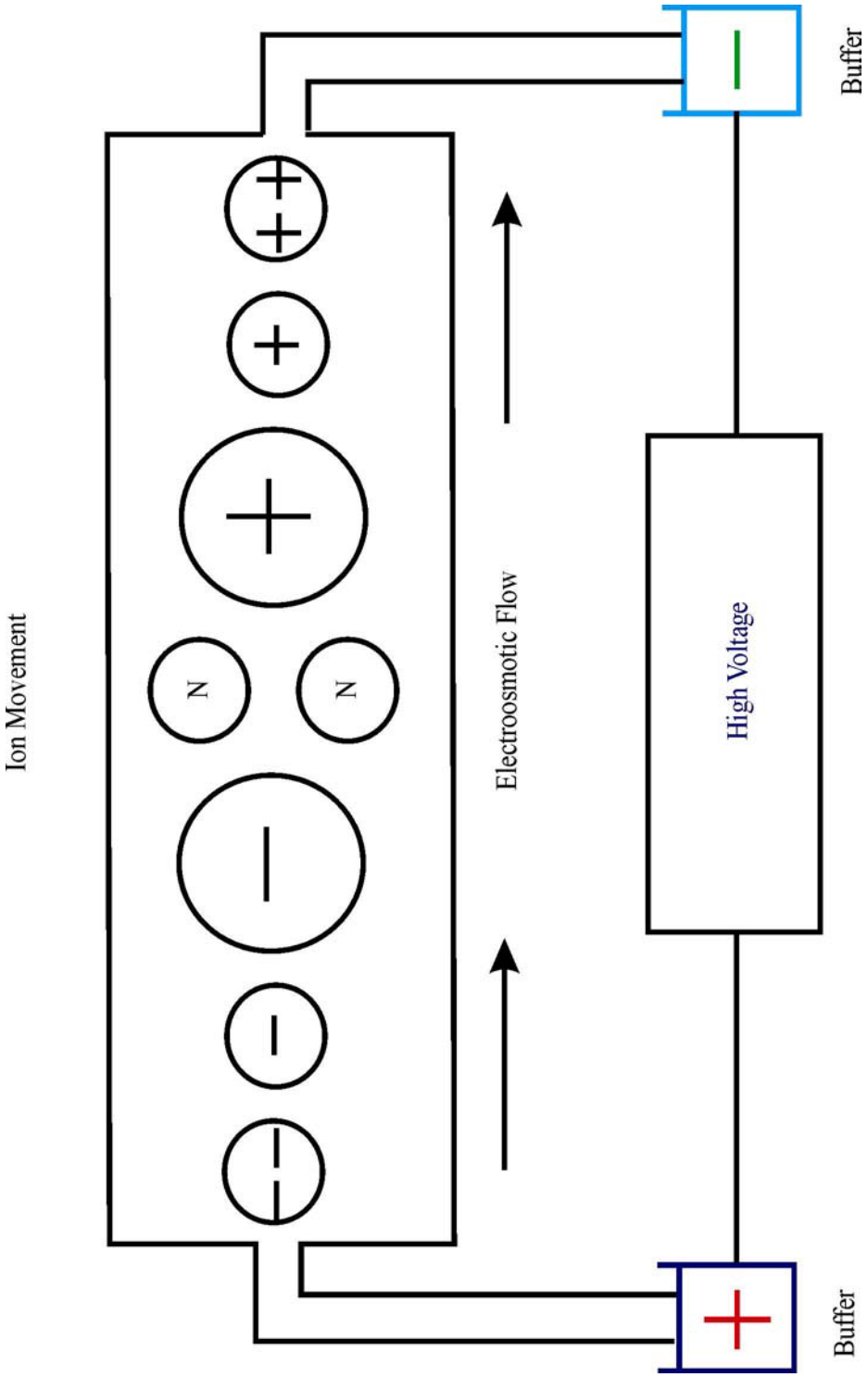
Buffer
Electroosmotic Flow
High Voltage
Ion Movement
N
N
Buffer

Another method that is commonly used to change the electroosmotic flow is to alter the inner wall of the capillary. These modifications generally fall into two different categories: charged and neutral coatings. The neutral coatings, polyacrylamide or polyethylene glycol, will eliminate or reduce the EOF. The charged coating modifications can be used to limit the solute adsorption on the capillary walls or to reverse the electroosmotic flow. By the correct choice of a capillary coating one can control the EOF and optimize the resolution and separation time.[27,39-41]

One advantage that CE has over the use of HPLC is the shape of flow profile during a separation. In HPLC, and other pressure driven separations, a laminar flow profile is seen. The force of the pressure pushing the liquid and the shear force at the wall of the column cause this parabolic shape. In capillary electrophoresis there is a flat flow profile. This is due to the driving force, which is the electrical current that is uniformly distributed along the column walls. There is a small drag that is produced very close to the walls but has relatively little effect on the overall separation. Figure 7 depicts the two different flow profiles, plug (a) and laminar (b), as seen in CE and HPLC respectively.

Capillary electrophoresis, like other separation techniques, can be performed in a number of different modes to achieve optimized separations. The most commonly used mode is capillary zone electrophoresis (CZE) because of its ease of use and simplicity. This mode involves the separation of charged molecules that migrate toward the anode or cathode under the influence of an electric field. As mentioned above, the movement of ions through the capillary is depicted in Figure 6. There is a number of applications that can be performed using this technique as long as the species can be ionized and are soluble in the buffer. These include amino acids, peptides, ionic species, enantiomers, proteins, and carbohydrates.

An important technique that is related to CE is capillary electrochromatography (CEC). This method involves the combination of chromatographic and electrophoretic

Figure 1.7 a: Plug flow profile

b: Laminar flow profile

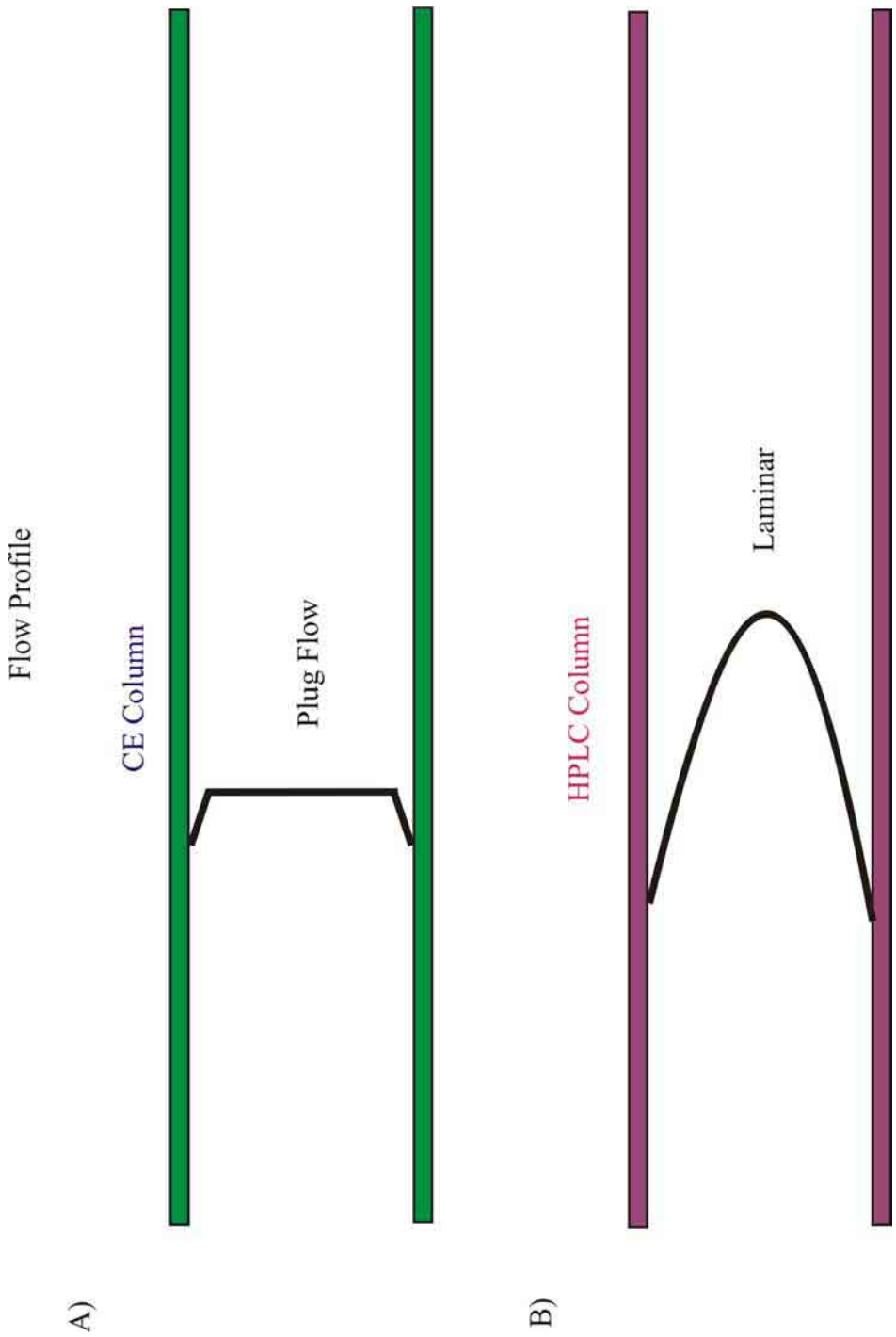
Flow Profile
CE Column
Plug Flow
A)
HPLC Column
Laminar
B)

separations. Figure 8 shows a diagram of a packed capillary electrochromatographic column. This method was first reported in 1974 when a methanol/water separation was studied in a glass tube packed with octane-coated Partisil.[42] Even though the separation was unsuccessful, the groundwork had been laid. The electroosmotic flow of the packed CEC column has three advantages over pressure driven systems. First, even though there is packing within the column, the plug flow characteristics seen in normal CZE hold true in CEC. The differences in the flow profiles in the pressure driven system and the electroendosmotic driven system are seen in Figure 9. The flow rates seen in the pressure driven systems tend to be high when compared to the rates seen in CEC. The EOF driven system is pulse free and operates at atmospheric pressure, which is an advantage when interfaced to MS or other spectrometric detectors.

The retention in CEC is based on the partitioning between the stationary and mobile phases of the solutes. This retention allows for the separation of neutral compounds as well as the charged ions. The use of CEC combines the best aspects of capillary zone electrophoresis such as rapid analysis times and high separation efficiencies with the best aspects of HPLC including selectivity mechanisms, the ability to analyze polar compounds, and an increased sample capacity.[43] Band broadening is the same in CEC as it is in CZE, with the added variable of eddy diffusion. This is not as great of a problem in CEC as it is in HPLC because of the flow mechanisms seen in CEC. The disadvantages of CEC are the production of capillaries, bubble formation in the mobile phase, and the complexity of gradient elution equipment on certain instruments.

CE Instrumentation

Under normal operation a capillary electrophoresis system is very simple. A CE system is designed with two electrodes connected to a high voltage power supply, a capillary column, buffer and sample vials, automated sample control, and a detector.

Figure 1.8 Diagram of a packed capillary electrochromatography column

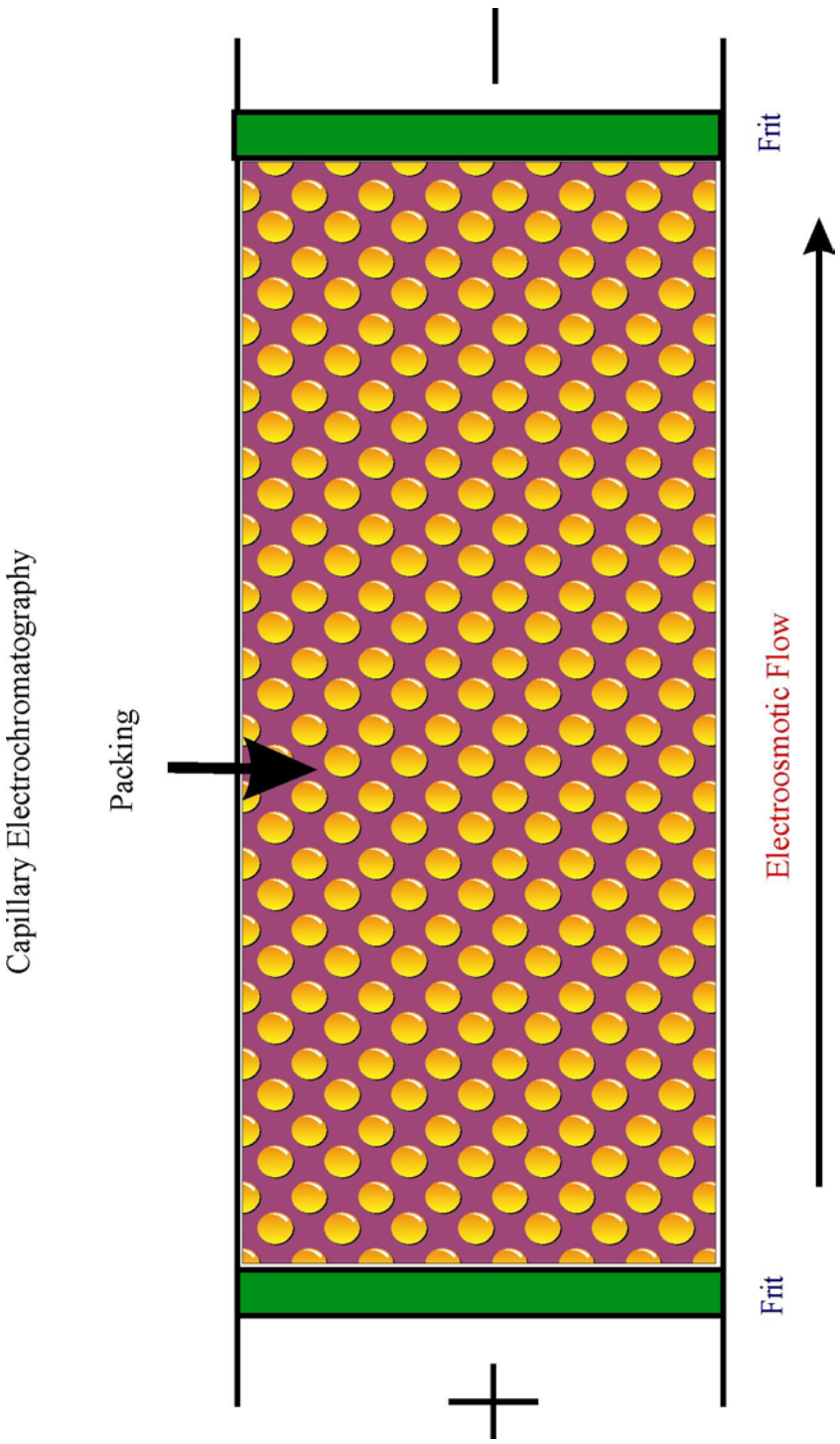
Capillary Electrochromatography
Packing
Frit
Frit
Electroosmotic Flow

Figure 1.9 a: Pressure driven flow profile through a packed column

b: Electroendosmotic driven flow profile through a packed column

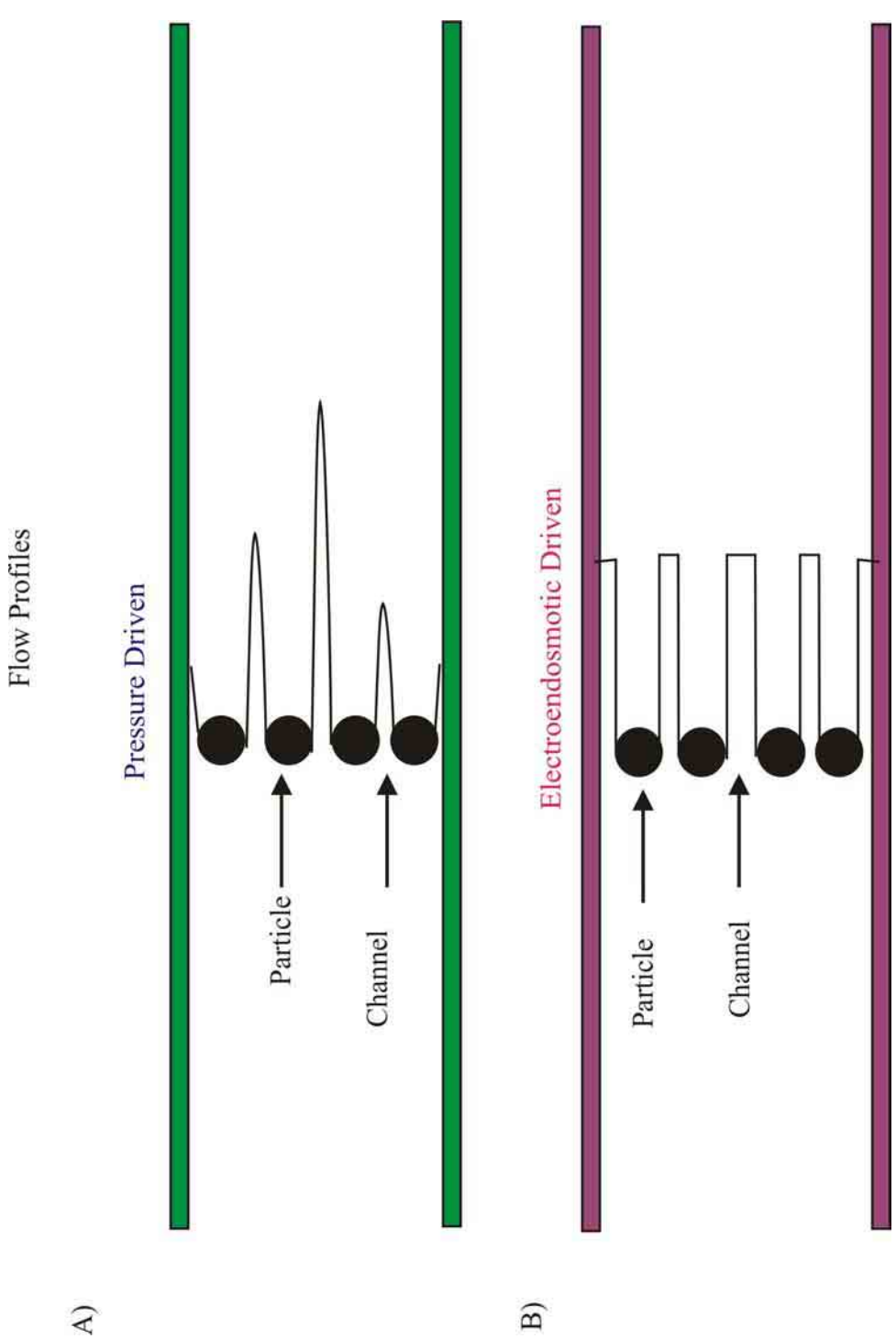
Flow Profiles
A)
Pressure Driven
Particle
Channel
B)
Electroendosmotic Driven
Particle
Channel

Figure 10 shows a diagram of a complete capillary electrophoresis system. To load the sample into the capillary, CE systems follow two commonly used methods. One method is to use electrophoretic injection, where a charge is placed upon the inlet sample vial and the outlet buffer vial. A large amount of sample solution is needed even though a very small amount of the sample is actually injected. The other popular method for sample introduction is pressure injection. In this method pressure is applied to the sample vial at the inlet of the capillary. This pressure can also be used to clean the column between runs and when condition of the column calls for it to be cleaned. Both of these injection methods load on the order of a nanoliter or less depending on the time and type of sample being injected. Once the sample has been loaded, the inlet and outlet of the capillary are immersed in the run buffer. A high voltage is applied across the column and separation begins. As mentioned above, the voltage, temperature, and buffer concentration can be adjusted to increase or decrease the run time as needed.

Most CE systems use a number of different types of detectors such as UV, fluorescence, mass spectrometry, refractive index, conductivity, and amperometry. The most widely used of these is on-line UV detection. To prepare the capillary for UV detection roughly 0.5 mm of the polyamide coating is removed by burning. The window that is formed should be no larger then 300 μm in length. If the window is too large there may be a loss of signal due to scattering of the radiation. The radiation passes through the window and analyte, and then onto the detector. Depending on the amount of signal obtained other detection methods may need to be used.

Fourier transform infrared microspectrometry

Fourier transform infrared microspectrometry is a very important method in the study of small quantities of materials. It has also gained popularity in the study of small biological samples. FT-IR microspectrometry has been used to study sample concentrations as low as the picogram level.[44-47] With sample extraction and synthetic

Figure 1.10 Diagram of an entire capillary electrophoresis instrument

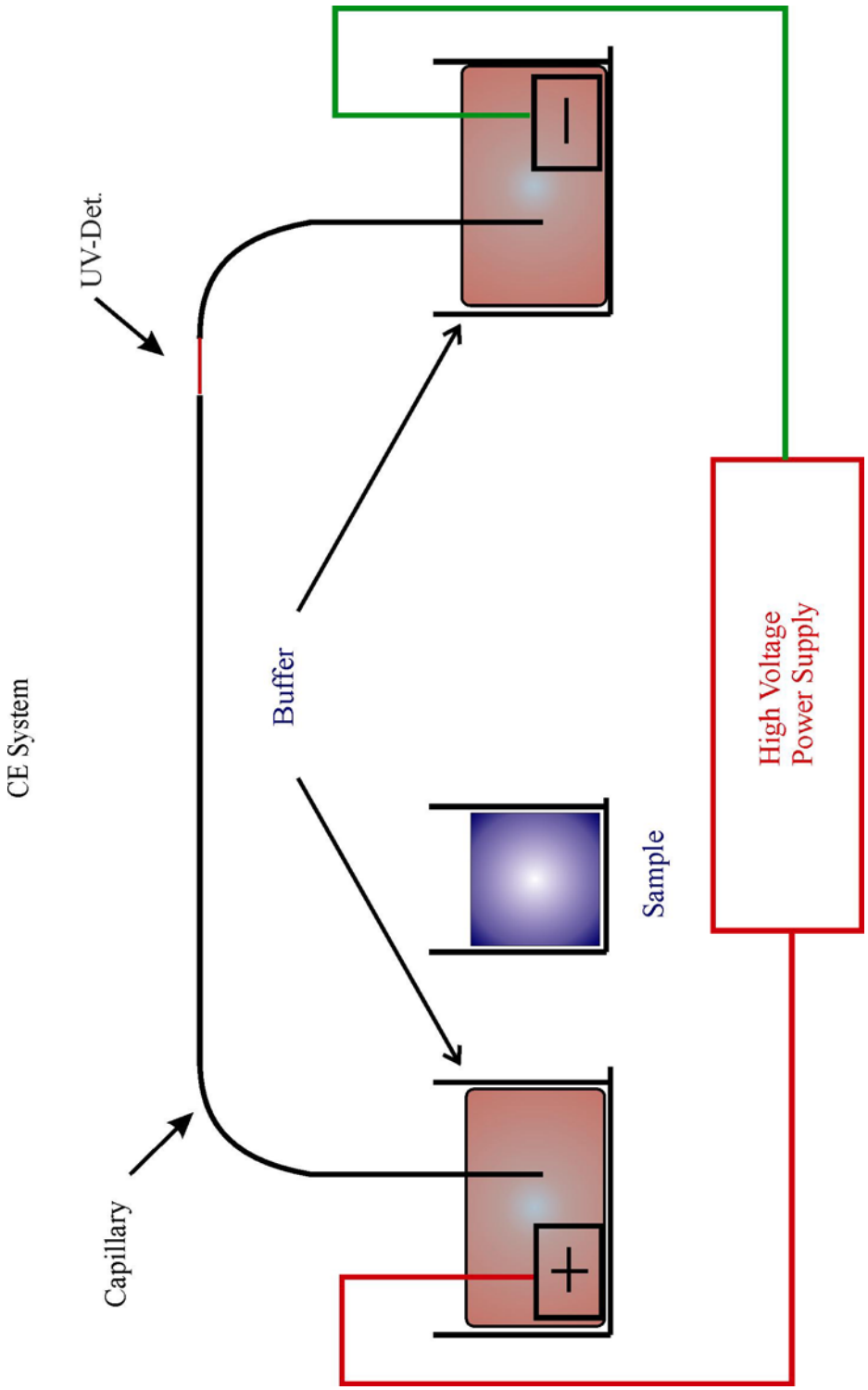
CE System
UV-Det.
Capillary
Buffer
Sample
High Voltage
Power Supply
−
+

methods becoming better, the ability to study small amounts of sample has become important to a number of different areas within the scientific community. This technique combines the areas of spectrometry and microscopy. IR microspectrometry techniques can also be used on a number other types of samples, including those in the textile, polymeric, forensics, and biological fields.[48-57]

Most FT-IR microscope systems have a video unit attached that allows for exact positioning of the beam path allowing for sampling from a number of points within the sample area. An IR microscope is somewhat different from a conventional optical microscope in that the IR scope has two separate beam paths. The first beam is the optical beam for the visible radiation. This visible beam is sent to the optical objective or in most cases, a video camera for display. Figure 11 shows the beam path for the optical mode of an FT-IR spectrometric microscope system. The infrared beam and He:Ne laser beam are blocked while the microscope is used in visible mode. The visible beam enters near the base of the microscope and then bounces off of mirror 3. From there the beam enters cassegrain 1. The beam is focused onto the sample position and then enters the second cassegrain. This cassegrain focuses the beam through the remote aperture, which can be set to a number of different sizes depending on the sample of interest. The beam is then sent onto the optical microscope or video camera. Here the area of the sample that is going to be analyzed can be brought into focus and the correct size of the aperture can be chosen. The infrared beam used in transmission experiments follows a different path than the visible radiation. Figure 12 shows the beam path of the infrared radiation in a FT-IR spectrometric microscope. The IR beam enters the microscope from the source and reflects off of mirror 2. This focuses the beam onto mirror 3 and then the beam enters cassegrain 1. The cassegrain focuses the beam onto the sample area and then into the second cassegrain. The beam is then focused through the remote aperture and instead of going onto the microscope's visible objective, a mirror is moved into the beam path. The beam is reflected off of mirror 4

Figure 1.11 Infrared Microscope Beam path for Optical viewing in transmission mode

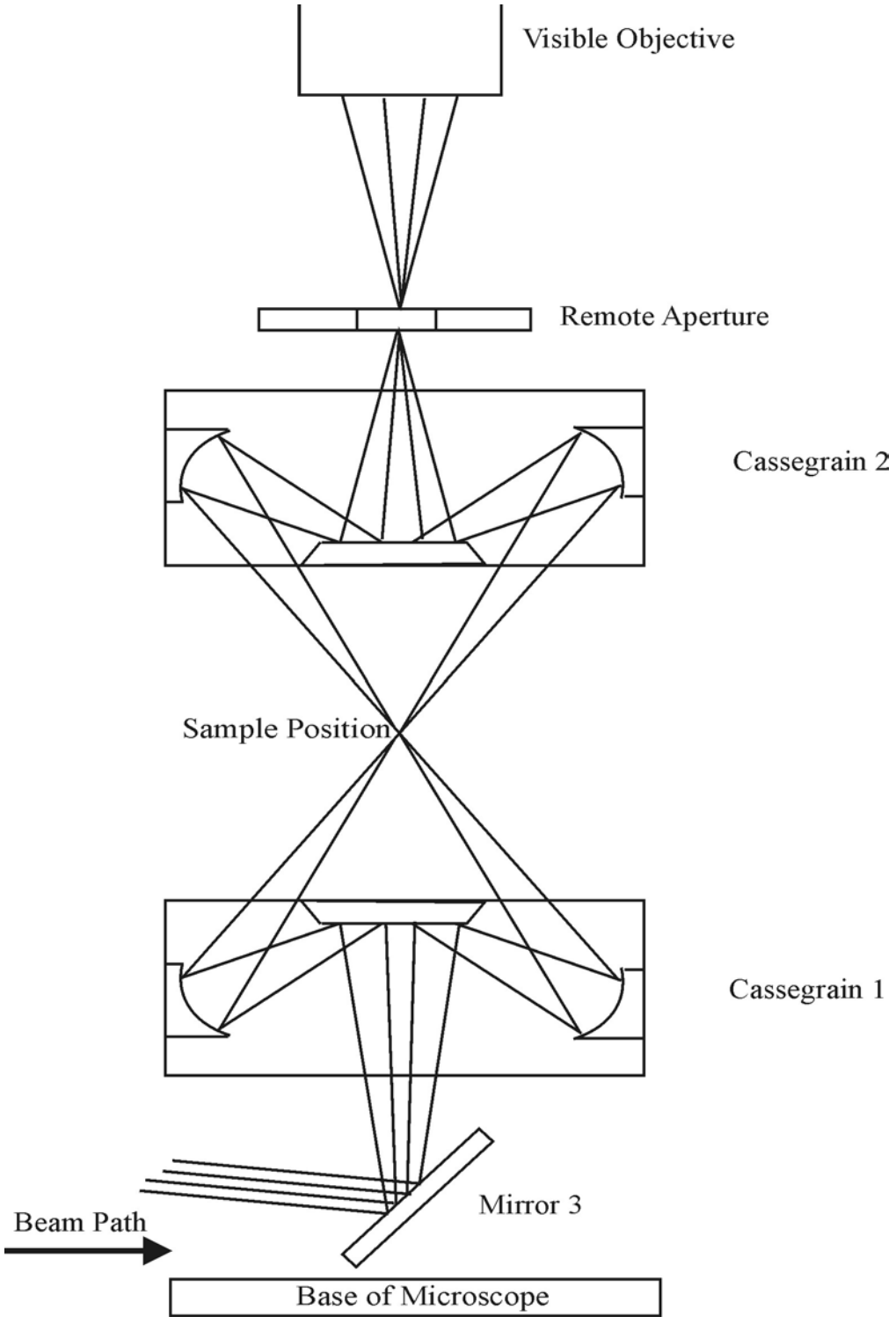
Visible Objective
Remote Aperture
Cassegrain 2
Sample Position
Cassegrain 1
Mirror 3
Beam Path
Base of Microscope

Figure 1.12 Infrared Microscope Beam Path for Infrared Scanning in transmission mode

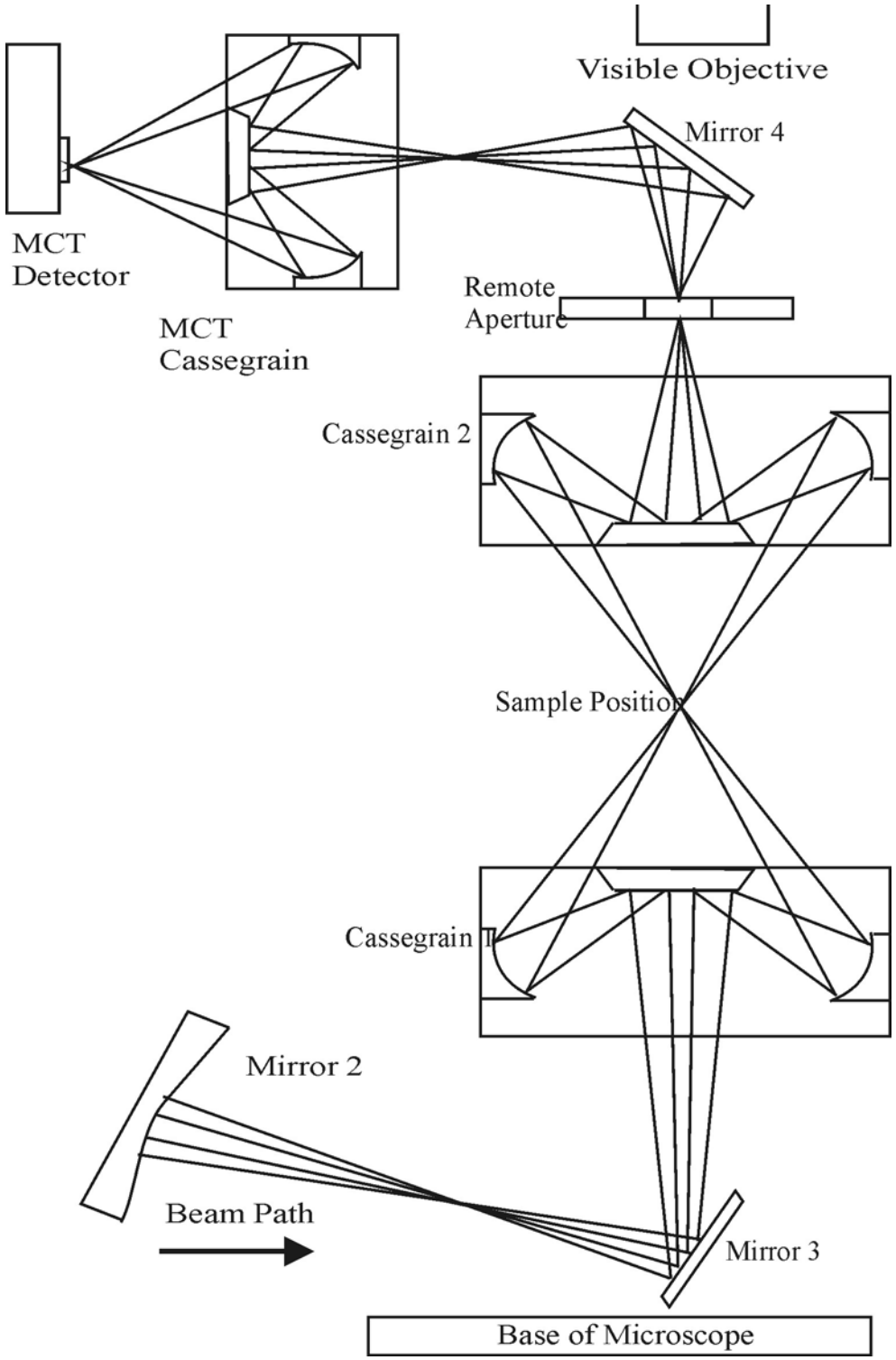
Visible Objective
Mirror 4
MCT
Detector
MCT
Cassegrain
Remote
Aperture
Cassegrain 2
Sample Position
Cassegrain 1
Mirror 2
Beam Path
Mirror 3
Base of Microscope

and sent to the mercury cadmium telluride (MCT) cassegrain mirror. This cassegrain focuses the beam onto the MCT detector, where the interferogram is collected. FT-IR microscopes can also be used in reflectance mode, however this is beyond the scope of this dissertation.

In a FT-IR spectrometer the signal-to-noise ratio (SNR) is an important measure of the performance of the instrument. The signal-to-noise ratio is defined by the following equation:

$$SNR = \frac{U_\nu(T) \cdot \Theta \cdot \Delta\nu \cdot \xi \cdot \sqrt{t}}{\sqrt{A_D}} \tag{5}$$

$$\Theta = \Omega \times A_L \tag{6}$$

$U_\nu(T)$ is the spectral energy density, Θ is the throughput which is described by equation 6, Ω is the solid angle, A_L is the limiting aperture, $\Delta\nu$ is the resolution, t is measurement time, the ξ is the spectrometer efficiency, and A_D is the area of the detector.[58] In an FT-IR spectrometric microscope system the spatial resolution is the most important consideration when performing sample analysis. As the infrared beam passes through the sample there is a large amount of radiative scattering that occurs. When an aperture is placed within the beam path the amount of the diffraction can be greatly reduced. In some microscope systems a second aperture can be placed within the beam path before it reaches the sample of interest thus removing a great deal of the instrument scattering.

When interfacing any separation method to a Fourier transform infrared spectrometer the following equation for the sensitivity of the analysis is used:

$$Sensitivity = SNR \times \frac{Sample\ Quantity \times Absorptivity \times Pathlength}{Area\ of\ the\ Sample} \tag{7}$$

To optimize the sensitivity of the analysis it is ideal if the area of sample matches the area of the limiting aperture A_L, seen in equation 5. If the area of the sample is smaller than the area of the detector then there will be an increase in the noise and a decrease in the sensitivity of the measurement. There is also a loss of sensitivity if the area of the sample is much larger than the area of the limiting detector due to the loss of signal that is not passing through or hitting the detector window. In the case of the FT-IR spectrometric microscope system in our laboratory, a Perkin-Elmer Spectrum 2000 coupled with a Perkin-Elmer *i*-series FT-IR microscope, the limiting aperture is the MCT detector. The detector element is roughly 50 μm square. The CE/FT-IR interface developed here is able to produce deposits on the order of 100 μm, which is well-matched to the detector element size.

Attenuated Total Reflection Spectrometry

Infrared spectroscopy is one of the most powerful analytical techniques in use today. With its growth the need for surface and bulk analysis using internal and external reflections has also grown.[59-69] Over the past decade the need for a nondestructive microsampling infrared spectrometry method has increased. There has been a great deal of work done in the development of attenuated total reflection (ATR) accessories in the area of infrared spectroscopy.[70-76] These accessories have an important advantage over many other accessories in transmission FT-IR spectrometry, such as microscopes and beam condensers. In transmission, the sample must be optically thin to be measured. Most samples are not optically thin, hence a method for sample preparation must be developed before they can be measured. Most of the methods involved in making optically flat samples involve the use of dilution or compression that can lead to sample destruction, or at least a change in morphology. The use of internal reflection spectrometry does not have the same sampling problems seen in transmission experiments. The sample is placed in contact with the surface of

the accessory, thus little, if any, sample preparation is needed before analysis. There is often no need for anything other than minor pressure application to the sample and thus loss of the sample integrity is not as pronounced. This technique also allows for the analysis of small samples that are in liquid, irregular solid, or powder form, as long as adequate contact between the sample and the ATR element is made. Many studies today that involve the use of ATR accessories investigate solution mixtures and minute amounts of sample.

There is a number of different designs used for the internal reflection elements (IRE) in ATR accessories. The designs fall into two categories, single and multi-bounce elements. The geometry of the single bounce elements is either fixed angle, such as prisms, or variable angle such as hemisphere and hemicylinder. Multiple reflection elements are described in detail by Harrick and will not covered here.[70] Figure 13 shows the design of a single bounce or reflection prism element. This design does not allow for the beam of light to be focused onto a small area, thus the size of the beam entering the prism will determine the active area of the IRE element. This works well for bulk materials and situations in which contact between the sample and the surface is easily maintained. This technique can be difficult when there is a small amount of sample available for analysis, due to the large active area, on the order of a millimeter, that is often seen with these types elements. To reduce these large active areas the use of the hemisphereical design has been employed.[71-73] In this design the bottom of the element is in the shape of a hemisphere. This design causes a large convergence of the beam, which in turn helps to increase the sensitivity when examining very small amounts of samples. Figure 14 shows a diagram of a hemispherical single reflection element. Once the beam enters the crystal the path is bent toward the center of the element. The active site of the element can vary in size but a commercially available element from Harrick scientific is ~250 μm in diameter. A diagram of this type of element, a Split-Pea™, is shown in Figure 15. Although the

Figure 1.13 Prism Internal Reflection Element: Beam Defocusing

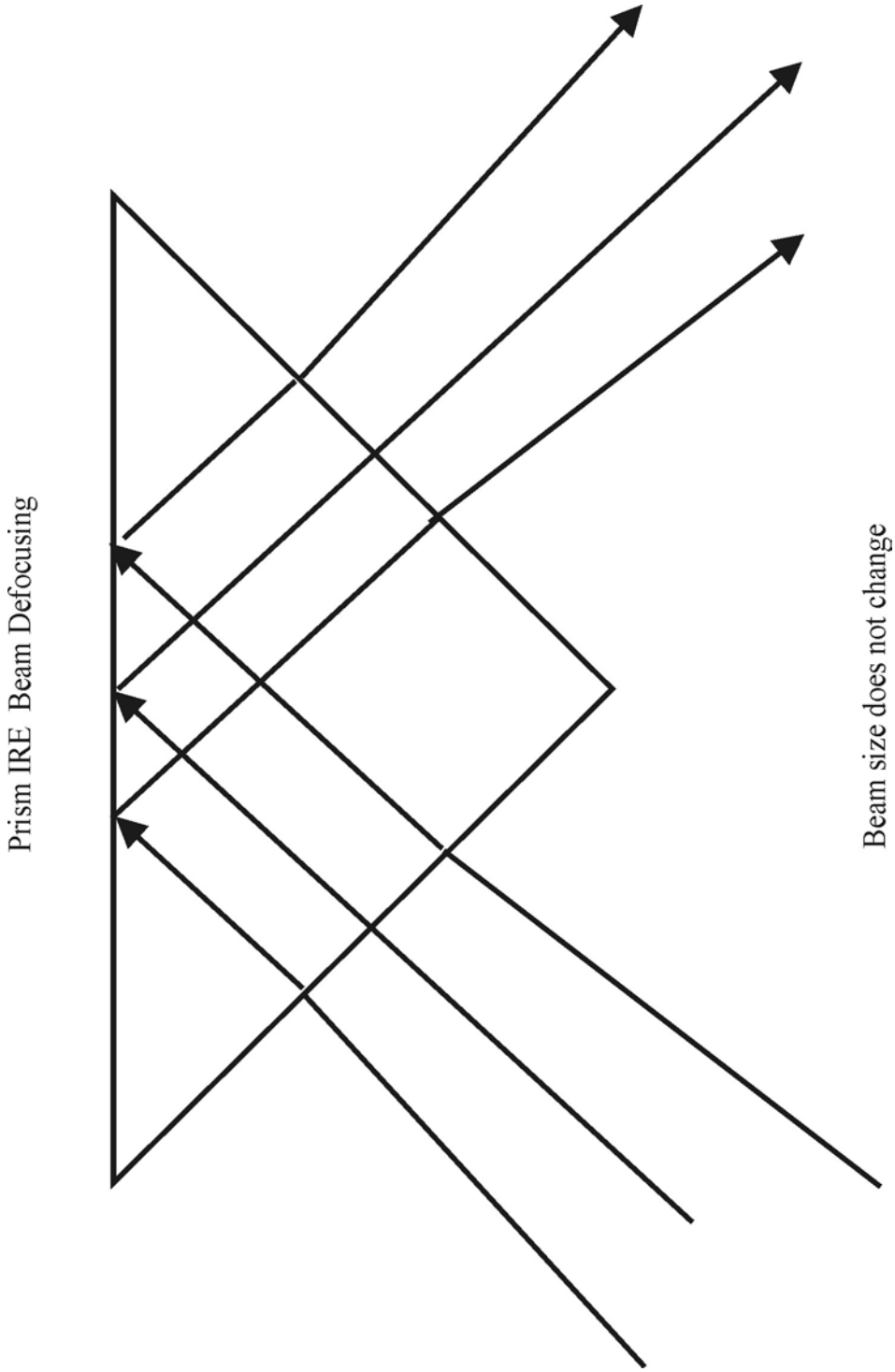
Prism IRE Beam Defocusing
Beam size does not change

Figure 1.14 Hemisphere Internal Reflection Element : Beam Non-Defocusing

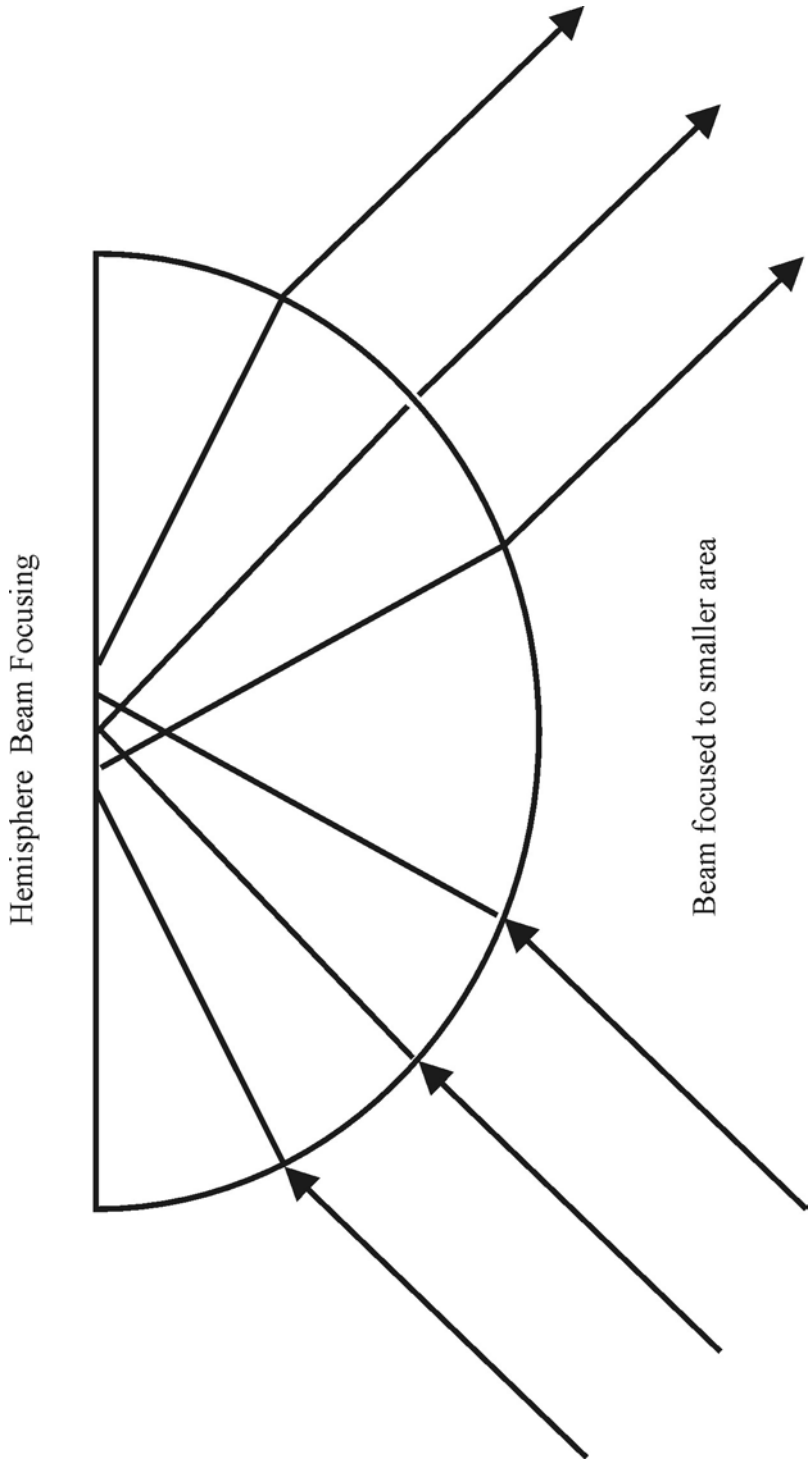
Hemisphere Beam Focusing
Beam focused to smaller area

Figure 1.15 Internal Reflection Element Active Site

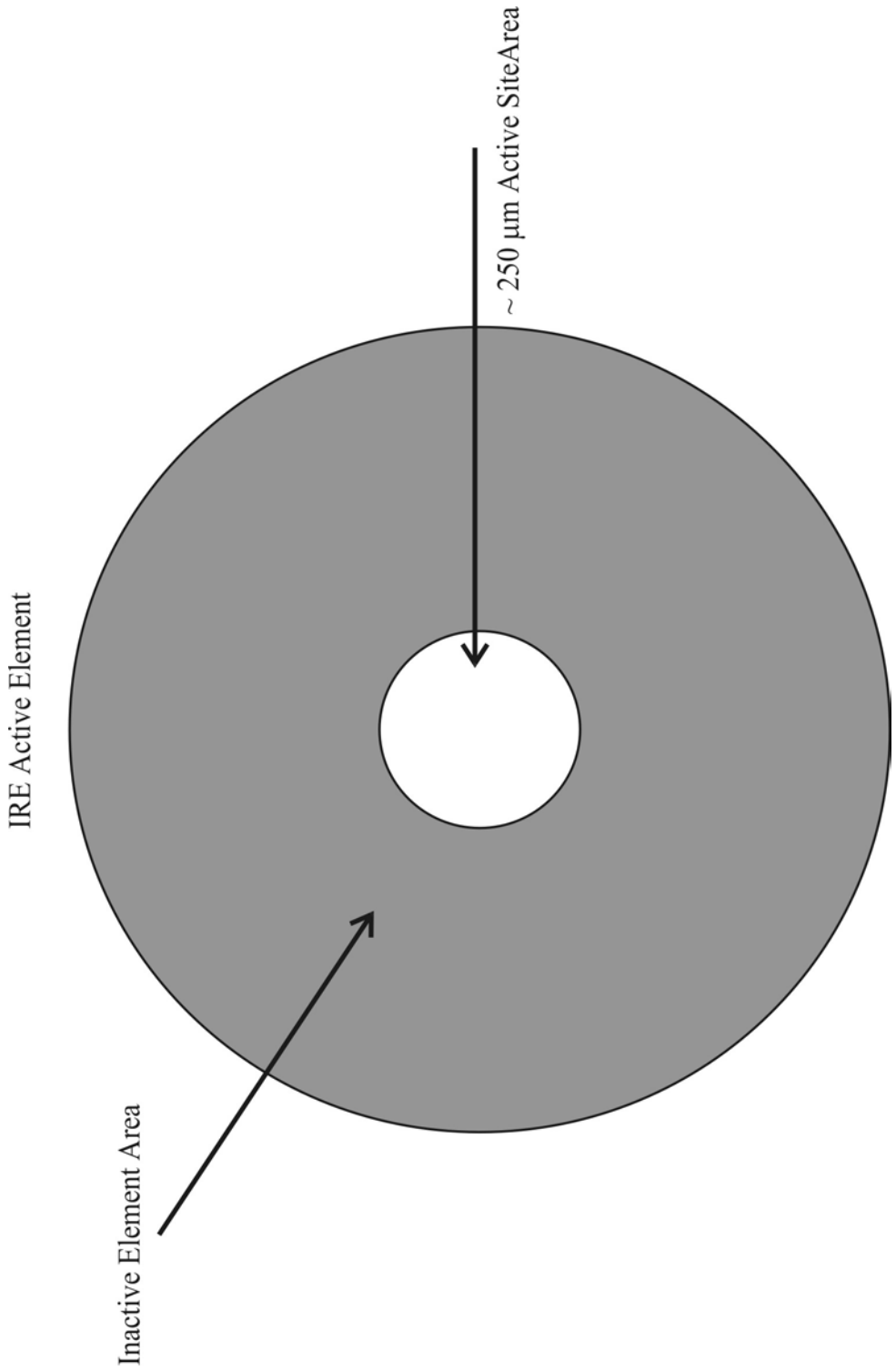
IRE Active Element
~ 250 µm Active SiteArea
Inactive Element Area

entire element is ~1000 μm in size, only a small part of the light beam is allowed to penetrate into the sample.

One important factor when using a single bounce internal reflection element is the choice of the material for the IRE. The material will have an effect on the depth of penetration of the light beam into the sample. The lower the refractive index of the material the greater the depth of penetration. The two most commonly used materials are germanium and silicon. The refractive index of these two materials is 4 and 3.5 respectively. In the mid IR region, 4000 cm^{-1} to 660 cm^{-1}, the depth of penetration varies from 0.181 μm to 1.10 μm if silicon is used for the IRE. To calculate the depth of penetration the following equation is used:

$$d_p = \frac{\lambda}{2\pi\eta_1(\sin^2\theta - \eta_{21}^{\ 2})^{1/2}} \tag{8}$$

where λ wavelength of the input radiation, η_1 is refractive index of element, η_{21} is η_2/η_1 the ratio of the refractive index of the sample divided by that of the element, θ is the angle of incidence. A pictorial description of the depth of penetration is shown in Figure 16. As the radiation wave penetrates through the crystal into the sample, the wave decreases exponentially the farther in it goes. For qualitative analysis, on a homogenous sample, the depth of penetration is inconsequential. Small deposits can still be made as long as the signal is large enough to overcome the baseline noise. The depth of penetration does, however, become an important factor when quantitative analysis is required.

In our laboratory the number and composition of a mixture of oligosaccharides is being determined. To build a model using single bounce IRE the depth of penetration needs to be covered to maximize the absorbance of the bands of each component. Once the model has been built all subsequent analyses must be performed in the same

Figure 1.16 Depth of Penetration for Internal Reflection Element

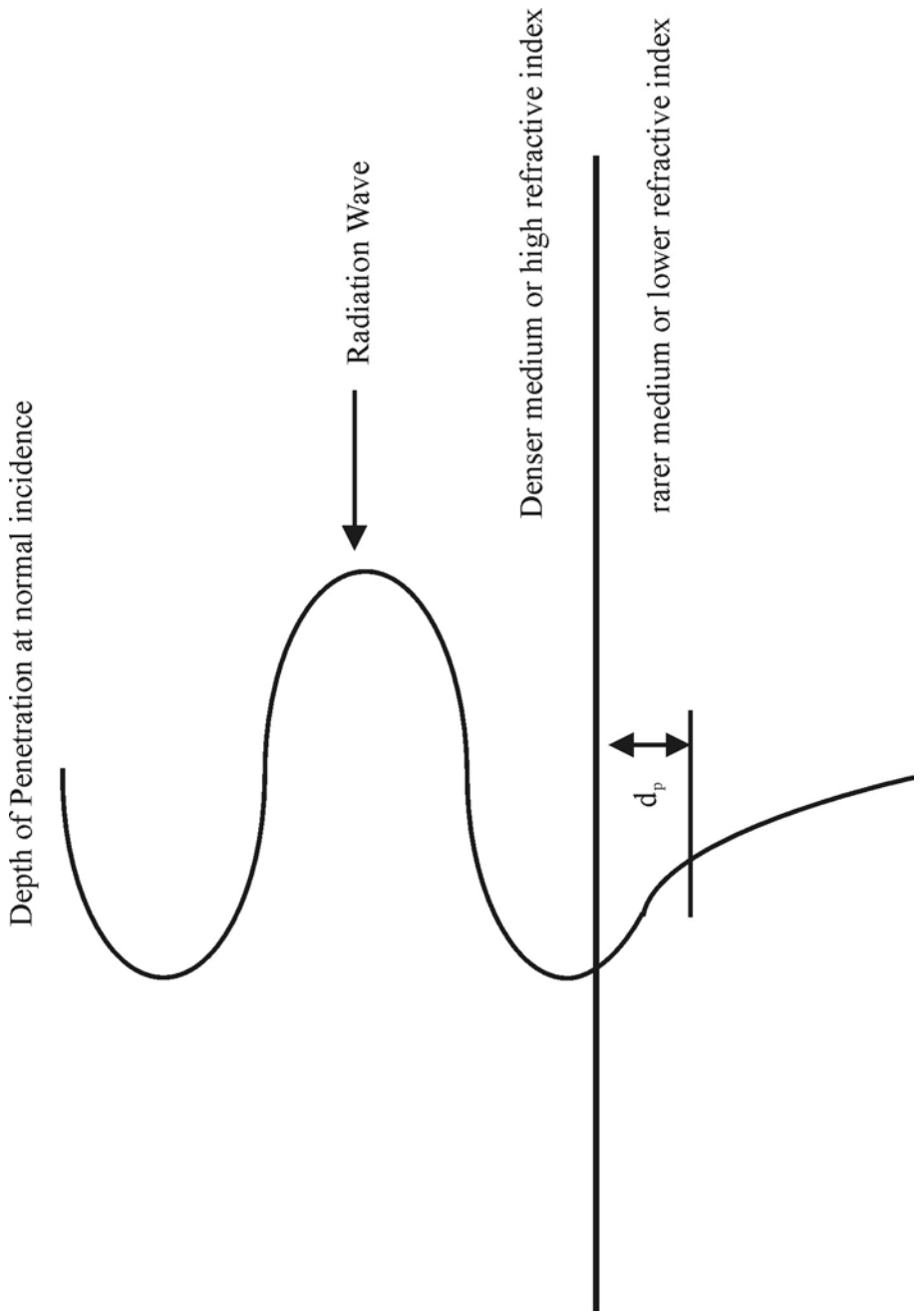
Depth of Penetration at normal incidence
Radiation Wave
Denser medium or high refractive index
rarer medium or lower refractive index
d_p

manner. If the model is not consistent, then the amount of each component will not be accurately reported.

Single bounce hemispherical internal reflection elements come in a number of different designs. We use a design developed by Harrick scientific called a Split-Pea™. This accessory attaches in the sample compartment of an FT-IR instrument. Figure 17 shows how the light beam enters the Split-Pea™ and moves toward the IRE element. Mirrors 1 and 2 direct the beam toward an ellipsoidal mirror, mirror 3, which focuses the radiation onto the element. The reflected beam is collected by another ellipsoidal mirror, mirror 4, and is then sent to mirrors 5 and 6 toward the detector. As seen in Figure 15 the active site of the element is roughly 250 μm in diameter. Both liquid and solid samples can analyzed using this accessory. For the solid samples a pressure applicator is provided. This can be brought down on top of the sample so that good contact can be maintained and reproducible spectra can be collected, however this is not needed for direct deposition. In our laboratory, the use of direct deposition involves the placement of a liquid sample upon the active area of the IRE element, then the sample is allowed to dry and its spectrum is collected. Chapter 4 discusses the use of the Split-Pea™ IRE accessory combined with a semi-automated sample direct deposition system to help with the analysis of monosaccharides, oligosaccharides and carbohydrates.

Figure 1.17 Split Pea™ Beam Path

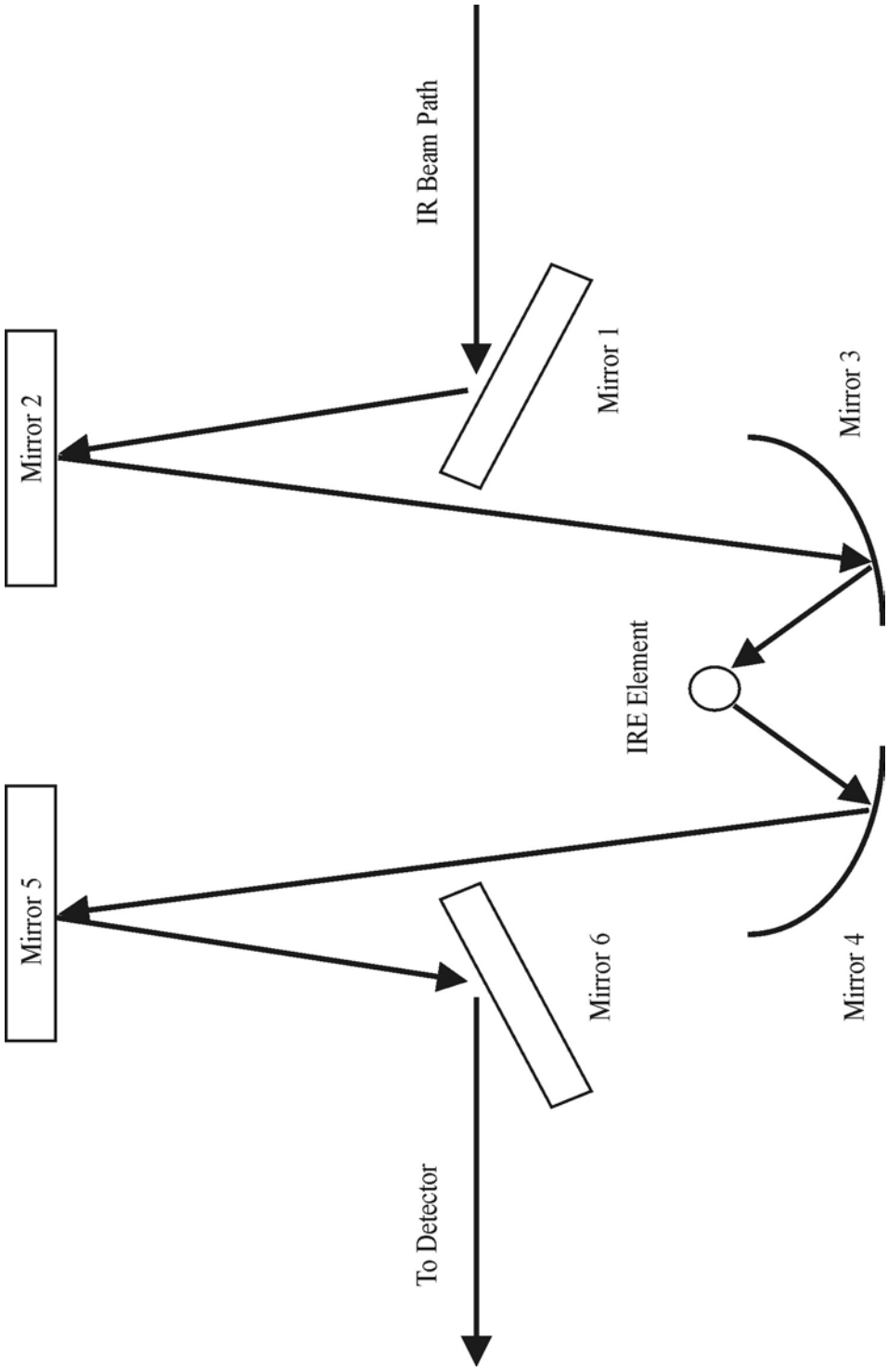
IR Beam Path
Mirror 1
Mirror 2
Mirror 3
IRE Element
Mirror 5
Mirror 6
Mirror 4
To Detector

References

1. Y. Lee and T. Lin, J. Chromatogr. B **681,** 87 (1996).

2. H. El Khadem *Carbohydrate Chemistry* (Academic Press, Inc., New York, 1988).

3. M. Legaz, M. Pedrosa, R. de Armas, C. Rodriguez, V. de los Rios, and C. Vicente, Anal. Chim. Acta **372,** 201 (1998).

4. A. Vorndran, P. Oefner, H. Scherz, and G. Bonn, Chromatographia **33,** 163 (1992).

5. P. Oefner, A. Vorndran, E. Grill, C. Huber, and G. Bonn, Chromatographia **34,** 308 (1992).

6. S. Hoffstetter-Kuhn, A. Paulus, E. Gassmann, and H. Widmer, Anal. Chem. **63,** 1541 (1991).

7. A. Paulus and A. Klockow, J. Chromatogr. A **720,** 353 (1996).

8. T. Garner and E. Yeung, J. Chromatogr. **515,** 639 (1990).

9. J. Zhao, P. Diedrich, Y. Zhang, O. Hindsgaul, and N. Dovichi, J. Chromatogr. B **657,** 307 (1994).

10. Y. Huang, Y. Mechref, and M. Novotny, Carbohydr. Res. **323,** 111 (2000).

11. E. Hounsell *Glycosciences, Status and Perspectives*, H.-J. Gabius, Ed. (Chapman and Hall, London, 1997), p.22.

12. R. Laine and *Glycosciences, Status and Perspectives*, H.-J. Gabius, Ed. (Chapman and Hall, London, 1997), p.1.

13. F. Dang, Y. Chen, Q. Guo, and G. Xu, Chemical Journal of Chinese Universities **21,** 206 (2000).

14. J. Delaney and P. Vouros, Rapid Commun. Mass Spectrom. **15,** 325 (2001).

15. M. Hadley, M. Gilges, J. Senior, A. Shah, and P. Camilleri, J. Chromatogr. B **745,** 177 (2000).

16. S. Honda, J. Okeda, H. Iwanaga, S. Kawakami, A. Taga, S. Suzuki, and K. Imai, Anal. Biochem. **286,** 99 (2000).

17. K. Hutterer, H. Birrell, P. Camilleri, and J. Jorgenson, J. Chromatogr. B **745,** 365 (2000).

18. B. Lagane, M. Treilhou, and F. Couderc, Biochem. Molec. Bio. Ed. **28,** 251 (2000).

19. X. Li, H. Ren, X. Le, M. Qi, I. Ireland, and N. Dovichi, J. Chromatogr. A **869,** 375 (2000).

20. S. Ma and W. Nashabeh, Chromatographia **53,** 75 (2001).

21. D. Newburg, Z. Shen, and C. Warren, Short and Long Term Effects of Breast Feeding On Child Health **478,** 381 (2000).

22. D. Newburg, Z. Shen, and C. Warren, Glycobiology **10,** (2000).

23. V. Pacakova, S. Hubena, M. Ticha, M. Madera, and K. Stulik, Electrophoresis **22,** 459 (2001).

24. T. Raju, Anal. Biochem. **283,** 125 (2000).

25. Z. El Rassi, Electrophoresis **20,** 3134 (1999).

26. Z. Shen, C. Warren, and D. Newburg, Anal. Biochem. **279,** 37 (2000).

27. R. Kuhn, S. Hoffstetter-Kuhn, and *Capillary Electrophoresis Principles and Practice* (Springer Laboratory, New York, 1993).

28. W. Lu and R. Cassidy, Anal. Chem. **65,** 2878 (1993).

29. S. Angyal, Adv. Carbohy. Chem. Biochem. **47,** 1 (1989).

30. J. Kennedy and G. Pagliuca *Carbohydrate Analysis: A Practical Approach,* M. Chaplin and J. Kennedy, Eds. (Oxford, England, 1994), p.43.

31. Z. Rassi and W. Nashabeh, "Carbohydrate Analysis, High Performance Liquid Chromatography and Capillary Electrophoresis," in *Journal of Chromatography Library Vol 58,* Z. Rassi, Ed. (Elsevier, New York, 1995), p.267.

32. L. Colon, R. Dadoo, and R. Zare, Anal. Chem. **65,** 476 (1993).

33. R. Virtanen, Acta Polytechnica Scandinavica-Chemical Technology Series 1 (1974).

34. J. Jorgenson and K. Lukacs, J. Chromatogr. **218,** 216 (1981).

35. J. Jorgenson and K. Lukacs, Anal. Chem. **53,** 1302 (1981).

36. K. Altria, J. Chromatogr. A **856,** 443 (1999).

37. R. StClaire, Anal. Chem. **68,** 569 (1996).

38. Polymicro, "Flexible Fused Silica Capillary Tubing", http://www.polymicro.com/tsp.htm, 1998.

39. D. Heiger *High performance capillary electrophoresis* (Aglient Technologies, Germany, 2000).

40. D. Baker *Capillary Electrophoresis* (John Wiley & Sons, Inc., New York, 1995).

41. R. Weinberger *Practical Capillary Electrophoresis* (Academic Press, New York, 2000).

42. V. Pretoriu, B. Hopkins, and J. Schieke, J. Chromatogr. **99,** 23 (1974).

43. I. Lurie, T. Conver, and V. Ford, Anal. Chem. **70,** 4563 (1998).

44. A. Meyer, H. Budzinski, J. Powell, and P. Garrigues, Polycyclic Aromatic Compounds **13,** 329 (1999).

45. M. Filippelli, Appl. Organomet. Chem. **8,** 687 (1994).

46. B. Smith *Fundamentals of Fourier Transform Infrared Spectroscopy* (CRC Press, Boca Raton, FL, 1996).

47. Spectra-Tech, "Contaminant Analysis by FT-IR Microsocpy", Spec-Tech Inc., Stamford, CT, No. 2 (1).

48. E. Bartick, M. Tungol, and J. Reffner, Anal. Chim. Acta **288,** 35 (1994).

49. T. Nakano and S. Kawata, Scanning **16,** 368 (1994).

50. M. Cohenford, L. Qiao, and B. Rigas, Gastroenterology **108,** 457 (1995).

51. N. Ferrer, Mikrochim. Acta **14,** 329 (1997).

52. W. Fu and W. Lien, Journal of Food Science **63,** 80 (1998).

53. V. Rampon, R. Robert, N. Nicolas, and E. Dufour, Journal of Food Science **64,** 313 (1999).

54. L. Cho, J. Reffner, B. Gatewood, and D. Wetzel, Journal of Forensic Sciences **44,** 275 (1999).

55. K. Yano, S. Ohoshima, Y. Gotou, K. Kumaido, T. Moriguchi, and H. Katayama, Anal. Biochem. **287,** 218 (2000).

56. J. Gardette, Spectroscpy Europe **28,** 30 (1993).

57. P. Lang and Richwine L.J. *Practical Sampling Techniques in Infrared Analysis*, P. Coleman, Ed. (CRC, Boca Raton, 1993), p.145.

58. P. R. Griffiths and J. A. de Haseth *Fourier Transform Infrared Spectrometry* (John Wiley & Sons, New York, 1986), Chap. 18.

59. F. Deblase, N. Harrick, and M. Milosevic, J. Appl. Polym. Sci. **34,** 2047 (1987).

60. N. Harrick, Phys. Rev. Lett. **4,** 226 (1960).

61. N. Harrick, Phys. Rev. **125,** 1165 (1962).

62. N. Harrick, Annals of the New York Academy of Sciences **101,** 928 (1963).

63. N. Harrick, Anal. Chem. **36,** 188 (1964).

64. N. Harrick, Appl. Opt. **4,** 1664 (1965).

65. N. Harrick, Appl. Opt. **5,** 1 (1966).

66. N. Harrick, Anal. Chem. **40,** 1755 (1968).

67. N. Harrick, Appl. Spectrosc. **25,** 142 (1971).

68. R. Levitt and N. Harrick, J. Opt. Soc. Am. **56,** 557 (1966).

69. N. Winograd and N. Harrick, Appl. Spectrosc. **25,** 143 (1971).

70. N. Harrick *Internal Reflection Spectroscopy* (Harrick Scientific Corp., Ossining, New York, 1987)

71. N. Harrick, M. Milosevic, and S. Berets, Am. Lab. **24,** 50 (1992).

72. N. Harrick, M. Milosevic, and S. Berets, Am. Lab. **24,** 29 (1992).

73. N. Harrick, M. Milosevic, and S. Betets, Appl. Spectrosc. **45,** 944 (1991).

74. G. Powell, M. Milosevic, J. Lucania, and N. Harrick, Appl. Spectrosc. **46,** 125 (1992).

75. A. Sommer and M. Hardgrove, Vib. Spectrosc. **24,** 100 (2000).

76. J. Coates, Spectroscopy **12,** 16 (1997).

CHAPTER 2

A METAL NEBULIZER CAPILLARY ELECTROPHORESIS/FT-IR SPECTROMETRIC INTERFACE[1]

[1]Todebush, R.A.; L.T. He; J.A. de Haseth. 2001. To be submitted to *Analytical Chemistry*.

Abstract

A capillary electrophoretic (CE) system has been successfully interfaced to a Fourier transform infrared (FT-IR) spectrometer. The advantage of such an interface is that analytes may be detected and often unequivocally identified without analyte derivatization. The interface consists of a stainless steel tube in which the CE capillary is placed and the two are in contact with the use of a metal tee. A solvent elimination approach is used with the interface, so that analytes are deposited onto an infrared transparent window, that is CaF_2, and measured with the use of an infrared microscope. A critical component of this design is to provide an electrical connection at the end of the CE column to permit stable separations that allow for efficient transport of the sample onto the window. The interface produces an aerosol that is directed at the surface of the infrared transparent window. The use of a volatile electrolyte, along with the flow of helium, allows for the evaporation of the electrolyte in flight and the deposition of "dry", or neat, analyte onto the surface of the window.

Introduction

Since the early development of FT-IR spectrometry, interfaces have been important tools in separation and analysis. Gas chromatography/Fourier transform infrared (GC/FT-IR) spectrometry has been commercially available for over two decades. The use of light-pipe,[1,2] direct deposition (DD),[3,4] and Matrix Isolation (MI)[1,5,6] GC/FT-IR spectrometric interfaces have been used extensively. Other areas that have seen extensive use of interface technology are high performance liquid chromatography (HPLC) and supercritical fluid chromatography (SFC). The use of a flow cell interface for HPLC/FT-IR spectrometry has been investigated by Mattson[7] and Taylor;[8] however, this approach has severe sensitivity limitations caused by infrared absorption of the mobile phase. The flow cell approach has given way to the use of interfaces that are able to remove the interference from the mobile phase. An HPLC/FT-IR spectrometric interface has been developed and used in our laboratory for a number of years[9-17] and a number of other researchers has employed different HPLC/FT-IR spectrometric designs.[18-30] Solvent elimination and direct deposition is the method of choice for sample deposition. This approach has also been used successfully with SFC/FT-IR spectrometry.[31,32] It has been used with thermospray,[22] electrospray,[29] concentric flow nebulization,[20,23,24,29,33-35] ultrasonic nebulization,[28,36] and particle beam desolvation.[9-17]

Capillary Electrophoresis has become a powerful tool for separations since its inception in the early eighties by Jorgenson and Lukacs.[37,38] CE has been combined with a number of other spectrophotometric techniques such as, UV spectrometry, LIF (Laser Induced Fluorescence),[39] Raman spectrometry,[40] MS (Mass Spectrometry),[41,42] and ICP-MS (Inductively Coupled Plasma Mass Spectrometry).[43] These interfaces work well with CE as the electrolytic solutions commonly used pose very little interference with the detection methods. CE/UV, CE/LIF, and CE/Raman spectrometries can also be built to detect the analytes in question by on-column

methods. A new interface has been developed that combines the high resolving power of CE and the ability to obtain very strong spectral signals from a Fourier transform infrared microscope spectrometer.

The design and feasibility of the interface has to overcome three major obstacles: the electrical contact point has to be maintained at the end of the CE column to produce stable electric current for reproducible separations; a volatile buffer or electrolyte to produce electroosmosis that does not produce interference in the infrared region of the spectrum; and the size of the sample deposition needs to be as small as possible to help increase the infrared sensitivity. The stainless steel nebulizer CE/FT-IR spectrometric interface described herein took into consideration these points and successfully met all three.

Experimental

Chemical Reagents. The following electrolytic solutions were used in separate experiments: ammonium acetate (NH_4Ac) (Fisher Scientific, Atlanta, GA); ammonium carbonate ($(NH_4)_2CO_3$), acetic acid (CH_3CO_2H), ammonium hydroxide (NH_4OH), sodium phosphate ($NaH_2PO_4 \cdot H_2O$) (Baker, Phillipsburg, NJ); sodium borate ($Na_2B_4O_7 \cdot 10\ H_2O$), (Sigma, St. Louis, MO), and potassium hydroxide (KOH) (EM Scientific, Gibbstown, NJ). All were used as received.

The concentrations of the electrolytic solutions varied between 0.8 M and 1.25×10^{-3} M depending upon the experimental parameters. Certain electrolytic solutions used were made at higher concentrations to try to attain a large enough current and to decrease the separation time. All of the electrolytic solutions were prepared in an aqueous solution of 18.0 MΩ deionized water prepared with a Barnstead Nano ultrapure H_2O system.

The following samples were used to test the stability of the interface: p-aminobenzoic acid, acetylsalicylic acid (Aldrich, St. Louis, MO); sodium benzoate,

N-acetyl-D -glucosamine (GlcNAc), nicotinamide (Sigma, St Louis, MO); caffeine, potassium chloride, and salicylic acid (Baker, Phillipsburg, NJ). The solutions were prepared with 18 MΩ water. The final concentrations of the solutions varied from 5.0×10^{-2} M to 1×10^{-3} M.

The samples were deposited onto zinc selenide (ZnSe) or calcium fluoride (CaF_2) (Spectral Systems, Hopewell Junction, NY) crystals.

Capillary Electrophoresis and FT-IR Microscopy. A Beckman P/ACE 5000 system capillary electrophoresis instrument (Beckman, Fullerton, CA) equipped with a P/ACE UV absorbance filter detector was used to separate the samples of interest. The system was controlled with Beckman System Gold™ software. CE/FT-IR spectra were collected with the use of a Perkin-Elmer Spectrum 2000 FT-IR spectrometer (Perkin-Elmer, Connecticut, USA). The spectrometer was coupled with a Perkin-Elmer *i*-series FT-IR microscope. The microscope was configured with a mercury cadmium telluride (MCT) detector cooled with liquid nitrogen, and an adjustable limiting aperture. The aperture allows for the beam to be restricted from 10 to 400 μm in diameter depending on the sample deposit size. The spectra were collected with PE Image™ software. Spectral manipulations, such as digital subtraction, baseline correction, and normalization were calculated with the use of GRAMS AI™ software (Galactic Industries, Salem, NH). Spectal searching was performed with the KnowItAll™ Analytical System (Sadtler Division of Bio-Rad Laboratories, Philadelphia, PA).

Fused silica capillaries (Polymicro Technologies, Phoenix, AZ), with an outer diameter of 360 μm and inner diameters of 75 μm and 48 μm, were used. The length of the capillary column varied from 78 cm to 110 cm. The distance between the inlet side and the UV detector was maintained at 50 cm.

Metal Nebulizer. A stainless steel nebulizer was designed with the use of a male tee and a flat hex nut (Swagelok, Solon, OH) through which a metal capillary tube was placed. The inner diameter of the capillary was large enough to hold the fused silica capillary in place and allow for electrical contact. The helium gas flow rate through the nebulizer was controlled manually.

Results and Discussion

Under normal operation, capillary electrophoresis works on the basis of movement of an analyte along a column in response to an applied voltage. The movement of the analyte is dependent on the charge and size of the species. The inlet side of the column is placed at a high positive potential with respect to the outlet end. With both ends of the capillary placed into reservoirs that contain the desired electrolyte solutions, electroosmotic flow is directed to the outlet end of the column. In order to perform CE/FT-IR spectrometry sample deposition, a number of modifications needed to be made to the instrument. First, the CE column was extended up to 60 cm from the outlet side electrode, to accommodate the interface. Next, the high voltage power supply connection had to be moved from the standard outlet side electrode and brought outside of the instrument to the interface. This was accomplished by connecting the voltage supply directly to the interface. Another important consideration with this interface design is the electrical contact point. If the electrical contact point is not at the end of the column, the electroosmotic flow will stop before the effluent exits the column. This can cause a loss of separation and droplet formation at the end of the column, which in turn leads to analyte mixing and peak broadening. In commercial CE/MS systems, the electrical contact point may be maintained by the use of a sheath liquid.[44] This is not a practical approach for use with the CE/FT-IR spectrometric interface as the sheath liquid would not allow for solvent elimination, small deposit sizes, and possible sheath liquid/analyte interference. To alleviate this problem, the end

of the column was placed inside of a 4 cm long stainless steel tube. With the column placed at the tip of this tube, the electrical contact point was moved to the end of the column. To test the feasibility of the interface and the placement of the electrical contact point, an electropherogram of sodium benzoate in a sodium borate electrolyte was obtained (Figure 1). As can be seen from the electropherogram that sample migrated as expected and there were no current anomalies.

The main problem with the CE/FT-IR spectrometric interface is the electrical contact point. As stated above, this problem was easily solved, with the use of a stainless steel tube. The problem remained to develop a method whereby the analyte would be deposited for spectral collection. The use of a tee in the design allows for both the CE column and helium sheath gas to exit concentrically in order to nebulize the effluent stream. Figure 2 shows the design of the metal nebulizer CE/FT-IR spectrometric interface. Figure 3 presents a UV electropherogram of a four-component mixture of caffeine, salicylic acid, p-aminobenzoic acid, and sodium benzoate along with resulting CE current plot. The current plot demonstrates that the electrical contact is good even with the application of the helium sheath gas. The helium gas also helped with another problem the CE/FT-IR spectrometric interface faced, which was the flow rate coming from the capillary column. Flow rates in CE are generally on the order of a few hundreds of nanoliters per minute and at these rates the production of a nebulized stream of effluent can be very difficult. With the helium gas the effluent is swept away from the end of the capillary and toward the window. Another way to try to increase the flow is to add pressure to the separation. If 0.5 psi helium is added to the input electrolyte vial the flow will increase and help to create a better nebulization. The problem with this is if the peaks are not well resolved before the pressure is added then there will be a loss of resolution when the pressure is applied. It should also be mentioned that the helium flow to the interface should only be turned on after the sample has been injected and the high voltage has been applied. If not, the CE current

Figure 2.1 UV electropherogram and CE current when the electrical contact at the outlet is a stainless-steel capillary. Sample: sodium benzoate, electrolyte: 1.25 x 10^{-2} M borate, voltage: 30 kV, detection 214 nm

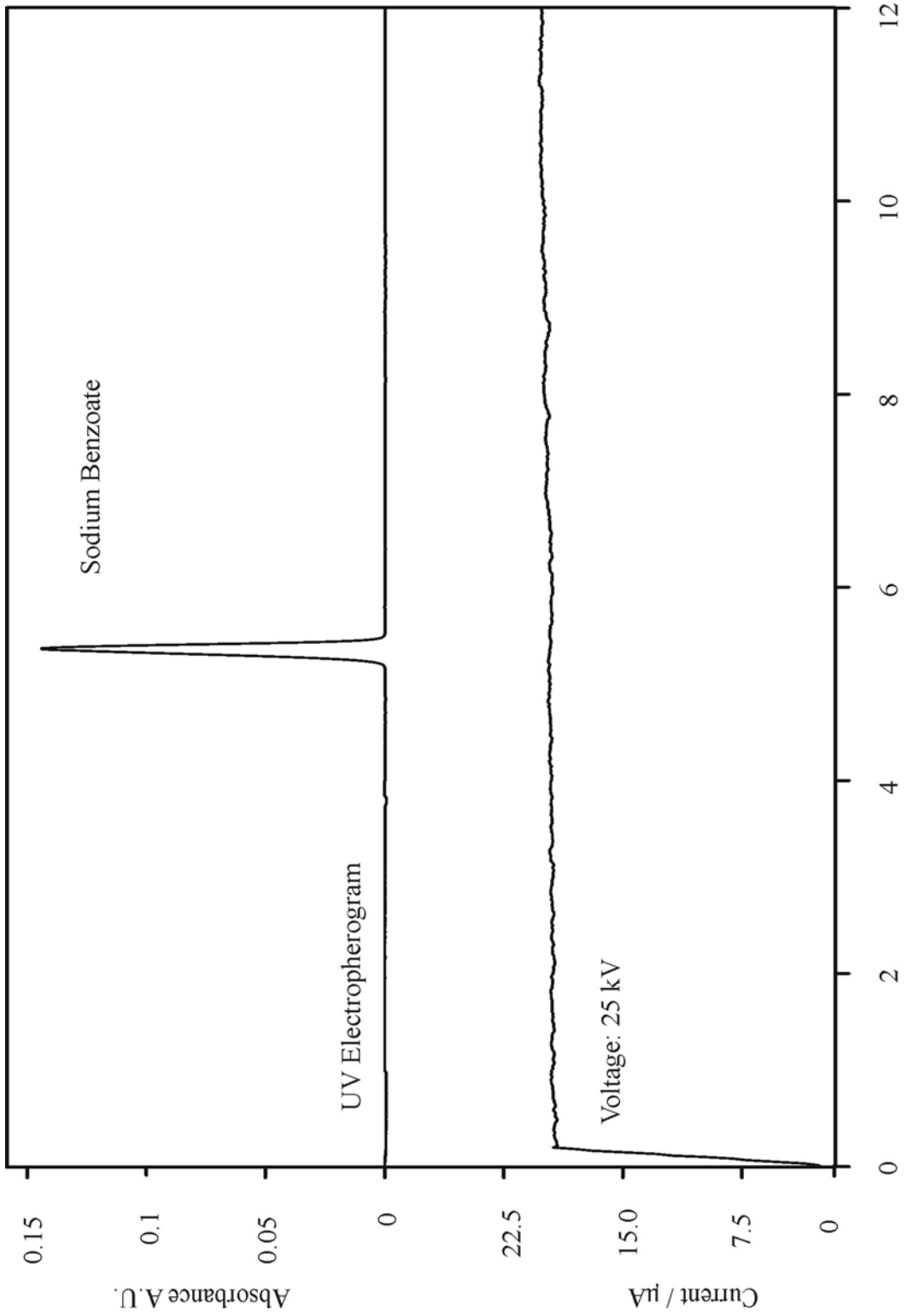
Sodium Benzoate
UV Electropherogram
Voltage: 25 kV
Absorbance A.U.
Current / μA
Time / Min
0.15
0.1
0.05
0
22.5
15.0
7.5
0
0
2
4
6
8
10
12

Figure 2.2 Metal nebulizer CE/FT-IR interface. The ground potential of the high voltage supply is connected to the metal Nebulizer

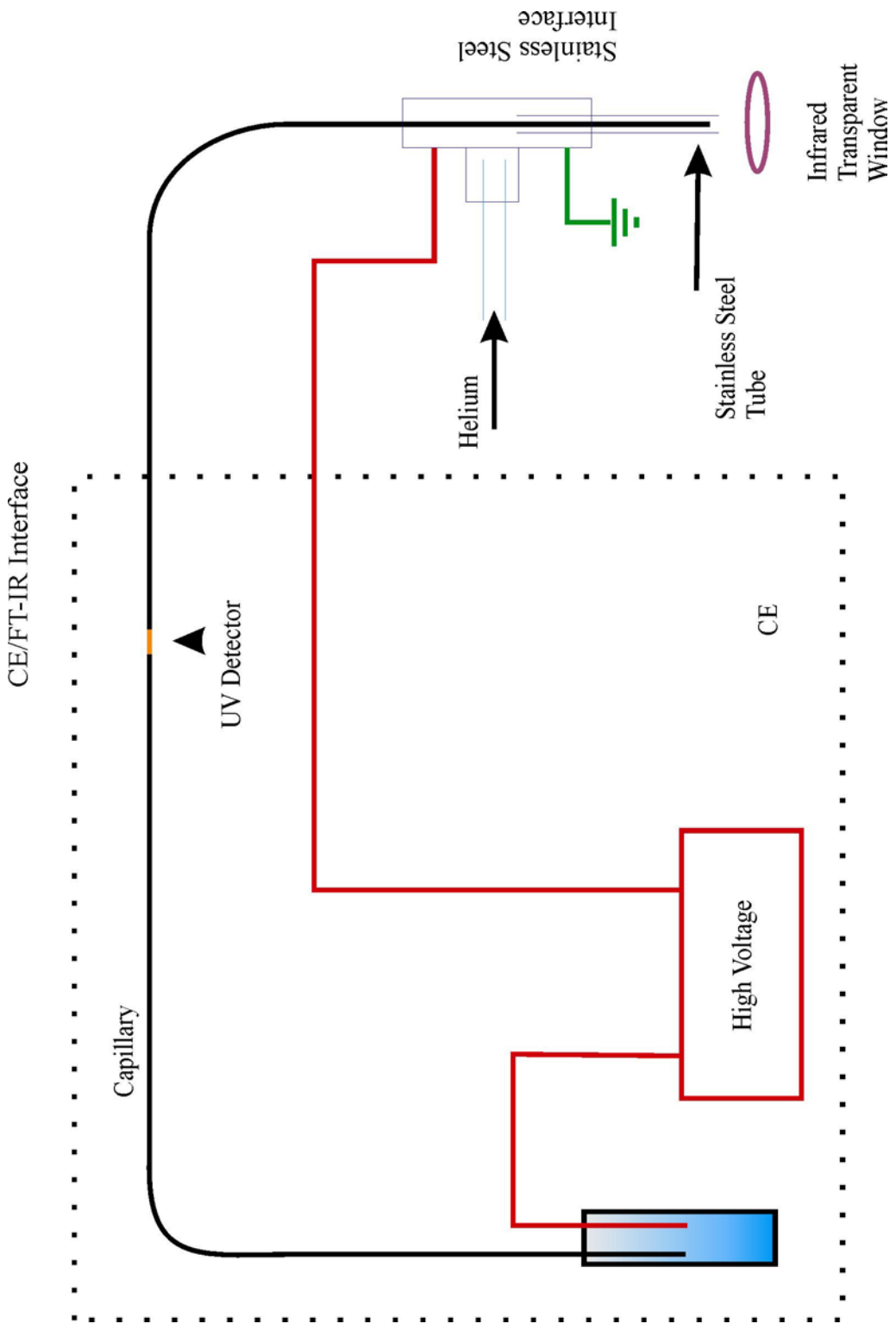
CE/FT-IR Interface
UV Detector
Capillary
CE
High Voltage
Helium
Stainless Steel
Tube
Infrared
Transparent
Window
Stainless Steel
Interface

Figure 2.3 UV electropherogram and CE current using the metal nebulizer CE/FT-IR interface. Sample: caffeine, salicylic acid, p-aminobenzoic acid, sodium benzoate, concentration: 1×10^{-3} M, voltage: 25 KV, electrolyte: 5.0×10^{-2} M ammonium acetate, detection wavelength: 214 nm. Column: 75 μm i.d., 110 cm long, CE/UV/FT-IR column. Nebulization: 12 psi sheath helium

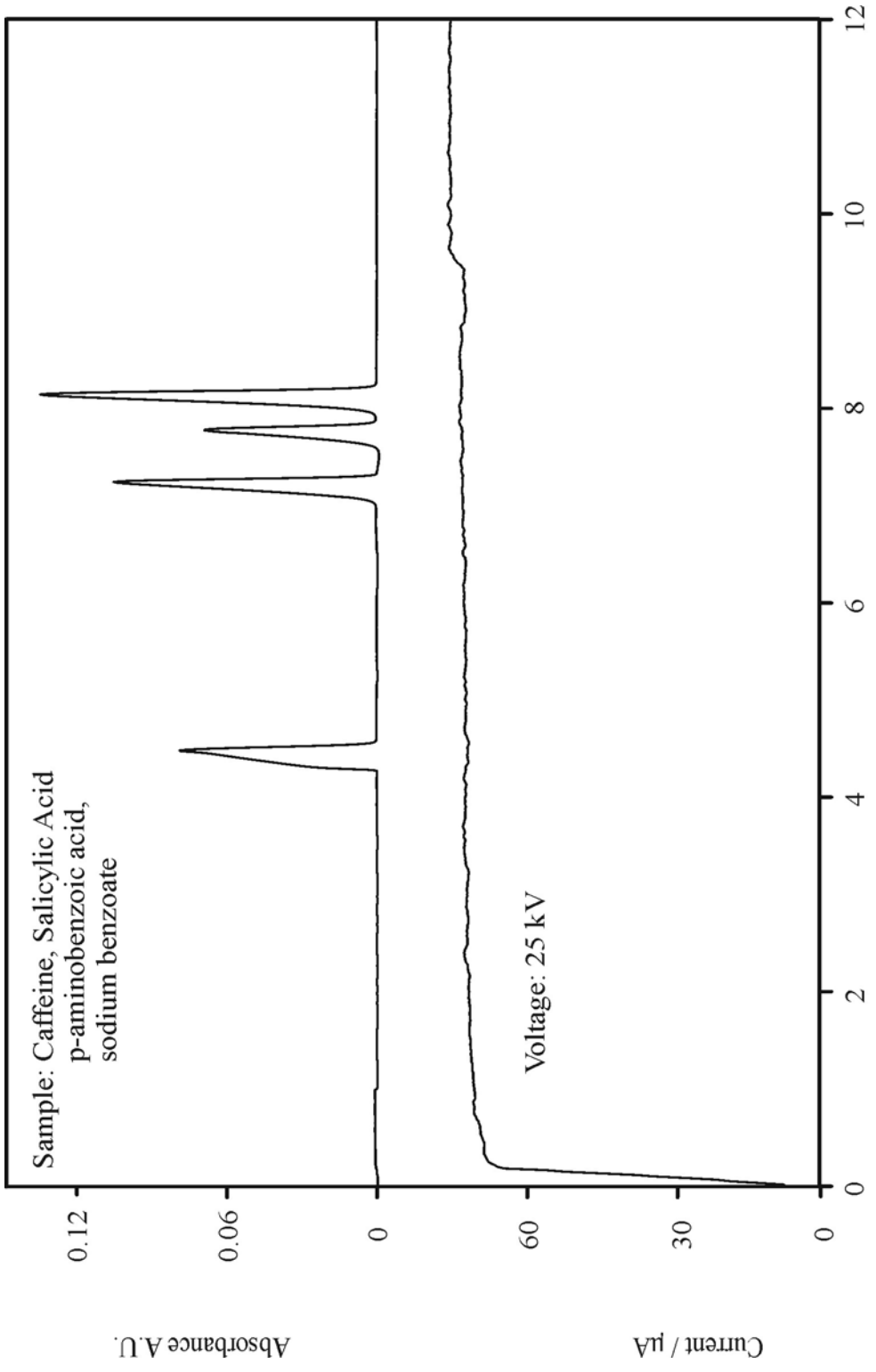
Sample: Caffeine, Salicylic Acid
p-aminobenzoic acid,
sodium benzoate
Voltage: 25 kV
Absorbance A.U.
Current / μA
Time / Min
0.12
0.06
0
60
30
0
0
2
4
6
8
10
12

is not maintained, and the separation is interrupted. One explanation for this is a backpressure is created when the helium is turned on before the high voltage has been applied. The helium gas will cause the solution to travel toward the inlet side of the column, thus there will be no liquid at the end of the column to make contact with the metal and form the electrical contact needed for electrophoresis.

A number of CE methods use either sodium borate or sodium phosphate electrolyte systems. These electrolyte systems, however, have strong IR absorbances, thus it is necessary to choose a system that is transparent in the infrared. Potassium chloride (KCl) was tested as a possible electrolyte system, however, the IR spectrum showed a very strong absorbance. The spectrum of the deposited potassium chloride was very similar to a spectrum taken of an evaporated solution of potassium hydroxide. It is understood that in solution, KCl will disassociate into K^+ ions and Cl^- ions. The K^+ ions will migrate toward the outlet side electrolyte (cathode) and form KOH with the OH^- ions from the water during nebulization and deposition. To try to alleviate this problem, volatile electrolyte systems such, as ammonium acetate, ammonium carbonate, ammonium hydroxide, and acetic acid, were used. The IR spectra of these electrolytic solutions show no evidence of band shifts due to adduct formation. Deposits of analytes from the volatile electrolytic solutions have a low residual absorbance of the electrolytes in the infrared, and they can be easily subtracted from the analyte spectra. There are residual absorbances because a minute quantity of the electrolyte is trapped within the deposit and is unable to evaporate. The residual absorbance from the electrolytic solutions was on the order of 0.05 absorbance units. Figure 4 shows a CE separation of a four component mixture in the presence of ammonium acetate, ammonium hydroxide, and borax (borate), respectively. The peak shapes seen in the NH_4Ac and NH_4OH electropherograms suggest that the column was overloaded by the mixture.

Figure 2.4 Comparison of UV electropherograms with volatile and electrolytes. Sample: caffeine, salicylic acid, p-aminobenzoic acid, and sodium benzoate, concentration: 1×10^{-3} M, Voltage: 15 kV, detection wavelength: 214 nm

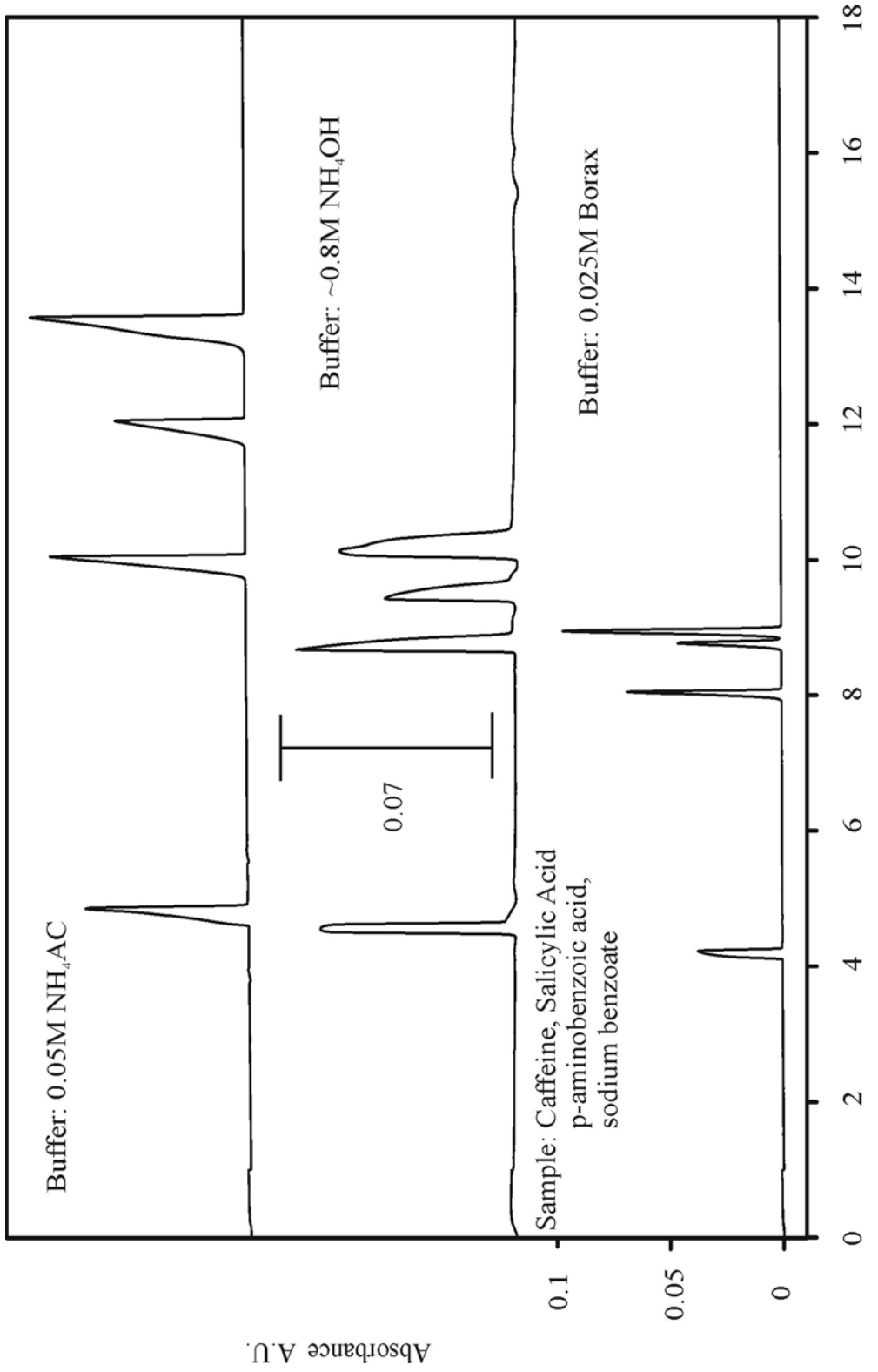
Buffer: 0.05M NH_4AC
Buffer: ~0.8M NH_4OH
Buffer: 0.025M Borax
0.07
Sample: Caffeine, Salicylic Acid
p-aminobenzoic acid,
sodium benzoate
Absorbance A.U.
0.1
0.05
0
0
2
4
6
8
10
12
14
16
18
Time / Min

As noted above, an important part of the stainless steel nebulizer is to maintain the electrical contact point at the end of the column. The solvent elimination process is aided by the use of helium sheath gas. Helium gas is needed to eliminate the solvent and deposit the analyte onto the ZnSe or CaF_2 window. If the flow rate is too high, the sample will splatter onto the surface. The window should be placed no more than 0.5 cm away from the nebulizer. The distance can vary by a few tenths of a centimeter and depends on the flowrate of the helium gas. If the window is held too far away, then the analyte will cover too great an area, and there is a possibility that the separated components will overlap. The window must be moved manually between deposits so that the components will not mix on the surface. Figures 5 and 6 show the CE/FT-IR deposit images of analytes with ammonium acetate electrolyte. Both deposits were made onto CaF_2 windows. Figure 6 shows that a poor choice of the electrolyte system can lead to an evaporation rate that is insufficient for solvent elimination before the analyte strikes the surface. The images of both deposits also displayed a great deal of splattering around the central deposit of interest. This splatter is due to the nebulizer design and lack of appropriate orifice. The orifice must be irregular to accommodate both contact with the electrolytic solution and to allow sheath gas to pass around the capillary. Provided subsequent depositions are made a reasonable distance apart there is no problem with cross contamination. The colored areas seen in the deposit in Figure 6 are interference patterns. These patterns are seen when a nonuniform surface is placed atop an optically flat surface. The change in radiation pathlength traveled causes these visible patterns to appear. These patterns can offer some information on the thickness of the deposits. The colors of the patterns lead to the conclusion that the deposits are on the order of the wavelength of visible radiation in thickness. That is, the deposits appear to be about 400 to 800 nm in thickness, but the deposits are not uniform, as shown by the range of values. These thickness variations in irreproducible deposits, and spectra from replicate deposits have varying absorbances. The deposit

Figure 2.5 CE/FT-IR deposit image. Sample: sodium benzoate, electrolyte: ammonium acetate, Deposit Size: ~200 μm

CE/FT-IR Deposit of Sodium Benzoate in NH_4AC

Figure 2.6 CE/FT-IR deposit image. Sample: p-aminobenzoic acid, electrolyte: ammonium acetate, Deposit size: ~200 μm

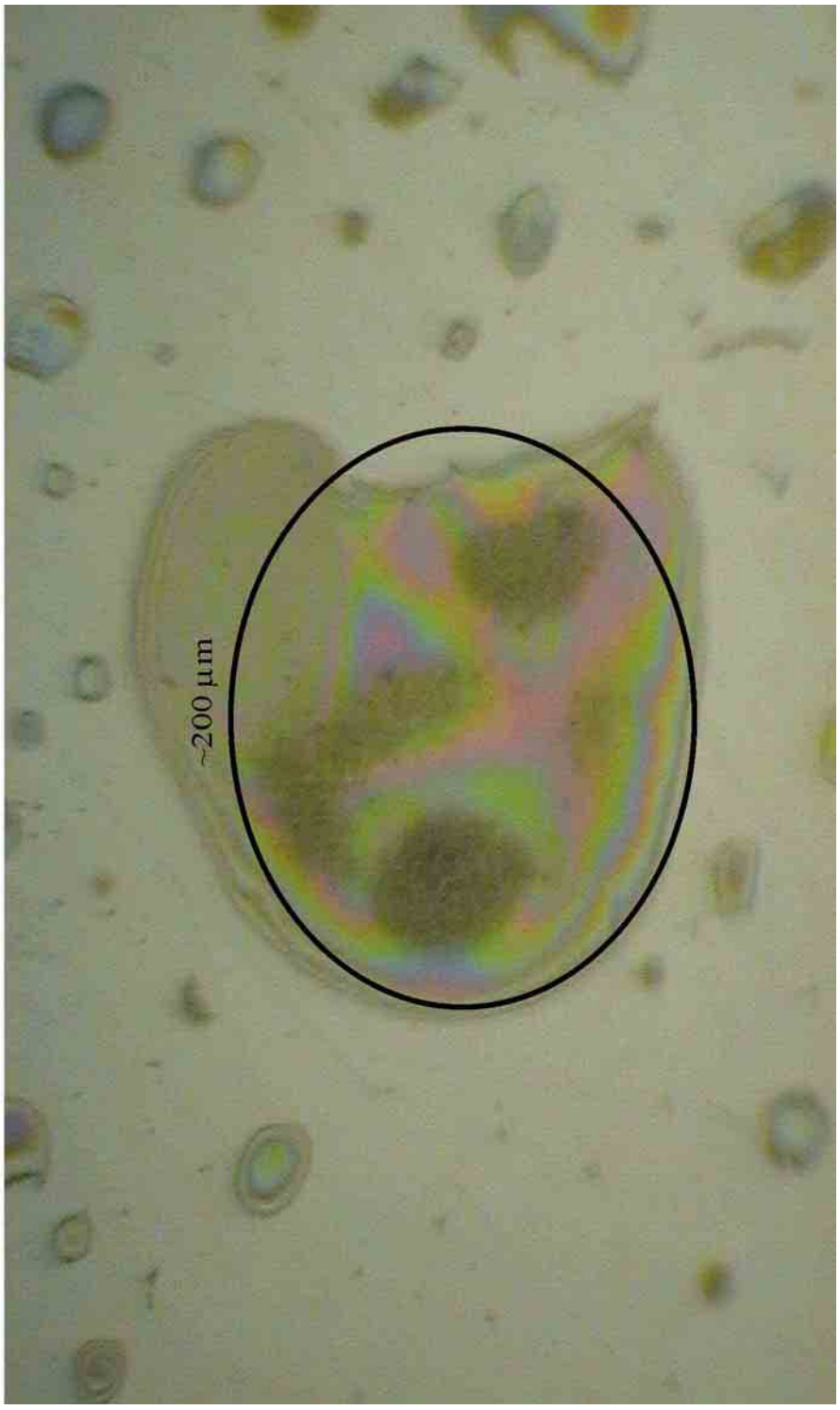

CE/FT-IR Deposit of p-Aminobenzoic Acid in NH_4AC

sizes varied from 100 to 200 μm in diameter, but with improvements in the design of the interface it should be possible to reduce the deposit sizes to 50 to 100 μm.

Spectra of the sample deposits were measured off-line with a Perkin Elmer *i*-series infrared microscope. All CE/FT-IR spectra were obtained in transmission with 100 co-added scans at a resolution of 4 cm^{-1}. For comparison, reference FT-IR spectra were collected with the infrared microscope by direct manual deposition of aqueous solutions. Figures 7 and 8 show the comparison between the CE/FT-IR spectra of GlcNAC and nicotinamide and their reference FT-IR spectra. The broadness, or increase in intensity, of some CE/FT-IR spectral bands (N-acetyl-D-glucosamine (GlcNAc), and nicotinamide) can be attributed to the fact that the samples were not sufficiently dry during the FT-IR scan and the interference patterns seen in the figures of the deposits.

In most cases, volatile electrolytic solutions, such as ammonium acetate and ammonium hydroxide, contribute little or no interference in the infrared spectra, thus spectral subtraction is not required. The CE/FT-IR spectra of acidic compounds, such as p-aminobenzoic acid (Figure 9) and acetylsalicylic acid (Figure 10), are very different from their respective direct deposition FT-IR spectra. It appears that the acidic compounds are ionized during the process of electrophoresis.

Figure 11 shows that spectra of caffeine can be obtained at a low nanogram level. The smallest quantity of caffeine deposited was 28 ng, yet the signal-to-noise ratio of the spectrum remains high. Under the current operating conditions the limit of detection is estimated to be less than 10 ng. The caffeine CE/FT-IR spectrum was run against a spectral library containing over 89,000 compounds and the first “hit” reported was for the structure of caffeine. This suggests that the spectra collected from the CE/FT-IR spectrometric interface are not affected by the choice of the volatile electrolytic solution.

Figure 2.7 N-Acetyl-D-glucosamine (GlcNAc) CE/FT-IR spectrum (electrolyte subtracted) and reference infrared spectrum. CE/FT-IR: 1.0×10^{-2} M GlcNAc, pressure injection: 5 seconds, voltage: 15 kV, electrolyte: 5.0×10^{-2} M NH_4Ac, column: 75 μm i.d. and 78 cm long. Reference infrared spectrum: GlcNAc aqueous solution deposited on a ZnSe window and dried

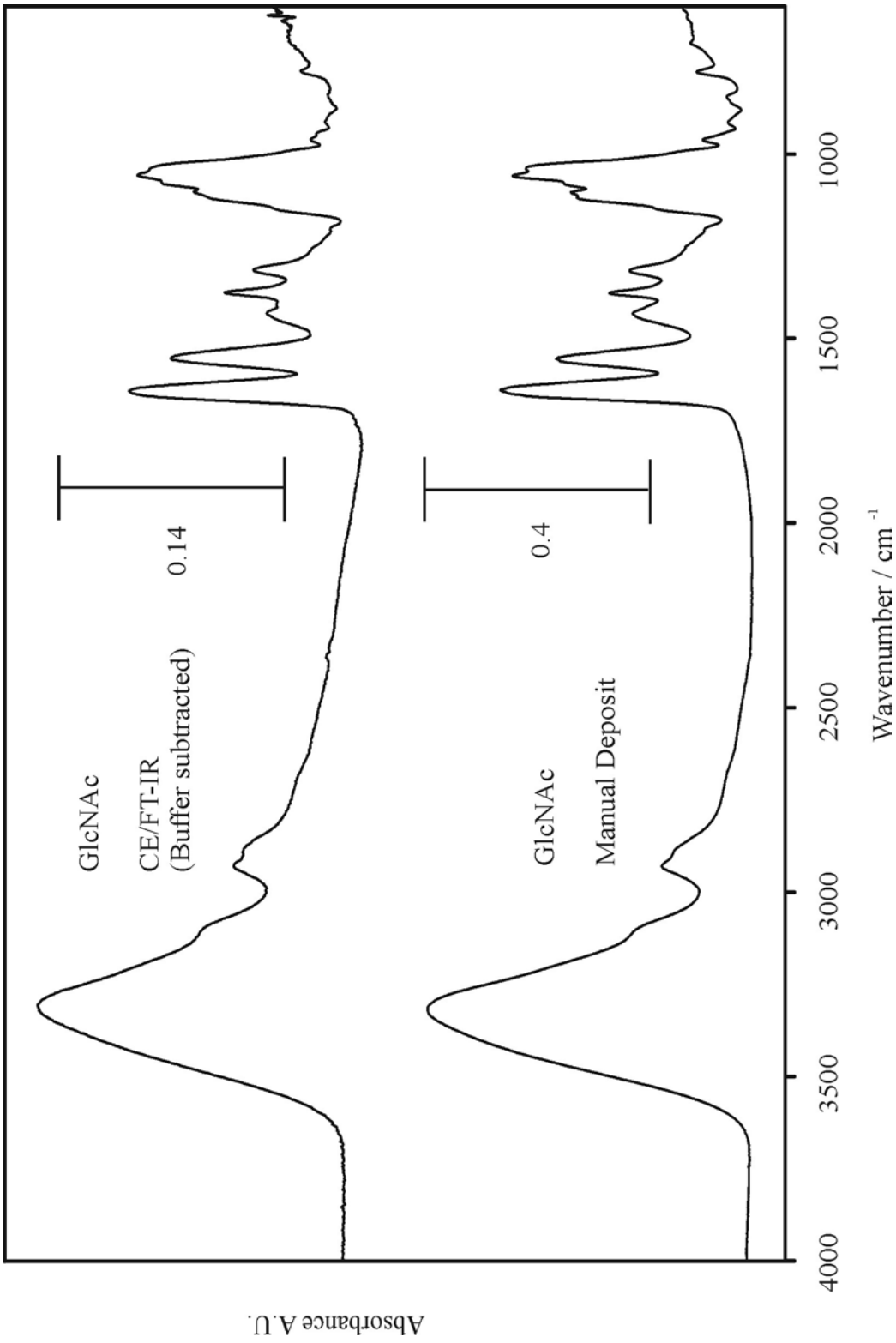
GlcNAc
CE/FT-IR
(Buffer subtracted)
0.14
GlcNAc
Manual Deposit
0.4
4000
3500
3000
2500
2000
1500
1000
Wavenumber / cm -1
Absorbance A.U.

Figure 2.8 Nicotinamide CE/FT-IR and reference infrared spectra. CE electrolyte: 5.0×10^{-2} M NH_4Ac

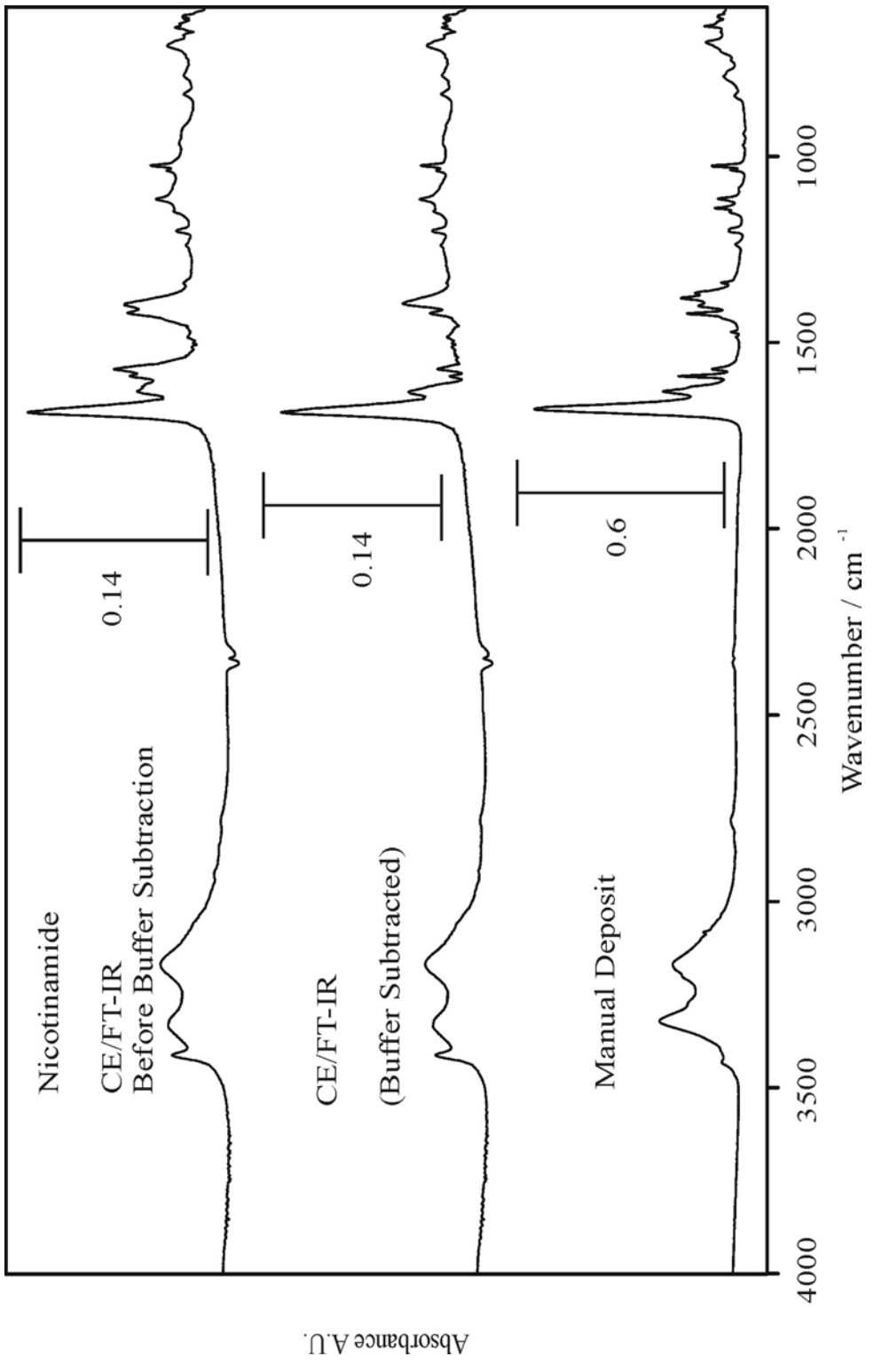
Nicotinamide
CE/FT-IR
Before Buffer Subtraction
0.14
CE/FT-IR
(Buffer Subtracted)
0.14
Manual Deposit
0.6
4000
3500
3000
2500
2000
1500
1000
Wavenumber / cm -1
Absorbance A.U.

Figure 2.9 p-Aminobenzoic acid CE/FT-IR and reference infrared spectra. CE electrolyte: 5.0×10^{-2} M NH_4Ac

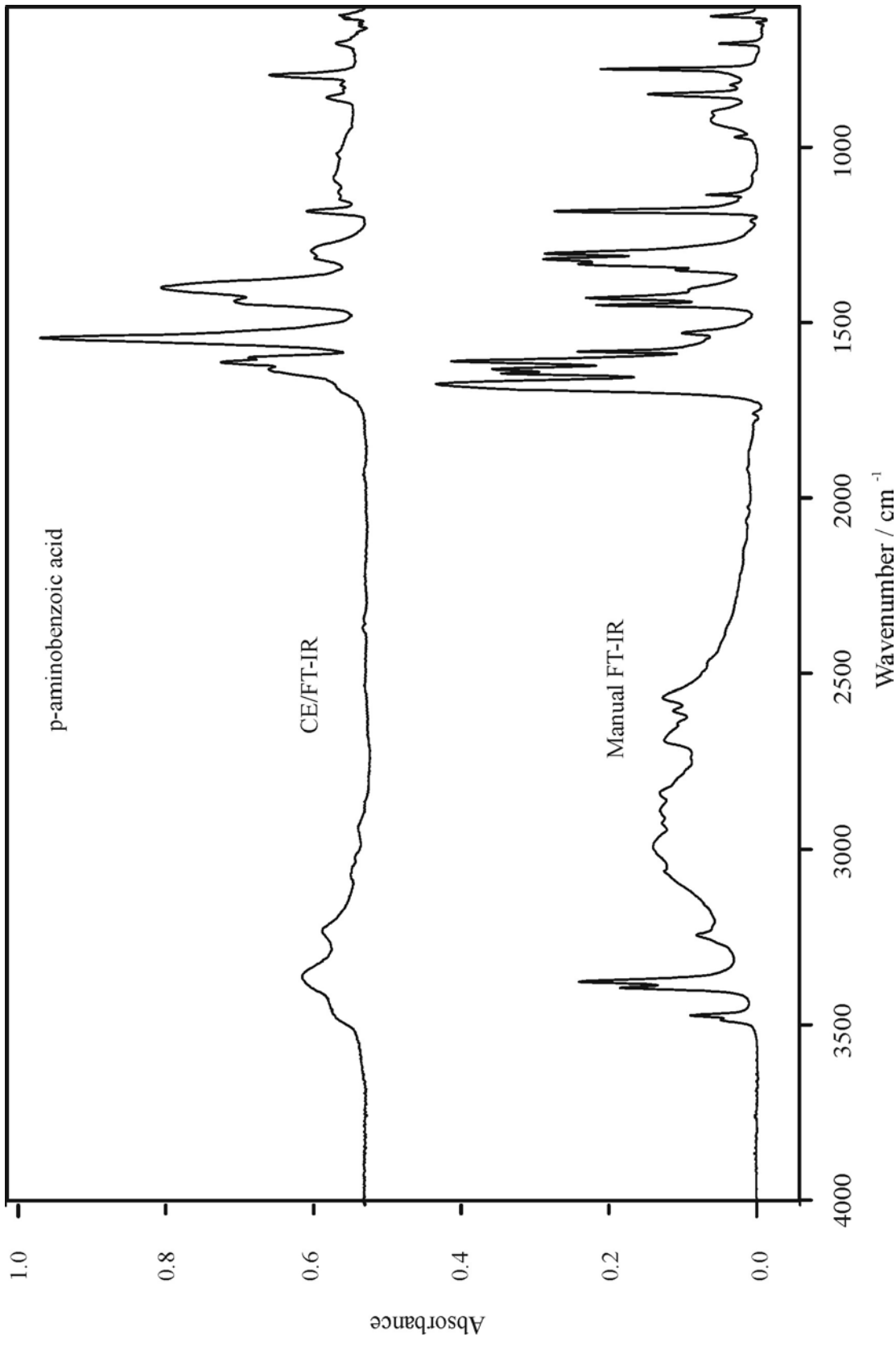
p-aminobenzoic acid
CE/FT-IR
Manual FT-IR
Absorbance
1.0
0.8
0.6
0.4
0.2
0.0
4000
3500
3000
2500
2000
1500
1000
Wavenumber / cm -1

Figure 2.10 Acetylsalicylic acid CE/FT-IR and reference IR spectra. electrolyte: 5.0×10^{-2} M NH_4Ac

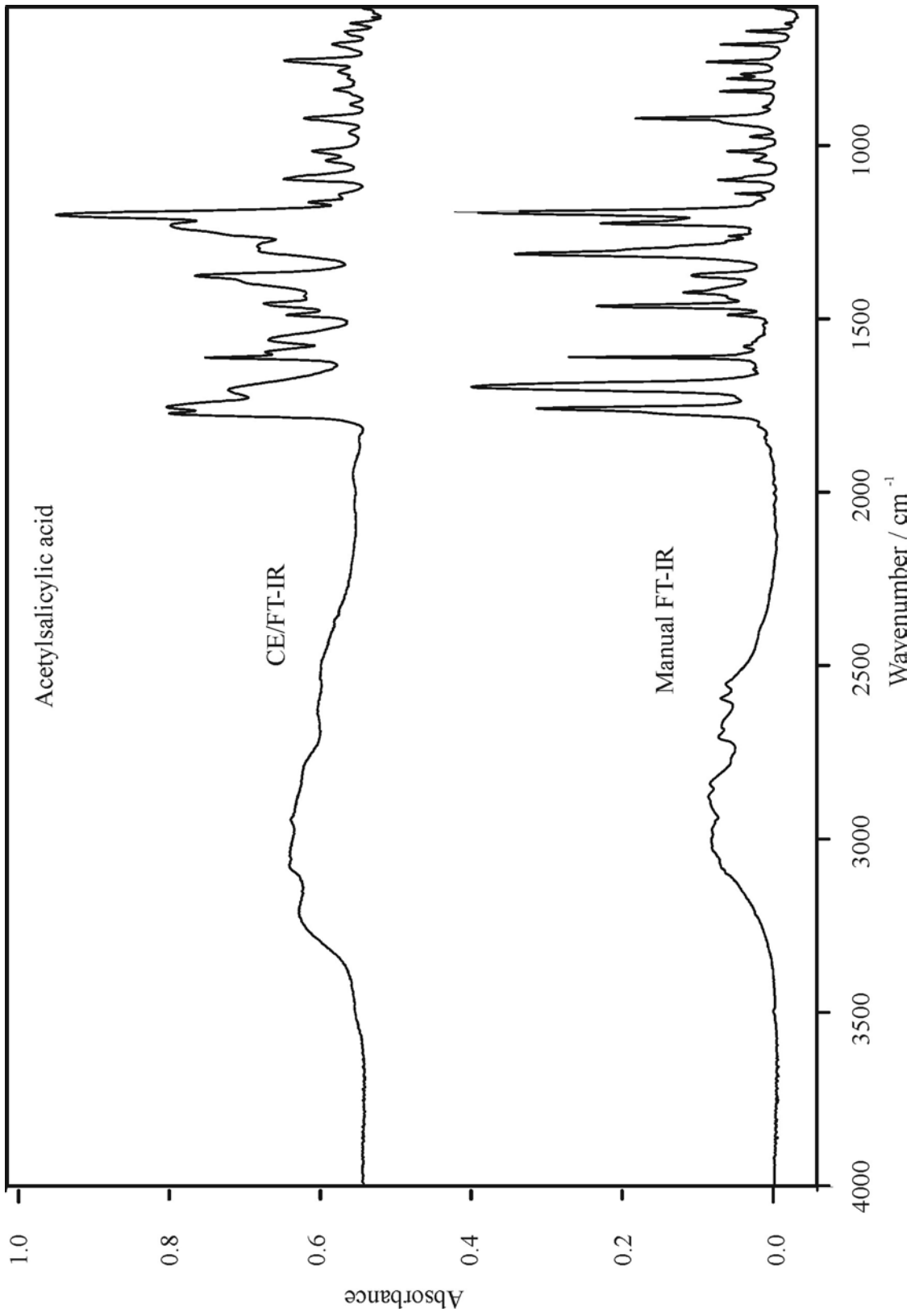
Acetylsalicylic acid
CE/FT-IR
Manual FT-IR
Absorbance
1.0
0.8
0.6
0.4
0.2
0.0
4000
3500
3000
2500
2000
1500
1000
Wavenumber / cm -1

Figure 2.11 Caffeine CE/FT-IR spectra with varying injection quantities and reference IR spectrum. Electrolyte: 5.0×10^{-2} M NH_4Ac

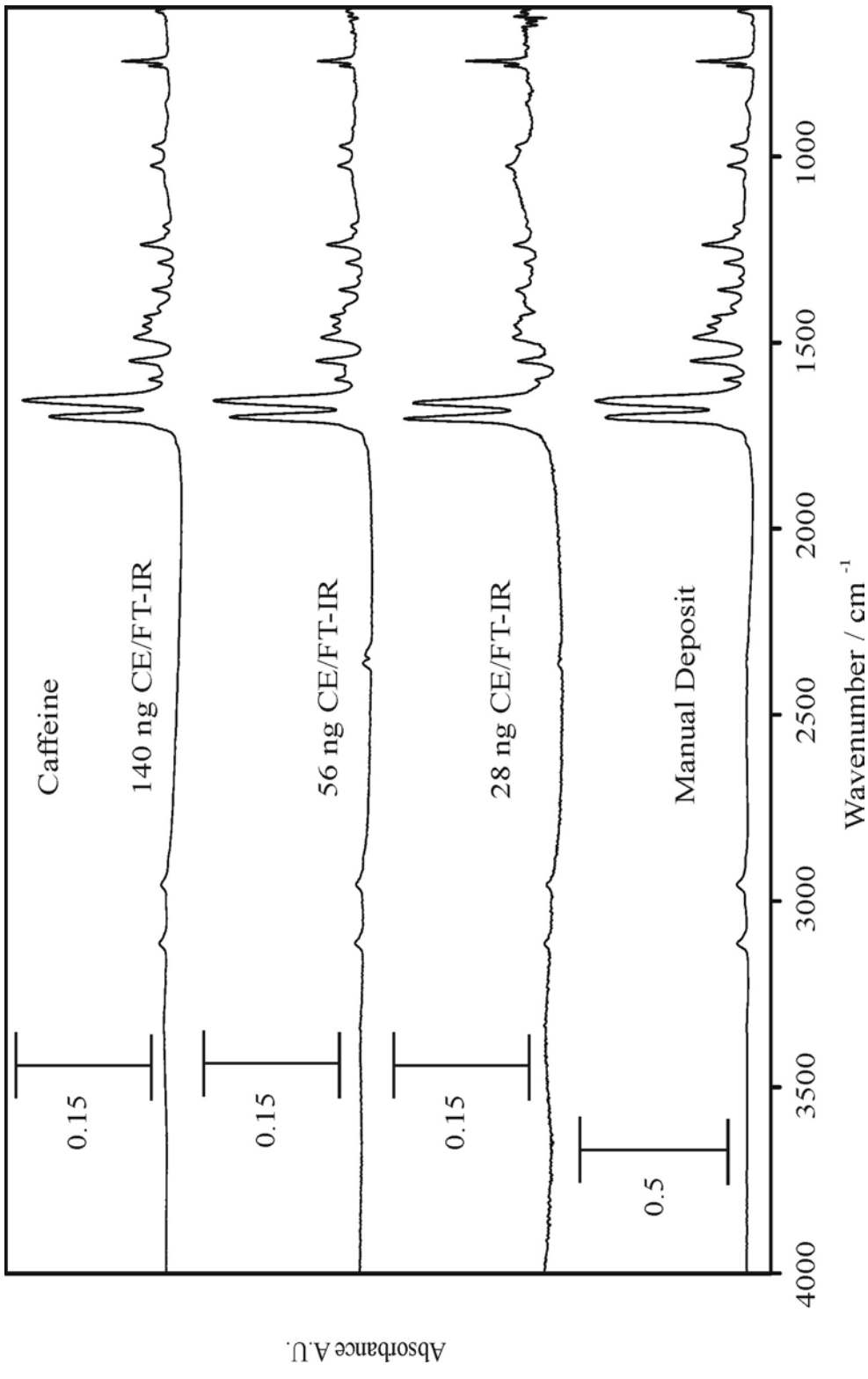
Caffeine
140 ng CE/FT-IR
56 ng CE/FT-IR
28 ng CE/FT-IR
Manual Deposit
0.15
0.15
0.15
0.5
4000
3500
3000
2500
2000
1500
1000
Wavenumber / cm -1
Absorbance A.U.

Conclusions

Our preliminary research has shown the feasibility of the stainless steel CE/FT-IR spectrometric interface. The ability to keep the electrical contact point at the end of the elongated column allowed for the consistent high resolving power of capillary electrophoresis. The process of desolvation and liquid jet formation does not appear to have caused any degradation or separation problems, despite the extremely low flow constraints of a CE system. From the infrared spectra collected from the deposits from the interface, there does not appear to be any contamination from other analytes present in the separation mixture. To help increase the "dryness" of the sample upon scanning, there is a need for a more volatile electrolyte system or a slower deposition rate. With the present interface, spectra of compounds at concentrations in the low nanogram level can be measured; however, it is projected that detection limits on the order of hundreds of picograms can be obtained. This will be possible when a more efficient interface is developed. When this can be accomplished the sample will be deposited in a smaller volume and the effective absorbance will increase.

It has been shown that the CE/FT-IR interface can successfully produce deposits for IR analysis. It has also been shown that the spectra obtained using the CE/FT-IR spectrometric interface match well with standard spectra. Work is in progress to improve the interface and extend its utility to other separation techniques. The interface is undergoing modifications that will reduce the area of the deposits, and it is projected that these modifications will produce deposition sizes of 50 to 100 μm in diameter. The deposit can theoretically be the same size as the inner diameter of the capillary column. The use of capillary electrochromatography (CEC) is also being investigated as a method for the separation of neutral compounds. It is planned to use the interface with CEC. The current interface is used as an off-line technique, nonetheless, future research is focused on the development of an at-line system, so that IR spectra can be obtained directly after deposition.

Acknowledgements

The authors would like to thank the University of Georgia Research Foundation (UGARF) and a National Institutes of Health Research Resource Grant (number 2P41-RR-05351) for financial support.

References

1. P. R. Griffiths and J. A. de Haseth *Fourier Transform Infrared Spectrometry* (John Wiley & Sons, New York, 1986), Chap. 18.

2. K. Krishnan, "Advances in Capillary Gas Chromatography-Fourier Transform Interferometry," in *Fourier Transform Infrared Spectroscopy : Applications to Chemical Systems*, J. R. Ferraro and L. J. Basile, Eds. (Academic Press, Orlando, 1985), Vol. 4, Chap. 3.

3. A. M. Haefner, K. L. Norton, P. R. Griffiths, S. Bourne, and R. Curbelo, Anal. Chem. **60,** 2441 (1988).

4. S. Bourne, A. M. Haefner, K. L. Norton, and P. R. Griffiths, Anal. Chem. **62,** 2448 (1990).

5. S. Bourne, G. T. Reedy, and P. T. Cunningham, J. Chromatogr. Sci. **17,** 460 (1979).

6. G. T. Reedy, S. Bourne, and P. T. Cunningham, Anal. Chem. **51,** 1535 (1979).

7. D. W. Vidrine and D. R. Mattson, Appl. Spectrosc. **32,** 502 (1978).

8. C. C. Johnson and L. T. Taylor, Anal. Chem. **56,** 2642 (1984).

9. R. M. Robertson, J. A. de Haseth, and R. F. Browner, Mikrochim. Acta **2,** 199 (1988).

10. V. E. Turula and J. A. de Haseth, Appl. Spectrosc. **48,** 1255 (1994).

11. V. E. Turula and J. A. de Haseth, Anal. Chem. **68,** 629 (1996).

12. V. E. Turula, R. T. Bishop, R. D. Ricker, and J. A. de Haseth, J. Chromatogr. A **763,** 91 (1997).

13. R. T. Bishop, V. E. Turula, and J. A. de Haseth, Anal. Chem. **68,** 4006 (1996).

14. R. T. Bishop, V. E. Turula, J. A. de Haseth, and R. D. Ricker, "Hyphenated HPLC Methodology for the Resolution and Elucidation of Peptides from Proteolytic Digests," in *Techniques in Protein Chemistry VIII*, D. R. Marshak, Ed. (Academic Press, San Diego, 1997), p.165.

15. J. de Haseth and R. Bishop, "Hypenated HPLC Methodology for the Resolution and Elucidation of Peptides from Proteoltic Digests", presented at the American Chemical Society, San Diego, CA (1997).

16. T. G. Venkateshwaran, J. T. Stewart, R. T. Bishop, J. A. de Haseth, and M. G. Bartlett, J. Pharm. Biomed. Anal. **17,** 57 (1998).

17. T. G. Venkateshwaran, J. T. Stewart, J. A. de Haseth, and M. G. Bartlett, J. Pharm. Biomed. Anal. **19,** 709 (1999).

18. D. Kuehl and P. R. Griffiths, J. Chromatogr. Sci. **17,** 471 (1979).

19. C. M. Conroy, P. R. Griffiths, P. J. Duff, and L. V. Azarraga, Anal. Chem. **56,** 2636 (1984).

20. A. J. Lange, P. R. Griffiths, and D. J. J. Fraser, Anal. Chem. **63,** 782 (1991).

21. V. F. Kalasinsky, K. G. Whitehead, R. C. Kenton, J. A. S. Smith, and K. S. Kalasinsky, J. Chromatogr. Sci. **25,** 273 (1987).

22. A. M. Robertson, D. Littlejohn, M. Brown, and C. J. Dowle, J. Chromatogr. **588,** 15 (1991).

23. J. J. Gagel and K. Biemann, Anal. Chem. **58,** 2184 (1986).

24. J. J. Gagel and K. Biemann, Anal. Chem. **59,** 1266 (1987).

25. C. Fujimoto, K. Jinno, and Y. Hirata, J. Chromatogr. **258,** 92 (1983).

26. G. W. Somsen, L. P. P. Vanstee, C. Gooijer, U. A. T. Brinkman, N. H. Velthorst, and T. Visser, Anal. Chim. Acta **290,** 269 (1994).

27. G. W. Somsen, E. W. J. Hooijschuur, C. Gooijer, U. A. T. Brinkman, N. H. Velthorst, and T. Visser, Anal. Chem. **68,** 746 (1996).

28. J. L. Dwyer, A. E. Chapman, and X. Liu, LC-GC **13,** 240 (1995).

29. M. W. Raynor, K. D. Bartle, and B. W. Cook, J. High Resolut. Chromatogr. **15,** 361 (1992).

30. G. W. Somsen, C. Gooijer, N. H. Velthorst, and U. A. T. Brinkman, J. Chromatogr. A **811,** 1 (1998).

31. R. Fuoco, S. L. Pentoney, and P. R. Griffiths, Anal. Chem. **61,** 2212 (1989).

32. K. L. Norton and P. R. Griffiths, J. Chromatogr. A **703,** 503 (1995).

33. G. W. Somsen, R. J. Vandenesse, C. Gooijer, U. A. T. Brinkman, N. H. Velthorst, T. Visser, P. R. Kootstra, and A. Dejong, J. Chromatogr. **552,** 635 (1991).

34. P. R. Griffiths and A. J. Lange, J. Chromatogr. Sci. **30,** 93 (1992).

35. A. J. Lange and P. R. Griffiths, Appl. Spectrosc. **47,** 403 (1993).

36. M. X. Liu and J. L. Dwyer, Appl. Spectrosc. **50,** 349 (1996).

37. J. Jorgenson and K. Lukacs, J. Chromatogr. **218,** 216 (1981).

38. J. Jorgenson and K. Lukacs, Anal. Chem. **53,** 1302 (1981).

39. T. W. Garner and E. S. Yeung, J. Chromatogr. **515,** 639 (1990).

40. M. Li and M. D. Morris, "Capillary Electrophoresis of Nucleosides with Real-Time Raman Spectroscopy Detection", presented at the Pittsburgh Conference on Analytical Chemistry and Applied Spectroscopy, Atlanta, Georgia (1997).

41. R. D. Smith, C. J. Barinaga, and H. R. Udseth, Anal. Chem. **60,** 1948 (1988).

42. W. M. A. Niessen, U. R. Tjaden, and J. Vandergreef, J. Chromatogr. **636,** 3 (1993).

43. J. W. Olesik, J. A. Kinzer, and S. V. Olesik, Anal. Chem. **67,** 1 (1995).

44. D. Wycherley, M. E. Rose, K. Giles, and D. Rimmer, "Biochemical and Environmental Applications of On-Line Capillary Electrophoresis and Electrospray Mass Spectrometry", Micromass UK Ltd, Cheshire, UK, No. 209.

CHAPTER 3

A GLASS NEBULIZER CAPILLARY ELECTROPHORESIS/FT-IR SPECTROMETRIC INTERFACE [1]

[1]Todebush, R.A.; J.A. de Haseth. 2001. To be submitted to *Applied Spectroscopy*.

Abstract

An improved capillary electrophoresis/Fourier transform infrared (CE/FT-IR) spectrometric interface has been designed in our lab. The interface consists of an inner glass capillary into which the CE column is inserted and a flow of helium around the capillary that helps to move the analyte toward the deposition surface. There is an outer glass capillary that holds the inner glass and a flow of nitrogen that assists with droplet formation and containment of the deposit. A solvent elimination approach is used in the design of the nebulizer, so that the analytes are deposited onto an infrared transparent window, which is made of CaF_2, and measured with an infrared microscope. This interface has a number of advantages over the original CE/FT-IR spectrometric interface reported by this laborotory: Electrical contact is made from the tip of the capillary thus allowing for a more streamline design, a second flow of gas has been introduced to help with containment of the deposit, and the tip of the newly designed interface is concentric with the flow gas which helps to produce a circular deposit.

Introduction

An important tool in the study of biological molecules is Fourier transform infrared (FT-IR) spectroscopy. This technique has been used with a number of different separation and deposition interfaces for over two decades. These interfaces include gas chromatography/Fourier transform infrared (GC/FT-IR) spectrometry[1,1-6] and supercritical fluid chromatography (SFC).[7,8] A high performance liquid chromatography/FT-IR (HPLC/FT-IR) interface has been developed and used in our laboratory for a number of years[9-17] and a number of different designs have been used by other research groups.[18-30] The method of choice for sample deposition and analysis is direct deposition. This method has been used with electrospray,[29] concentric flow nebulization,[20,23,24,29,31-33] and particle beam desolvation.[9-17]

Since the development of capillary electrophoresis (CE) in the early 80's, it has enjoyed success as a rapid and efficient separation technique.[34,35] CE is based upon the concept that when a voltage is placed across a small diameter fused-silica column, analytes with differing electrophoretic mobilities can be separated. There is a number of advantages to the use of capillary electrophoresis over other separation techniques. First, the capillaries allow for fast heat dissipation and thus a high separation voltage can be employed. Second, the volumes of samples, waste, and buffers are orders of magnitude less then other separation techniques. Third, small inner diameter capillaries and increased detection sensitivity allows for smaller sample amounts then used in many LC separations. These advantages have allowed CE to become a useful tool in the separation of biological molecules including saccharides, monosaccharides, oligosaccharides, and carbohydrates.[36,36-47] Under normal operation CE uses UV and fluorescence detection. Both the sugars and carbohydrates do not absorb strongly in these regions of the spectrum, thus methods such as chemical derivatization are often used. Another problem faced with saccharide separation is that they are not easily ionized once in solution. This problem can often be addressed by the use of a borate

electrolytic solution system, which helps to ionize the neutral saccharides and carbohydrates.[48-50]

To increase the usefulness of capillary electrophoresis, it has been combined with a number of different types of spectrophotometric detection techniques. These techniques include laser induced fluorescence (LIF),[49] Raman spectrometry,[51] inductively coupled plasma mass spectrometry (ICP-MS)[52] and mass spectrometry (MS).[53,54] MS has seen the greatest increase of use since it was first interfaced with CE in the late eighties.[53,55-60] This detection method also suffers from the inability to distinguish between steroisomers of mono- and oligosaccharides. It was from this need of a powerful detection method for underivatized saccharides and carbohydrates that the first CE/FT-IR interface was designed.[61]

The feasibility of this new design had to meet the same three criteria that the original design met. First, the electrical contact point has to be maintained at the end of the capillary column. This ensures that the formation of a stable current will help to produce reproducible separations. Second, the size of the deposit needs to be as small as possible to help increase the sensitivity of the spectrometric analysis. Lastly, an electrolytic system must be used that will not interfere in the infrared region of the spectrum yet it must be volatile enough so that the resulting analyte is neat and not contaminated by the electrolyte. The glass nebulizer CE/FT-IR spectrometric interface successfully meets all three of these criteria.

Experimental

Chemical Reagents. The following buffers were used in separate experiments: ammonium formate (NH_4CO_2H), ammonium acetate ($CH_3CO_2NH_4$) (Fisher Scientific, Atlanta, GA); ammonium carbonate ($(NH_4)_2CO_3$), acetic acid (CH_3CO_2H), ammonium hydroxide (NH_4OH), sodium phosphate ($NaH_2PO_4 \cdot H_2O$) (Baker, Phillipsburg, NJ);

sodium borate ($Na_2B_4O_7 \cdot 10\ H_2O$, Sigma, St. Louis, MO), and potassium hydroxide (KOH) (EM Scientific, Gibbstown, NJ). All were used as received.

The concentrations of the buffers varied between 0.8 M and 1.25×10^{-3} M, depending upon the experimental parameters. All of the buffers were prepared in an aqueous solution of 18.0 MΩ deionized water. The deionized water was prepared with a Barnstead Nano ultrapure H_2O system.

The following samples were used to test the stability of the interface: p-aminobenzoic acid, acetylsalicylic acid (Aldrich, St. Louis, MO); sodium benzoate, N-acetyl-D-glucosamine (GlcNAc), N-acetyl-D-galactosamine (GalNAc), D-Mannose (Man), N-acetyl-D-Neuraminic Acid (NANA), D-Glucose (Glc), and nicotinamide (Sigma, St Louis, MO); caffeine, potassium chloride, and salicylic acid (Baker, Phillipsburg, NJ). The solutions were prepared with 18 MΩ water. The final concentrations of the solutions varied from 5.0×10^{-2} M to 1×10^{-3} M.

The samples were deposited onto zinc selenide (ZnSe) or calcium fluoride (CaF_2) (Spectral Systems, Hopewell Junction, NY) crystals.

Capillary Electrophoresis and FT-IR Spectrometry Microscope. A Beckman P/ACE 5000 system capillary electrophoresis instrument (Beckman, Fullerton, CA) equipped with a P/ACE UV absorbance filter detector was used to separate the samples of interest. The system was controlled with Beckman System Gold™ software. CE/FT-IR spectra were collected with the use of a Perkin-Elmer Spectrum 2000 FT-IR spectrometer (Perkin-Elmer, Connecticut, USA). The spectrometer was coupled with a Perkin-Elmer *i*-series FT-IR microscope. The microscope was configured with a mercury cadmium telluride (MCT) detector cooled with liquid nitrogen, and an adjustable limiting aperture. The aperture allows for the beam to be restricted from 10 to 400 μm in diameter depending on the sample deposit size. The spectra were collected with PE Image™ software. Spectral manipulations, such as digital

subtraction, baseline correction, and normalization were calculated with the use of GRAMS™ software (Galactic Industries, Salem, NH).

Fused silica capillaries (Polymicro Technologies, Phoenix, AZ), with an outer diameter of 360 μm and inner diameters of 75 μm and 48 μm, were used. The length of the capillary column varied from 78 cm to 160 cm. The distance between the inlet side and the UV detector was maintained at 50 cm.

Glass Nebulizer. A glass nebulizer was designed (J.E. Meinhard, Santa Ana, CA) and coupled to the CE system with a male tee (Upchruch, Oak Harbor, WA) through which the CE capillary was inserted and a flow of helium was introduced. The helium flow was controlled manually. The CE column was fed through the interface to the tip of the inner glass capillary. Electrical contact was made through the silver paint, which coated the last 20 cm of the CE capillary, was obtained from Ernest Fullam (Latham, NY). A flow of nitrogen gas was introduced through a tubing connector (Swagelok, Solon, OH) into the outer glass capillary and was controlled manually. A lamp was placed above the deposit surface to help with evaporation of the deposited sample

Results and discussion

Normal capillary electrophoretic analysis involves the movement of a charged analyte along a column with an applied voltage. The movements of the analytes depend on relative sizes and charges. Under standard operating conditions, a high positive potential, with respect to the outlet potential, is placed upon the inlet side and both ends of the capillary are immersed in electrolytic buffer solutions. To design and create a usable CE/FT-IR spectrometric interface, a number of conditions have to be met. The requirements include moving the outlet of the CE column and the electrical contact from the electrolytic solution reservoir to the outside of the instrument, and employing a

volatile electrolytic solution system that will not interfere in the mid-IR region of the spectrum. The original design[61] met all of these conditions, but there was room for improvement. The deposits that were obtained from this design were not very circular and uniform in thickness, which made spectrometric scans difficult.

As with the original interface, the CE column had to be extended up to 80 cm from the normal outlet electrode in order to accommodate the interface. The first major design improvement for the glass nebulizer involved the method in which electrical contact was maintained. The first design placed the outlet of the CE column in contact with a stainless steel tube. The use of glass prohibited using this type of electrical connection, thus a new method was needed. In CE/MS, a commonly used method to maintain electrical contact is to coat the tip of the capillary column with a conductive metal, such as silver paint. Similarly, the CE column used with the glass nebulizer was coated with silver paint. The paint was applied with a brush and covered approximately 20 cm of the end of the column. With the silver paint in contact with the effluent from the column, the electrical contact point is maintained at the end of the capillary column. This type of connection provides a stable electrical current throughout the separation. It should be noted that the silver paint degrades and has to be reapplied after approximately 30 runs. To determine the paint condition, a standard mixture was analyzed to see if there is problem with current stability throughout the run. A large change in the current over the course of the analysis may have signaled it was time to reapply the silver paint to the column. Figure 1 shows a diagram of the glass nebulizer CE/FT-IR spectrometric interface.

The next major improvement was the design of the tip of the glass CE/FT-IR spectrometric interface. The tip of the stainless steel spectrometric interface had to be constructed to allow the end of the capillary column to come in contact with the stainless steel tube. This did not provide a concentric circular exit for the effluent from the interface. This caused the deposits to be nonuniform in shape, size and thickness

Figure 3.1 Glass nebulizer CE/FT-IR interface. The ground potential is connected to the CE column ~20 cm from the outlet coated with silver paint

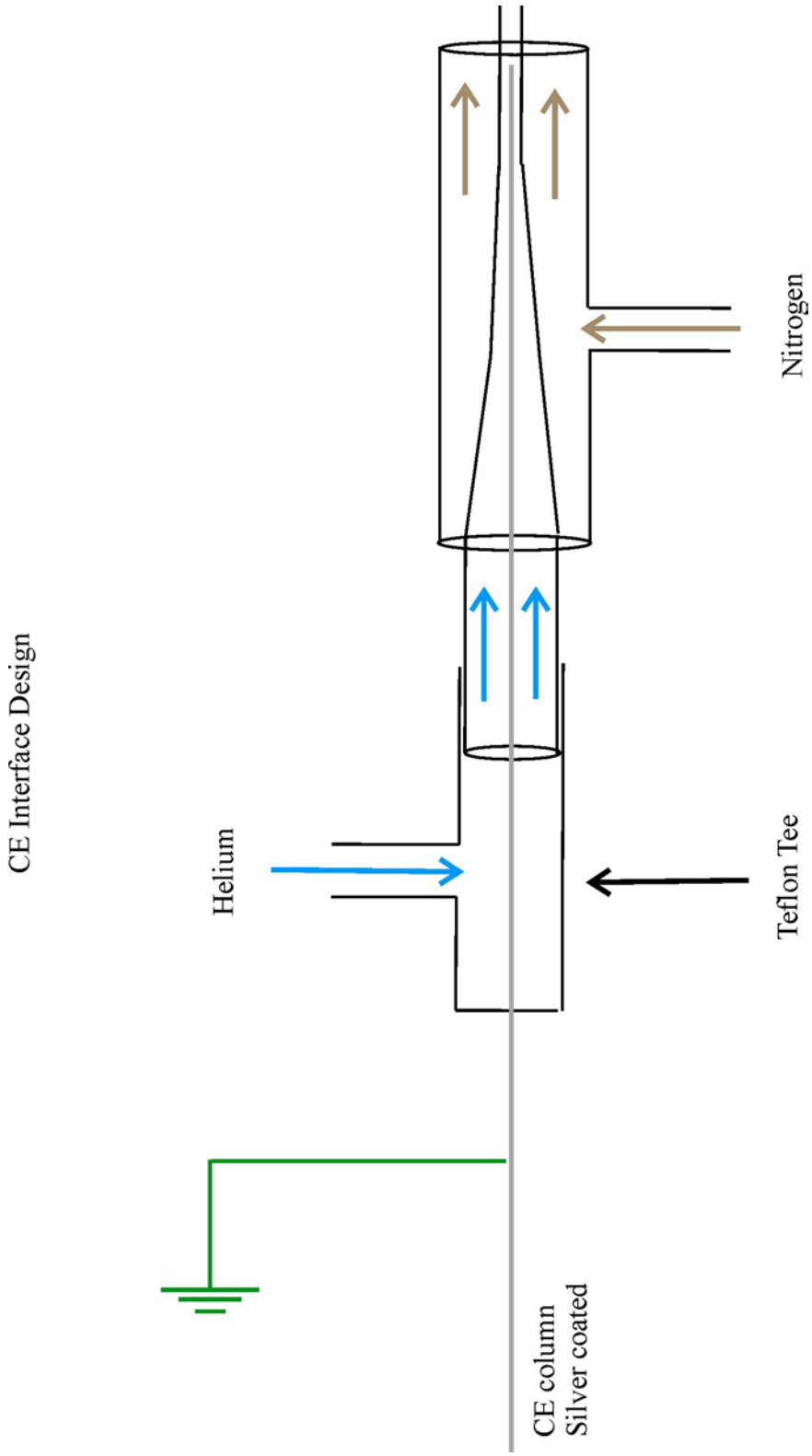
CE Interface Design
Helium
Nitrogen
Teflon Tee
CE column
Silver coated

and often resulted in deposit splatter. Figure 2 shows a diagram of the stainless steel interface tip. The thickness problems were easily seen in the form of interference patterns within the deposits that were obtained from the interface.[61] Changes in deposit thickness can lead to spectrometric errors, primarily associated with the reproducibility of the measurements. The glass nebulizer tip consisted of a series of concentric circles. Figure 3 shows a diagram of the glass interface tip. The tip has an inner glass capillary that holds the capillary column and allows for a flow of helium gas to move around the outside of the column. There is a larger outer glass capillary which houses the inner glass capillary and helps to provide a flow of nitrogen. The helium flow helps to produce the nebulization and evaporation of the analyte/electrolytic solution, while the nitrogen gas flow helps to direct and contain the deposit to the smallest area possible. This improved design provided uniform deposit sizes and shapes, which helps with the spectrometric analysis. With the glass CE/FT-IR spectrometric interface, the IR transparent window is placed roughly 1.0 cm away from the end of the nebulizer. This distance is due to the extra flow of gas that was added to the nebulizer. If the window is too close, the deposit will hit the surface to hard and splatter. If the window is too far away it is difficult to control deposit placement. Figures 4 and 5 show deposits that were produced using the glass CE/FT-IR spectrometric interface. Figure 4 shows a pure borate electrolytic solution deposit that is approximately 200 μm in diameter. Figure 5 is a sample of caffeine that eluted from an ammonium acetate electrolytic solution system. As seen in Figure 4 the caffeine deposit is approximately 200 μm in diameter. Both of the figures had to be digitally enhanced so they could be seen using the FT-IR microscope. The darkened edges were added to provide an outline of the deposit and provide some definition to the deposits.

As stated above, one of the major problems with the interface is the electrical contact point. If the contact point is somewhere other than the outlet end of the capillary column, there will be a loss of separation and the flow of the effluent from the

Figure 3.2 Metal nebulizer CE/FT-IR interface. The tip of the metal tube is not a concentric circle and thus produces deposits that are nonuniform in shape and size

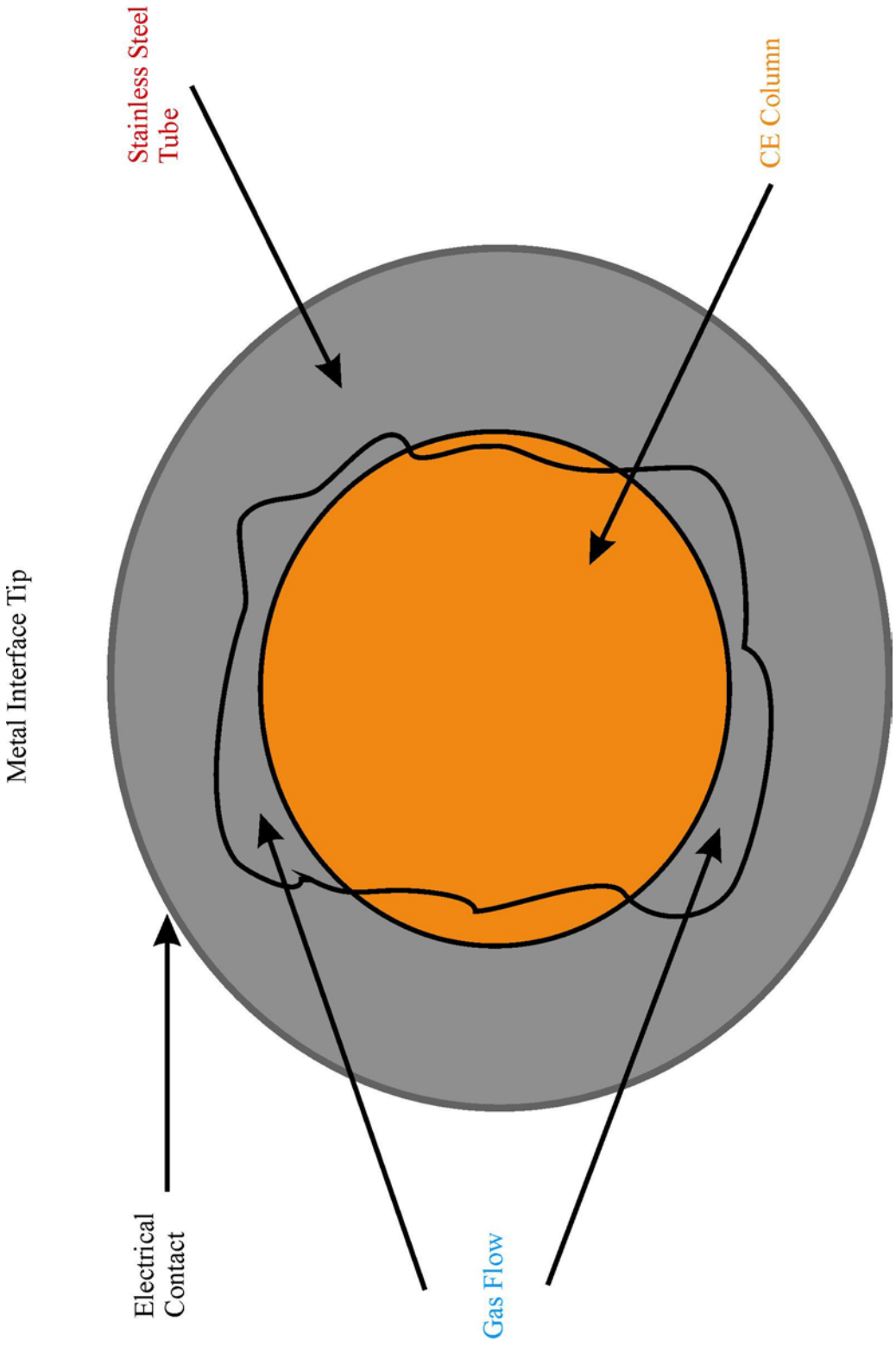
Stainless Steel Tube
CE Column
Metal Interface Tip
Electrical Contact
Gas Flow

Figure 3.3 Glass nebulizer CE/FT-IR interface tip. Concentric circles help with the deposit size and shape

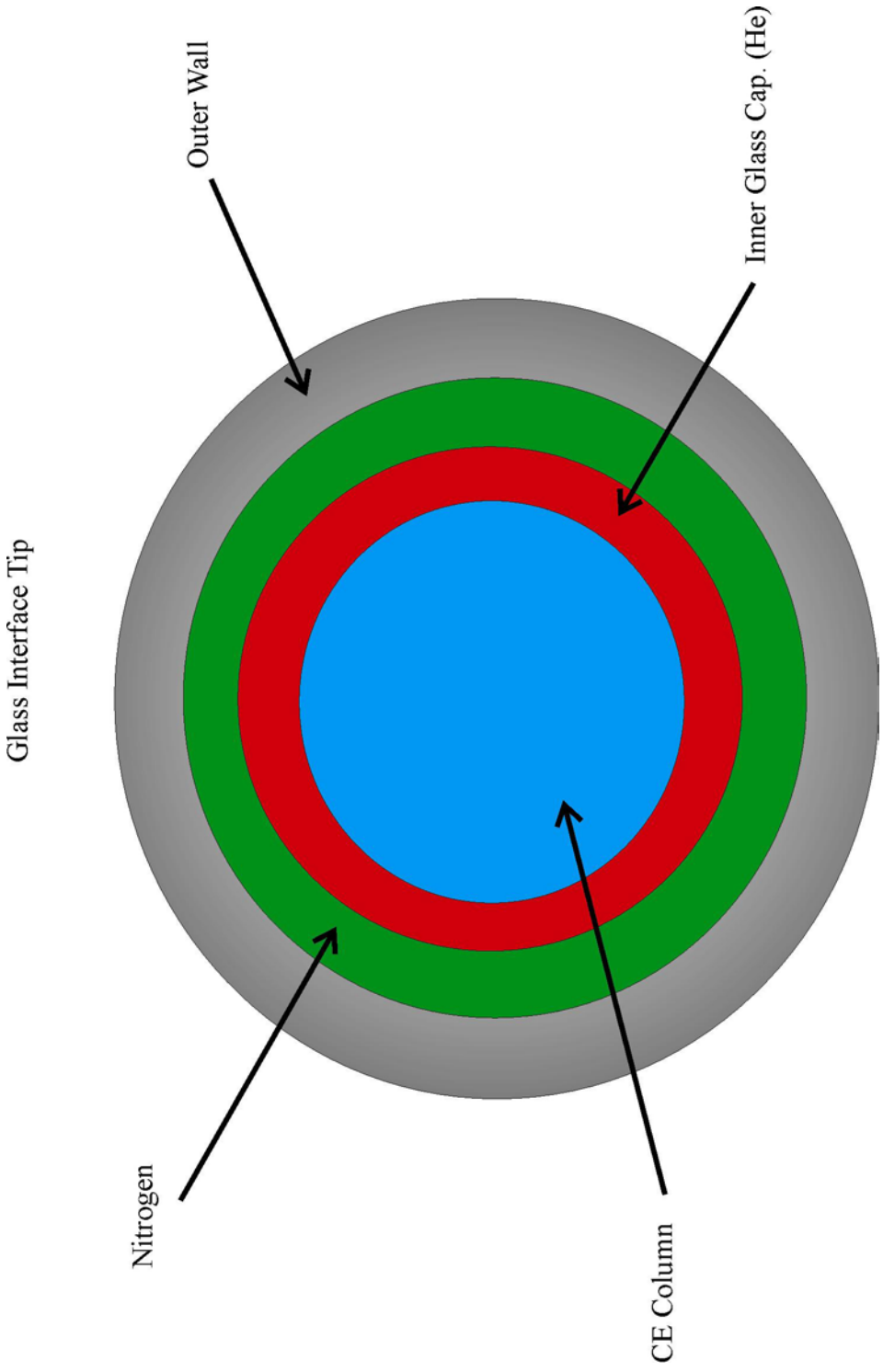
Outer Wall
Inner Glass Cap. (He)
Glass Interface Tip
Nitrogen
CE Column

Figure 3.4 CE/FT-IR deposit image. Borate electrolyte, Deposit size : ~200 μm

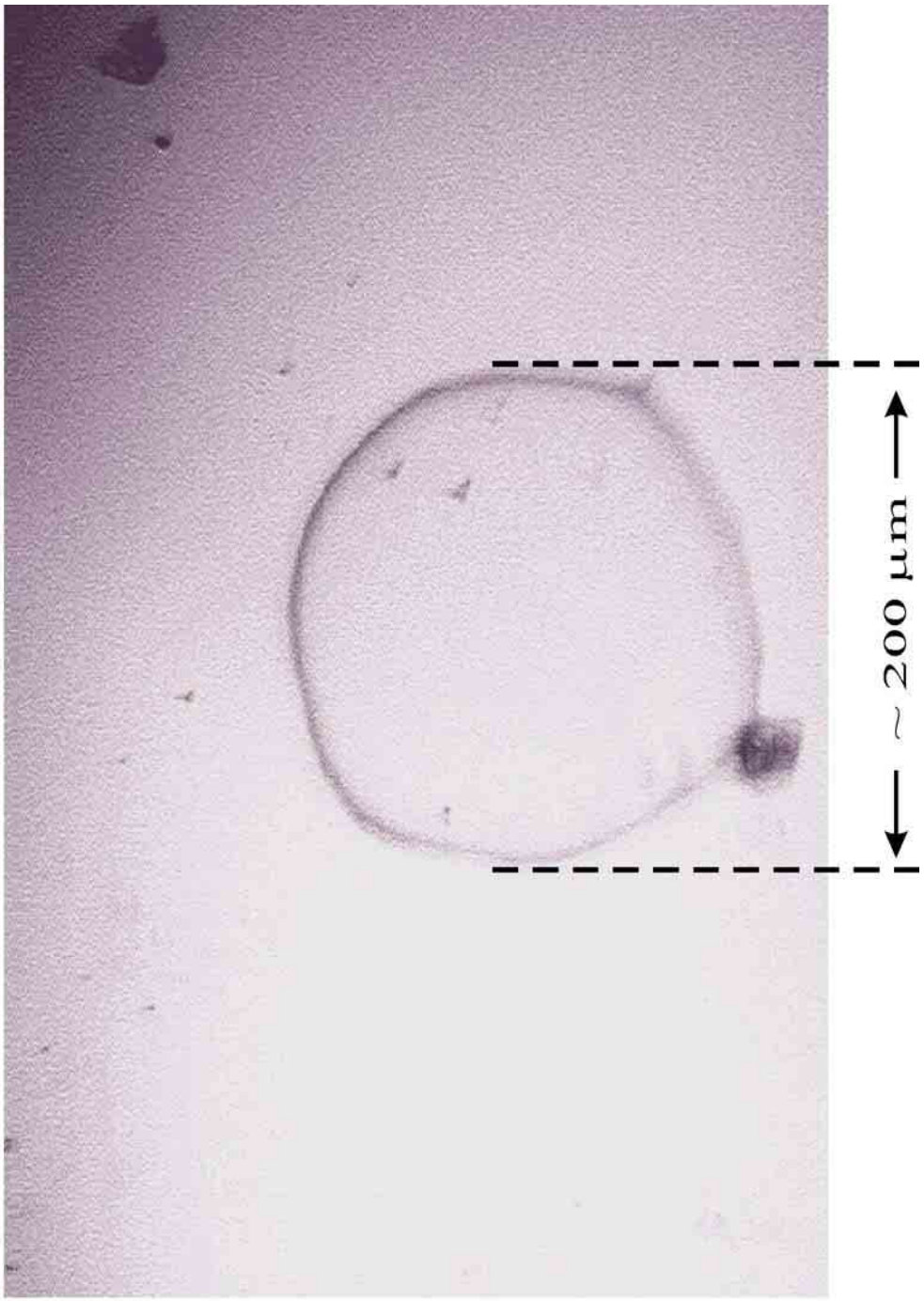

CE/FT-IR Deposit of Borate

Figure 3.5 CE/FT-IR deposit image. Sample: Caffeine electrolyte: ammonium acetate, Deposit Size: ~200 μm

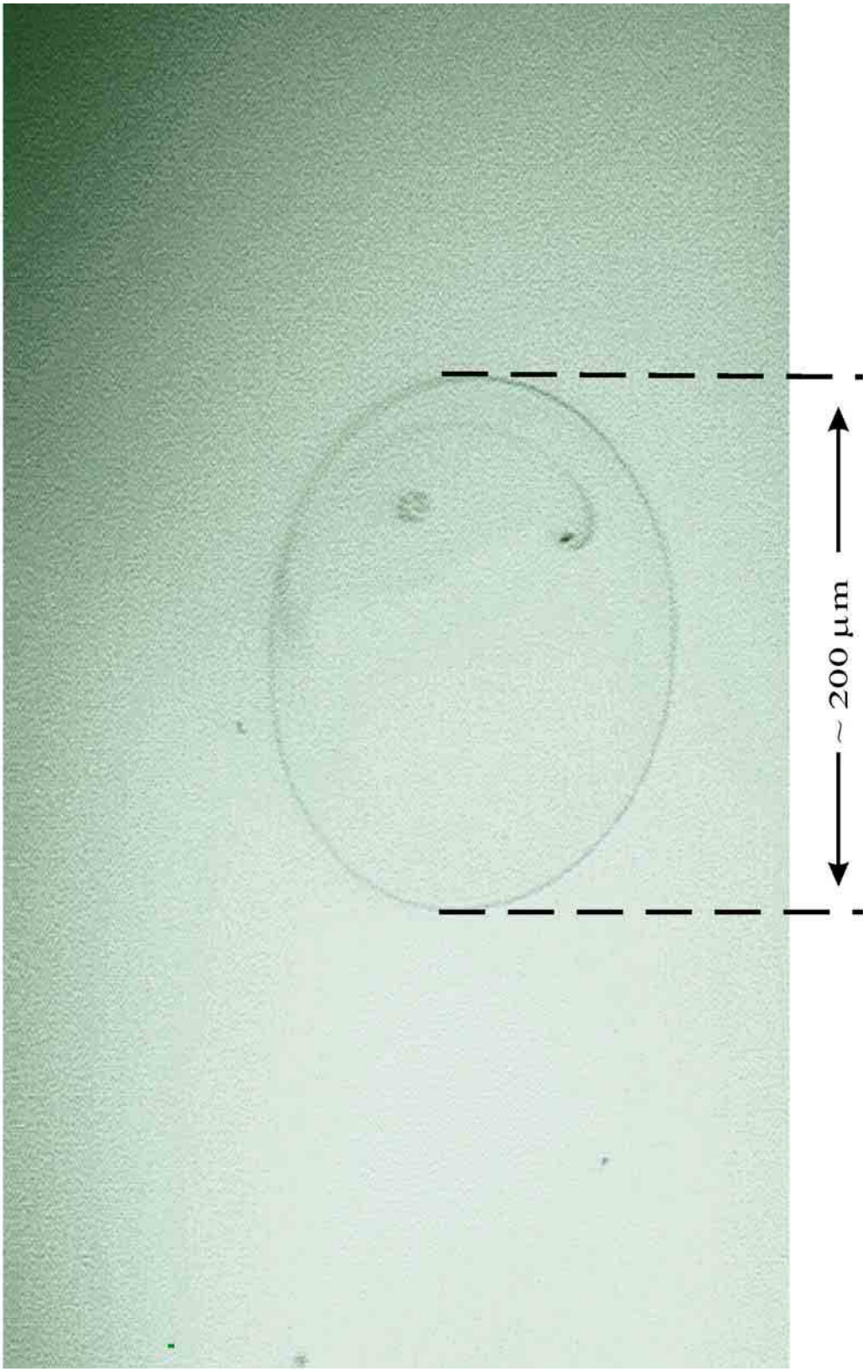

CE/FT-IR Deposit of Caffeine

column will be due to gravity and not the electroosmotic or electrophoretic flow. To test the stability of the interface under normal CE operation, a standard mixture was separated. The standard mixture contained caffeine, salicylic acid, p-aminobenzoic acid, and sodium benzoate, which were all made up in a sodium borate solution. The separation of this standard mixture is shown in Figure 6. The peak shapes suggest that the throughout the run the current remains stable. The peaks seen in Figure 6 also suggest that at this current and voltage there is very little problem with joule heating. The current remains relatively stable once the maximum voltage used for the separation has been reached. The fluctuation in current seen in Figure 7 is stable to within ± 0.3 μAmp or roughly 0.5% of the total current and is a representative current profile.

Monosaccharide separation using capillary electrophoresis can be a very difficult task if the correct electrolytic solution system is used. Monosaccharides and oligosaccharides are neutral when placed in solution and a charge is placed upon them in solution, thus they will travel together with the electroosmotic flow. A commonly used buffer system used for the separation of mono- and oligosaccharides is borate. The borate ion forms a complex with the sugars and facilitates their separation. Figure 8 shows a typical electropherogram of the separation of five monosaccharides: N-acetyl-D -glucosamine, N-acetyl-D-galactosamine, D-Mannose, N-acetyl-D-Neuraminic Acid, and D-Glucose. The peak shapes of the GlcNAc, Man, and Glc suggest that there is a mismatch of the borate and sugar concentrations. The concentration of the sugars was lowered to decrease the effect of electrodispersion, however, the sugars do not have a strong absorbance in the UV region, they are difficult to produce a suitable electropherogram. The current profile seen in Figure 8 suggests that the silver coated column is maintaining contact with effluent from the end of the column. The lack of fluctuations in the current profile seen in Figure 8 suggest that the silver coated column is marinating contact with the effluent coming from the end of the capillary. There are two major problems with the use of a borate as an electrolytic solution system in

Figure 3.6 UV Electropherogram of a standard separation mixture. Sample: caffeine, salicylic acid, p-aminobenzoic acid, sodium benzoate, concentration: 1×10^{-3} M, voltage: 30 kV. Electrolyte borate 1 X 10^{-3} M, detection wavelength: 214 nm. Column: 75 μm i.d. and ~140 cm long

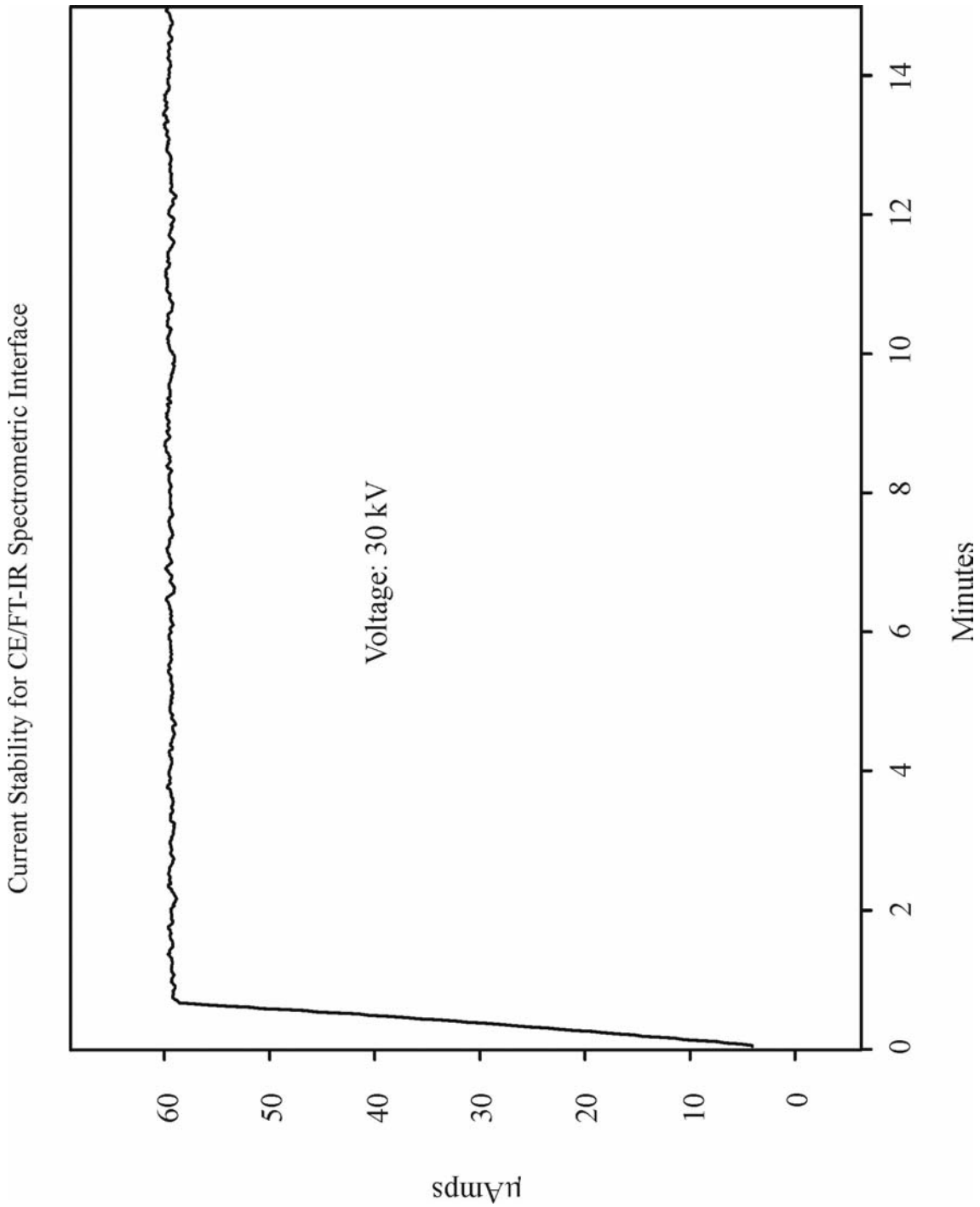
Current Stability for CE/FT-IR Spectrometric Interface
Voltage: 30 kV
μAmps
0
10
20
30
40
50
60
0
2
4
6
8
10
12
14
Minutes

Figure 3.7 CE current using the glass CE/FT-IR spectrometric interface.

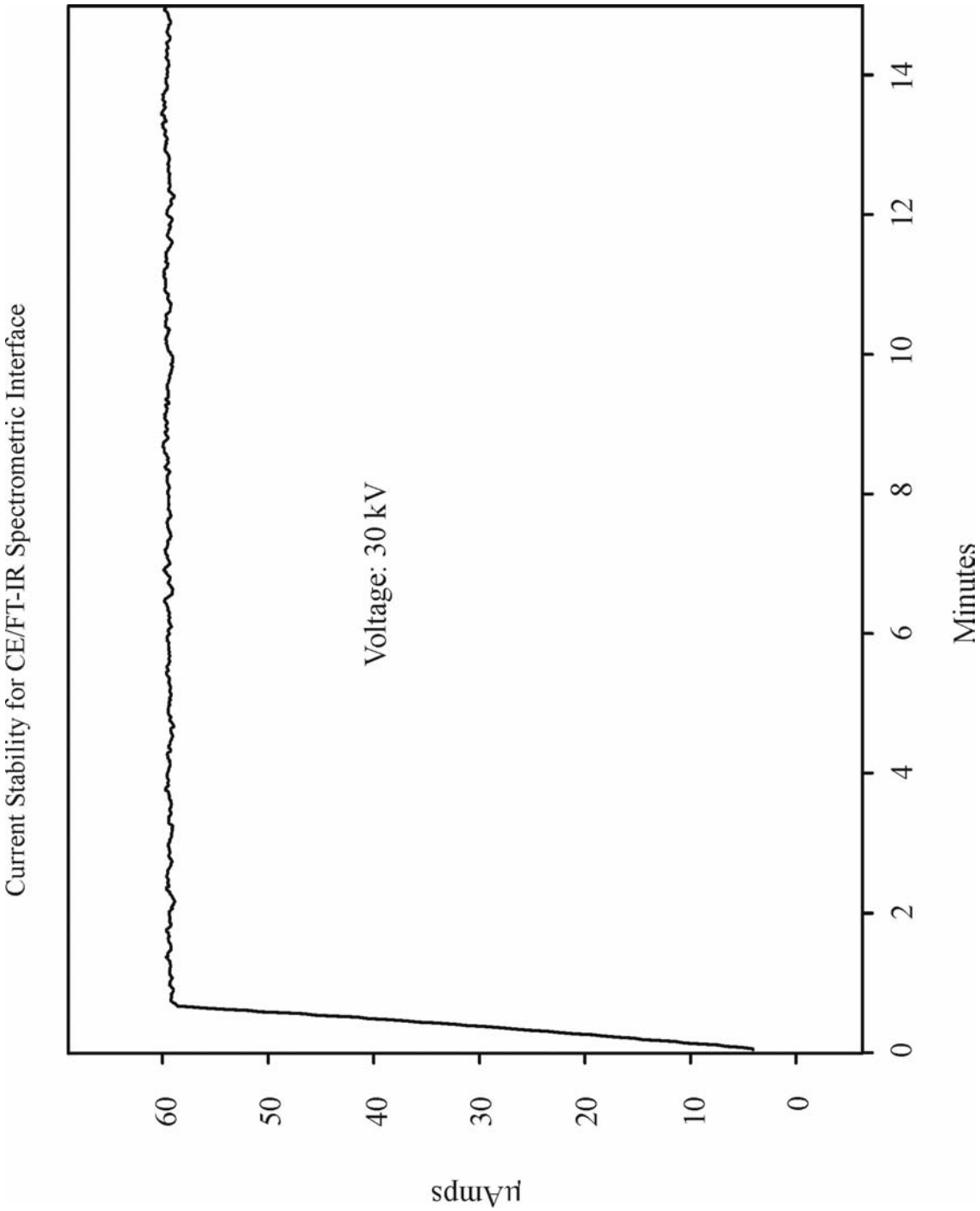
Current Stability for CE/FT-IR Spectrometric Interface
Voltage: 30 kV
μAmps
0
10
20
30
40
50
60
0
2
4
6
8
10
12
14
Minutes

Figure 3.8 UV Electropherogram and CE current using the glass CE/FT-IR spectrometric interface. Sample: N-acetyl-D-glucosamine, N-acetyl-D-galactosamine, D-Mannose, N-acetyl-D-Neuraminic Acid, and D-Glucose. Voltage: 25 kV. Detection wavelength: 200 nm. Temperature: 50 °C. Column ~142 cm long

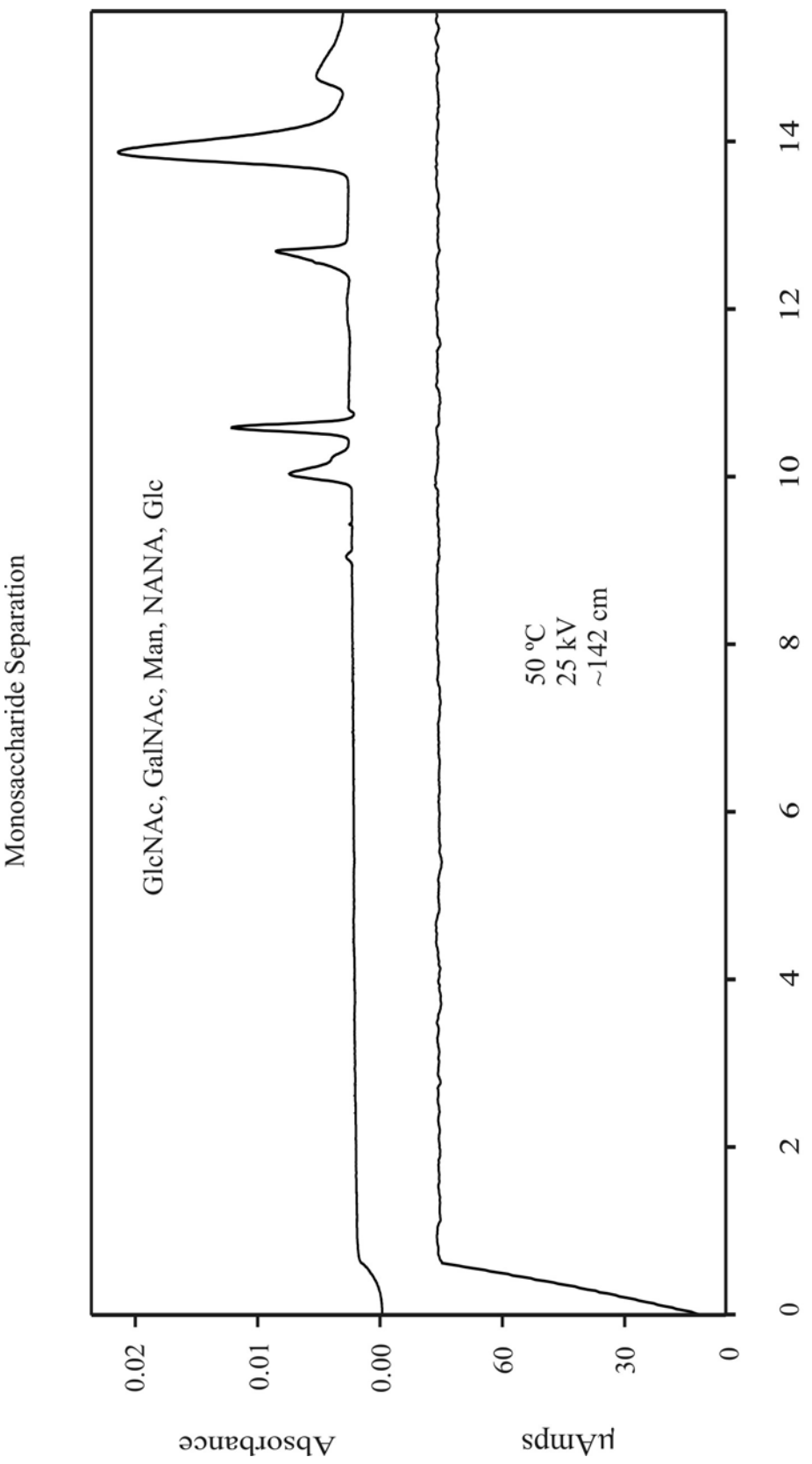
Monosaccharide Separation
GlcNAc, GalNAc, Man, NANA, Glc
50 ºC
25 kV
~142 cm
Absorbance
0.02
0.01
0.00
μAmps
60
30
0
0
2
4
6
8
10
12
14
Minutes

conjunction with the CE/FT-IR spectrometric interface. The first is that borate absorbs strongly in the mid-infrared region. The top spectrum in Figure 9 shows a CE/FT-IR of GlcNAc using a borate electrolytic solution system. As can be seen the borate interferes with the spectral bands from the GlcNAc. A manual deposit of an aqueous sample of GlcNAc is also shown. An electrolyte buffer that is transparent in the mid infrared would be preferable. There is a number of different electrolyte systems that do not have interference bands in the infrared region because they are volatile and evaporate when deposited. These include acetic acid, ammonium hydroxide, ammonium acetate, and ammonium formate. Although the buffers are volatile, some buffer remains trapped with the analyte hence the buffers leave low intensity absorbance bands, which can easily be subtracted from the analyte spectra. The middle spectrum in Figure 9 shows a deposit made from the nebulizer of GlcNAc using a formate electrolytic solution system. If the manual deposit and formate spectra are compared, there is very little difference between the two spectra. There is also no evidence of shifts in the analyte bands due to the formation of adducts between the electrolyte and GlcNAc. The second problem with the use of a borate electrolyte system is its lack of volatility. The aforementioned electrolyte systems do interfere in the infrared region, however there absorbances are weak compared to borate because of there volatility also are very volatile relative to borate. This volatility is important when making deposits from the CE/FT-IR spectrometric interface. Ideally, the evaporation rate should be high enough for sufficient solvent elimination to occur before the analyte strikes the surface. Desolvation helps to produce the smallest possible deposit and reduce the amount of splatter that may occur.

Conclusion

Our research has shown that the newly designed glass CE/FT-IR spectrometric interface provides smaller and more circular deposits than the original stainless steel CE/FT-IR interface. The ability to change the method in which electrical contact is

Figure 3.9 N-Acetyl-D-glucosamine (GlcNAc) CE/FT-IR spectra. Top: deposit with borate separation electrolyte. Middle deposit with formate separation electrolyte, Bottom manual deposit. Deposits made on CaF_2 crystal, 1000 scans at 4^{-1} cm resolution

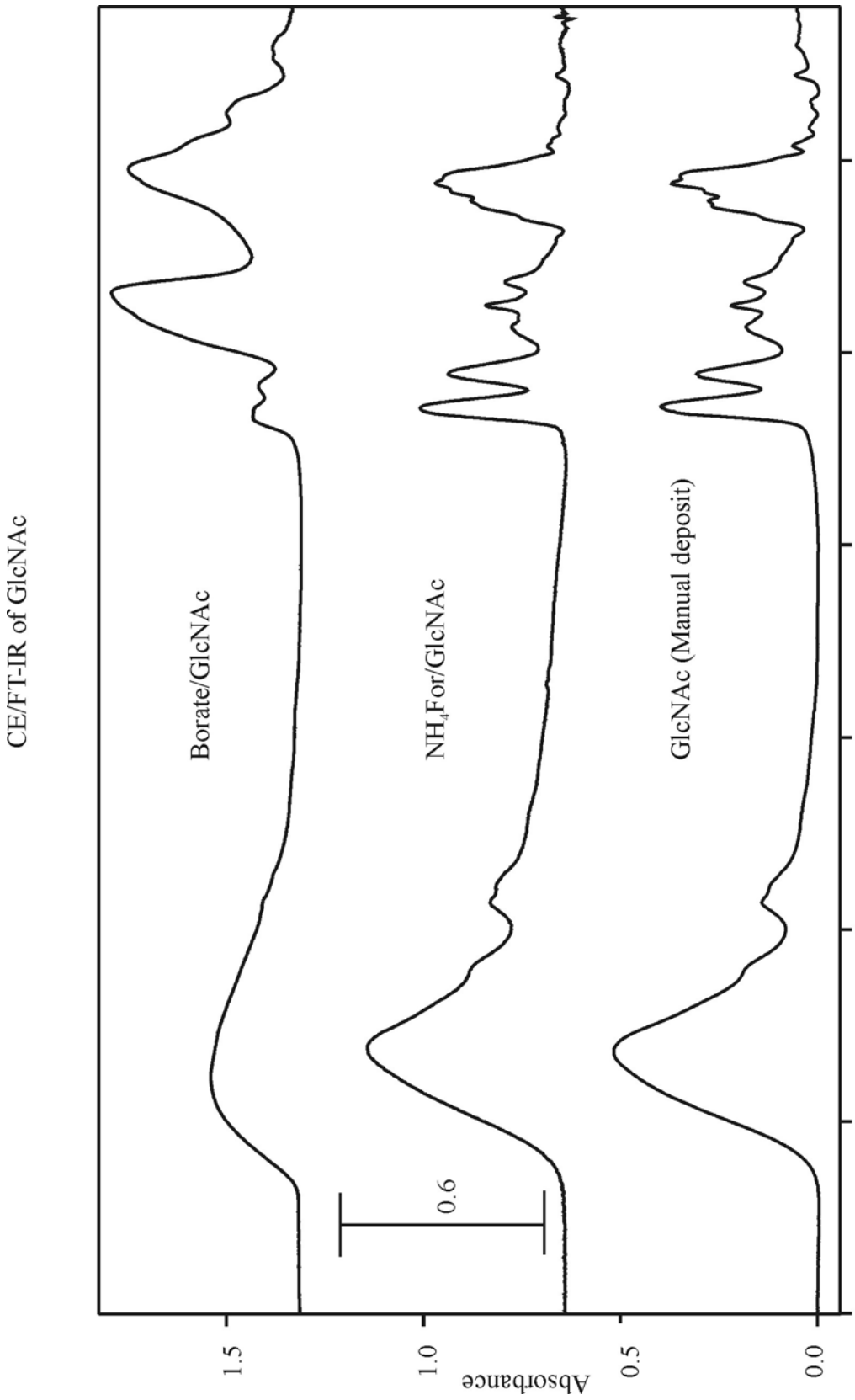
CE/FT-IR of GlcNAc
Borate/GlcNAc
NH4For/GlcNAc
GlcNAc (Manual deposit)
0.6
Absorbance
1.5
1.0
0.5
0.0
4000
3500
3000
2500
2000
1500
1000
Wavenumber/cm-1

made has allowed for easier operation. The original design required that the end of the CE column be in contact with the tip of the stainless steel tube, thus it was difficult to keep the interface clean and produce small concentric deposits. The silver paint coating allowed for electrical contact to be moved away from the tip and for a more functional design. The inner glass capillary was then decreased in diameter to closely match the outer diameter of the capillary column, with a flow of helium helping nebulize the effluent. A flow of nitrogen is sent through the outer glass capillary to help with evaporation and containment of the deposit. Currently, detection limits are as low as tens of nanograms. Deposits made using the stainless steel depositor also tended to be very thick and nonuniform in thickness. This was seen by the appearance of interference patterns the stainless steel nebulizer deposits. These patterns appear as colors, which give some insight into the thickness of the deposit in certain areas. These colors are not seen in the deposits made by the glass interface. Although there may appear to be a difference in deposit thickness seen in Figures 4 and 5, there were no visible color changes in the deposit and the deposits were enhanced digitally in order to be viewed.

A borate electrolytic solution system provided more robust separations than the volatile electrolytic solution systems. Borate electrolytic solution systems, however, are problematic because they interfere with absorbance bands of the samples in the mid-infrared region of the spectrum and are not very volatile. To overcome these drawbacks, a non-interfering volatile electrolytic solution system is essential in the use of the CE/FT-IR spectrometric interface. Thus leading to the use of ammonium volatile electrolytic solution systems. Work is in progress to develop a separation method involving capillary electrochromatography (CEC) with a volatile electrolytic solution system. CEC uses a packed CE column, adding chromatographic separation characteristics to the electrophoretic separation used in normal capillary electrophoresis. With the increased resolving power of CEC, the separation of neutral oligosaccharides

and other neutral compounds should increase the usefulness of CE/FT-IR interface. Work is in progress to develop a third generation interface. It is expected that these modifications will help to produce smaller deposits and keep them contained to a smaller area with less splatter. This interface is currently used as an off-line technique, although, future research is focused on the development of an on-line system, to facilitate IR spectral collection directly after deposition.

Acknowledgements

The authors thank the National Institutes of Health (grant number 2P41-RR-05351) for financial support in the form of a National Center for Research Resources.

References

1. P. R. Griffiths and J. A. de Haseth *Fourier Transform Infrared Spectrometry* (John Wiley & Sons, New York, 1986), Chap. 18.

2. K. Krishnan, "Advances in Capillary Gas Chromatography-Fourier Transform Interferometry," in *Fourier Transform Infrared Spectroscopy : Applications to Chemical Systems*, J. R. Ferraro and L. J. Basile, Eds. (Academic Press, Orlando, 1985), Vol. 4, Chap. 3.

3. A. M. Haefner, K. L. Norton, P. R. Griffiths, S. Bourne, and R. Curbelo, Anal. Chem. **60,** 2441 (1988).

4. S. Bourne, A. M. Haefner, K. L. Norton, and P. R. Griffiths, Anal. Chem. **62,** 2448 (1990).

5. S. Bourne, G. T. Reedy, and P. T. Cunningham, J. Chromatogr. Sci. **17,** 460 (1979).

6. G. T. Reedy, S. Bourne, and P. T. Cunningham, Anal. Chem. **51,** 1535 (1979).

7. R. Fuoco, S. L. Pentoney, and P. R. Griffiths, Anal. Chem. **61,** 2212 (1989).

8. K. L. Norton and P. R. Griffiths, J. Chromatogr. A **703,** 503 (1995).

9. R. Robertson, J. de Haseth, J. Kirk, and R. Browner, Appl. Spectrosc. **42,** 1365 (1988).

10. V. E. Turula and J. A. de Haseth, Appl. Spectrosc. **48,** 1255 (1994).

11. V. E. Turula and J. A. de Haseth, Anal. Chem. **68,** 629 (1996).

12. V. E. Turula, R. T. Bishop, R. D. Ricker, and J. A. de Haseth, J. Chromatogr. A **763,** 91 (1997).

13. R. T. Bishop, V. E. Turula, and J. A. de Haseth, Anal. Chem. **68,** 4006 (1996).

14. R. T. Bishop, V. E. Turula, J. A. de Haseth, and R. D. Ricker, "Hyphenated HPLC Methodology for the Resolution and Elucidation of Peptides from Proteolytic Digests," in *Techniques in Protein Chemistry VIII,* D. R. Marshak, Ed. (Academic Press, San Diego, 1997), p.165.

15. R. T. Bishop and J. A. de Haseth, Mikrochim. Acta [Suppl.] **14,** 721 (1997).

16. T. G. Venkateshwaran, J. T. Stewart, R. T. Bishop, J. A. de Haseth, and M. G. Bartlett, J. Pharm. Biomed. Anal. **17,** 57 (1998).

17. T. G. Venkateshwaran, J. T. Stewart, J. A. de Haseth, and M. G. Bartlett, J. Pharm. Biomed. Anal. **19,** 709 (1999).

18. D. Kuehl and P. R. Griffiths, J. Chromatogr. Sci. **17,** 471 (1979).

19. C. M. Conroy, P. R. Griffiths, P. J. Duff, and L. V. Azarraga, Anal. Chem. **56,** 2636 (1984).

20. A. J. Lange, P. R. Griffiths, and D. J. J. Fraser, Anal. Chem. **63,** 782 (1991).

21. V. F. Kalasinsky, K. G. Whitehead, R. C. Kenton, J. A. S. Smith, and K. S. Kalasinsky, J. Chromatogr. Sci. **25,** 273 (1987).

22. A. M. Robertson, D. Littlejohn, M. Brown, and C. J. Dowle, J. Chromatogr. **588,** 15 (1991).

23. J. J. Gagel and K. Biemann, Anal. Chem. **58,** 2184 (1986).

24. J. J. Gagel and K. Biemann, Anal. Chem. **59,** 1266 (1987).

25. C. Fujimoto, K. Jinno, and Y. Hirata, J. Chromatogr. **258,** 81 (1983).

26. G. W. Somsen, L. P. P. Vanstee, C. Gooijer, U. A. T. Brinkman, N. H. Velthorst, and T. Visser, Anal. Chim. Acta **290,** 269 (1994).

27. G. W. Somsen, E. W. J. Hooijschuur, C. Gooijer, U. A. T. Brinkman, N. H. Velthorst, and T. Visser, Anal. Chem. **68,** 746 (1996).

28. J. L. Dwyer, A. E. Chapman, and X. Liu, LC-GC **13,** 240 (1995).

29. M. W. Raynor, K. D. Bartle, and B. W. Cook, J. High Resolut. Chromatogr. **15,** 361 (1992).

30. G. W. Somsen, C. Gooijer, N. H. Velthorst, and U. A. T. Brinkman, J. Chromatogr. A **811,** 1 (1998).

31. G. W. Somsen, R. J. Vandenesse, C. Gooijer, U. A. T. Brinkman, N. H. Velthorst, T. Visser, P. R. Kootstra, and A. Dejong, J. Chromatogr. **552,** 635 (1991).

32. P. R. Griffiths and A. J. Lange, J. Chromatogr. Sci. **30,** 93 (1992).

33. A. J. Lange and P. R. Griffiths, Appl. Spectrosc. **47,** 403 (1993).

34. J. Jorgenson and K. Lukacs, J. Chromatogr. **218,** 209 (1981).

35. J. Jorgenson and K. Lukacs, Science **222,** 266 (1983).

36. Y. Huang, Y. Mechref, and M. Novotny, Carbohydr. Res. **323,** 111 (2000).

37. K. Hutterer, H. Birrell, P. Camilleri, and J. Jorgenson, J. Chromatogr. B **745,** 365 (2000).

38. B. Lagane, M. Treilhou, and F. Couderc, Biochem. Molec. Bio. Ed. **28,** 251 (2000).

39. D. Newburg, Z. Shen, and C. Warren, Glycobiology **10,** 212 (2000).

40. V. Pacakova, S. Hubena, M. Ticha, M. Madera, and K. Stulik, Electrophoresis **22,** 459 (2001).

41. T. Raju, Anal. Biochem. **283,** 125 (2000).

42. Z. El Rassi, Electrophoresis **20,** 3134 (1999).

43. Z. Shen, C. Warren, and D. Newburg, Anal. Biochem. **279,** 37 (2000).

44. F. Dang, Y. Chen, Q. Guo, and G. Xu, Chemical Journal of Chinese Universities **21,** 206 (2000).

45. J. Delaney and P. Vouros, Rapid Commun. Mass Spectrom. **15,** 325 (2001).

46. M. Hadley, M. Gilges, J. Senior, A. Shah, and P. Camilleri, J. Chromatogr. B **745,** 177 (2000).

47. S. Honda, J. Okeda, H. Iwanaga, S. Kawakami, A. Taga, S. Suzuki, and K. Imai, Anal. Biochem. **286,** 99 (2000).

48. A. Paulus and A. Klockow, J. Chromatogr. A **720,** 353 (1996).

49. T. W. Garner and E. S. Yeung, J. Chromatogr. **515,** 639 (1990).

50. R. Kuhn, S. Hoffstetter-Kuhn, and *Capillary Electrophoresis Principles and Practice* (Springer Laboratory, New York, 1993).

51. M. Li and M. D. Morris, "Capillary Electrophoresis of Nucleosides with Real-Time Raman Spectroscopy Detection", presented at the Pittsburgh Conference on Analytical Chemistry and Applied Spectroscopy, Atlanta, Georgia (1997).

52. J. W. Olesik, J. A. Kinzer, and S. V. Olesik, Anal. Chem. **67,** 1 (1995).

53. R. D. Smith, C. J. Barinaga, and H. R. Udseth, Anal. Chem. **60,** 1948 (1988).

54. W. M. A. Niessen, U. R. Tjaden, and J. Vandergreef, J. Chromatogr. **636,** 3 (1993).

55. J. Olivares, N. Nguyen, C. Yonker, and R. Smith, Anal. Chem. **59,** 1230 (1987).

56. K. D. Altria, J. Chromatogr. A **856,** 443 (1999).

57. J. Banks, Electrophoresis **18,** 2255 (1997).

58. K. Bateman, J. Am. Soc. Mass Spectrom. **10,** 309 (1999).

59. J. Cai and J. Henion, J. Chromatogr. A **703,** 667 (1995).

60. R. Smith, J. Olivares, N. Nguyen, and H. Udseth, Anal. Chem. **60,** 436 (1988).

61. R. Todebush, He L.T., and J. de Haseth, Submitted to *Analytical Chemistry* (2001).

CHAPTER 4

SEMI-AUTOMATED SAMPLE DEPOSITION SYSTEM FOR SINGLE BOUNCE ATR/FT-IR [1]

[1]Todebush, R.A.; J.L. Jarman; J.A. de Haseth. 2001. To be submitted to *Applied Spectroscopy.*

Abstract

The detection of minute samples is a concern in many areas of research and analysis, including biological, environmental, and forensic sciences. The use of manual solution direct deposition, combined with surface evaporation, is a very useful and convenient method for the transfer of an analyte to a spectroscopic sampling window. This transfer is performed with the use of a small pipette and manual placement of the analyte onto a specific area. For Fourier transform infrared (FT-IR) spectrometric analysis, the Harrick SplitPea™ can improve sensitivity by focusing the infrared beam onto a very small area, approximately 250 μm in diameter. Because the sample area is so small, manual placement of the analyte deposit on the active area of the sampling accessory must be carfully done. To achieve this, a novel direct deposition system has been developed. This system, a series of valves attached to a nebulizer, generates deposits that are reproducible and placement of the deposits is precise. The valves allow for the loading of the sample, nitrogen airflow to assist in the evaporation process, and cleaning of the nebulizer after deposition. To help contain the sample to a small area once deposition has taken place, a vacuum line is attached to the nebulizer. This simple semi-automated deposition system allows for higher sensitivity and run-to-run reproducibility for minute sample deposits.

Introduction

Optical spectroscopy is one of the most powerful analytical techniques in use today. With its growth, the need for surface and bulk analysis using internal and external reflections has also grown.[1-16] Over the past decade, the need for a nondestructive microsampling optical spectroscopy method has increased. There has been a great deal of work done in the development of attenuated total reflection (ATR) accessories for use in infrared spectroscopic analyses.[17-23] ATR accessories have an important advantage over accessories in transmission FT-IR spectrometry, such as microscopes and beam condensers. To be measured with microscopes and beam condensers, the sample must be optically thin. Most samples are not optically thin and are therefore not well suited for traditional analysis. Most of the methods involved in making optically flat samples involve the use of compression, which can lead to sample destruction. The use of internal reflection spectroscopy does not have the sampling problem found in transmission experiments. The sample is placed directly in contact with the surface of the accessory, which can eliminates certain sample preparation steps prior to analysis. Often, analysis can be performed without applying pressure, which reduces loss of the sample destruction. This technique also allows for the analysis of samples that are in liquid, irregular solid, or powder form, as long as adequate contact between the sample and the ATR element is made. Many studies today that involve the use of ATR accessories investigate solution mixtures and minute amounts of sample

There is a number of different designs used for the internal reflection elements (IRE) in ATR accessories. The type of sample being studied, e.g. liquid, solid, powder, thin film, often determines which design is used. The designs fall into two categories: single and multi-bounce elements. The available geometries for single bounce elements are: fixed angle (prisms) and variable angle (hemisphere and hemicylinder). Multiple reflection elements are described in detail by Harrick and are not presented here.[17] The fixed angle single bounce element does not allow for the beam to be focused onto a

small area, thus the size of the beam entering the prism will determine the active area of the IRE element. Fixed angle elements work well for bulk materials and materials for which contact between the sample and the surface is easily maintained. ATR analysis, however, can be difficult when there is only a small amount of sample available. This difficulty is due to the large active area, millimeters that is often characteristic of this type of element. To try to reduce these large active areas, a hemispherical design has been employed.[18-20] This geometry causes a large convergence of the beam, which helps to increase the sensitivity when examining very small amounts of sample. Once the beam enters the IRE through the hemisphere, the radiation is focused at the center of the planar surface of the hemispherical IRE. The active site of the element can vary in size, but a commercially available element from Harrick Scientific has as active site of only ~250 μm in diameter.

One important factor when using a single bounce internal reflection element is the choice of the material for the element. The crystal used affects the depth of penetration from the radiation beam into the sample; materials with a low refractive index value will allow a greater depth of penetration. The two most commonly used materials are germanium and silicon. The refractive index of these two materials is 4 and 3.5, respectively. In the mid IR region, 4000 cm^{-1} to 660 cm^{-1}, the depth of penetration varies from 0.181 μm to 1.10 μm if silicon is used for the IRE. To calculate the depth of penetration the following equation is used:

$$d_p = \frac{\lambda_1}{2\pi\eta_1(\sin^2\theta - \eta_{21}^{\ 2})^{1/2}} \tag{8}$$

where λ wavelength of the input radiation, η_{21} is η_2/η_1: the ratio of the refractive index of the sample divided by that of the element, and θ is the angle of incidence. As the radiation penetrates the IRE into the sample, the electric field strength decreases exponentially as a function of distance from the IRE surface. If only *qualitative*

analysis is being performed, the depth of penetration can exceed the sample thickness as long as the sample is homogenous. As long as the signal-to-noise ratio is large enough so as not to lose information in the noise of the baseline then very small deposits can be made onto the IRE. The depth of penetration, however, does become an important factor when *quantitative* analysis is required.

Single bounce hemispherical internal reflection elements are also available in a number of different designs. The work described herein uses a design developed by Harrick Scientific called a SplitPea™. This accessory is placed in the sample compartment of any FT-IR instrument and can be used to analyze both liquid and solid samples. For some solid samples, a pressure applicator is provided. The applicator can be pressed against the top of the solid sample to ensure that good contact is maintained and reproducible spectra are collected. In order to obtain suitable liquid sample deposits, several requirements must be met. An ideal deposit is of uniform thickness, round in shape, and just large enough to cover the IRE active site. The deposit must be made at ambient temperature and pressure and should dry quickly. The semi-automated sample deposition system should be placed close to the IRE for precise deposition, however it should also be allowed to move away from the IRE surface for cleaning.

Deposition methods have been used for a number of years as a way to easily measure liquid samples that are not easily analyzed using traditional FT-IR methods. There is a number of different methods used to make deposits onto infrared transparent windows. These include manual deposition, semi-automated deposition, and interface deposition. Manual deposition is often used in our laboratory to produce very small deposits for analysis with an FT-IR spectroscopic microscope and an ATR/FT-IR system. When liquid deposits evaporate the resulting deposits usually tend to dry thicker around the edges than in the middle. If the deposit is too thick, the spectra will deviate from linearity with Beers law, but if a deposit is too thin it prevents a strong signal-to-noise ratio from being obtained. Figure 1 depicts how the manual deposition

Figure 4.1 Manual deposition technique

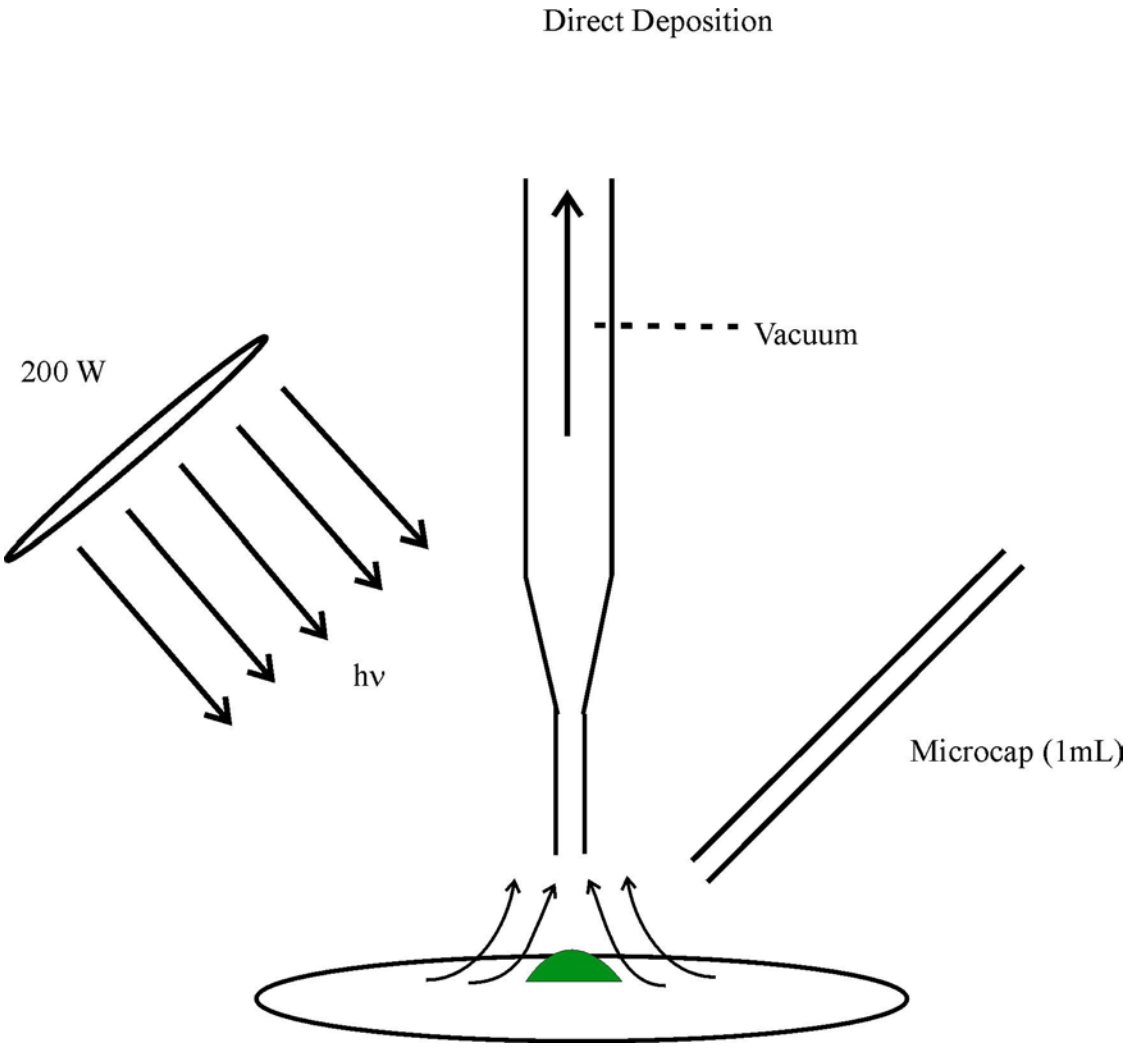
Direct Deposition
Vacuum
200 W
hν
Microcap (1mL)

is carried out in this laboratory. The sample is loaded into the microcapillary and then placed onto the infrared transparent window. Once the droplet is deposited, a vacuum apparatus is moved above the sample to aid in solvent evaporation. This apparatus consists of a glass pipette attached to a vacuum line and is placed about 3 mm above the center of the deposition area. This allows for air to be pulled up, over, and around the droplet to help with evaporation and deposition thickness, thus concentrating the sample into a smaller area. A white light source is placed near the droplet to provide radiant heat to increase the rate of evaporation. The vacuum and heat combination is used to help contain the deposit. Despite these measures, a number of deposits is generally required to find one that is suitable for spectral interrogation. When using volatile solvents, the deposit has a tendency to splatter upon expulsion from the microcapillary. Volatile solvents, therefore, can increase the number of deposits required to obtain a suitable one for analysis. The result of this method is an area of more uniform sample thickness on which to perform FT-IR transmission spectroscopy and ATR/FT-IR spectrometry.

Some of the inherent problems of the manual sample deposition system, such as deposit size, thickness, and the need to make multiple deposits, can be reduced or eliminated with the use of a semi or fully automated sample deposition system. Our group has previously shown that a semi-automated sample deposition system works well for making deposits from a high performance liquid chromatography (HPLC) particle beam system.[24-35] With this method, deposits of relatively uniform shape and thickness are produced and subsequently analyzed spectrometrically. While the particle beam works well as an interface for an HPLC, the length of the desolvation tube does not allow for close placement to the ATR element, and deposits cannot be made at ambient pressure. Using information gained from these interfaces and unpublished data[36]; a method for sample deposition onto small single bounce IREs has been created.

A novel system has been developed for use with a single bounce internal reflection element for the analysis of a number of different types of samples. A semi-automated depositor has been constructed to allow deposition of minute sample volume (Figure 2). The deposits are analyzed spectrometrically and compared with spectra of manual deposits. The deposits made with the new design are suitable for ATR analysis and can be made under normal conditions. The system is relatively simple and removes many variables and obstacles encountered with other deposition methods.

Experimental

Chemical Reagents.

Caffeine, sodium benzoate, and D- (+) cellobiose were purchased from Sigma-Aldrich Chemical Company (St. Louis, MO). All samples were made to 1.0×10^{-2} M with 18MΩ deionized water, which was obtained in-house with a Barnstead Nano ultrapure water purifier.

Manual Deposits.

The manual method of direct deposition was performed with 1 µL capillary tubes and modified Pasteur pipettes. The sample deposit is placed directly onto a Harrick SplitPea™ silicon IRE and allowed to dry. To expedite solvent evaporation, a 200 W light and the Pasteur pipette attached to a vacuum line was placed above the sample.

Semi-Automated Depositor.

The sample depositor was fashioned from fittings purchased from Upchurch Scientific (Oak Harbor, WA) and Swagelok (Solon, OH). The main body of the depositor was designed by the authors and manufactured by J. E. Meinhard Associates (Santa Ana, CA). Sample loading was accomplished with a 10 µL Hamilton syringe

Figure 4.2 Semi-Automated sample depositor

Sample Depositor

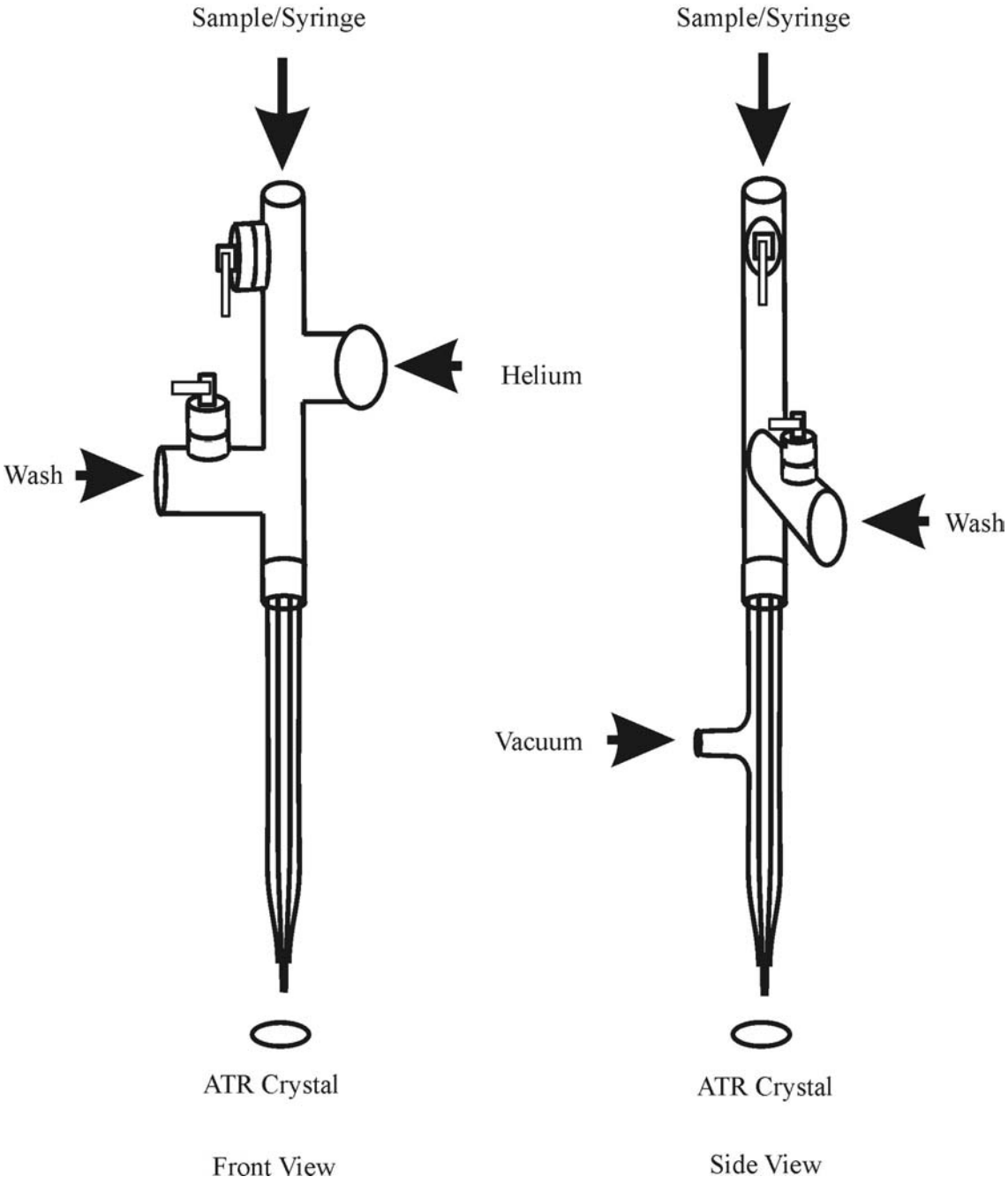

using 182 mm of fused silica (184 μm o.d., 50 μm i.d.) as the needle. Sample is injected into the tip of the depositor body and the syringe is withdrawn. All valves are closed off during injection, and the sample remains lodged in the depositor tip. Single deposits were made onto a Harrick SplitPea™ ATR element or other infrared transparent window and allowed to dry. The samples were expelled from the depositor tip with helium (National Welders Supply Co., Charlotte, NC) while vacuum was applied to the outer cavity of the depositor to increase the rate of evaporation and solvent elimination. Gas flow rates are varied to achieve desired deposit size.

Deposit Measurements.

Size determination of the manual and semi automated deposits was carried out with a Perkin-Elmer Spectrum 2000 FT-IR spectrometer (Perkin-Elmer, Connecticut, USA). The spectrometer was coupled with a Perkin-Elmer *i*-series FT-IR microscope. The microscope is equipped with a remote aperture that can be used in conjunction with the spectrometer software to obtain the size of the deposits. Pictures were obtained using an ausJENA stereomicroscope (Jenavert, Germany) with a Hitachi digital camera (Hitachi, USA).

ATR/FT-IR Spectrometry.

Infrared spectra of manual and semi-automated deposits were collected with a Bio-Rad FTS-60A/896 spectrometer with a DTGS detector. A total of 1000 scans were collected at a resolution of 4 cm^{-1} and co-added. The single bounce IRE SplitPea™ silicon element was generously donated from Harrick Scientific Corporation (Ossining, NY).

Results and Discussions

In order to determine the feasibility of the semi-automated sample deposition system, a series of studies was conducted. A number of aqueous and volatile deposits was obtained by both semi-automatic and manual deposition. Each deposit was compared visually and spectroscopically to determine the advantages of the deposition system over manual deposition. Visual analysis revealed that manual deposits exhibited non-uniform evaporation patterns and thickness variations throughout the entire series of deposits. Evidence of this is found in Figure 3, which shows the thickened edge of a representative deposit of an aqueous caffeine solution. Typically, manual deposits had dimensions on the order of ~1000 μm and were oblong in shape, as shown in Figure 4. In contrast, the semi-automatic deposits measured between 300 and 600 μm in diameter and were consistently circular. Additionally, semi-automatic deposits did not exhibit evidence of uneven evaporation patterns and thickness variations. Figure 5 shows a semi-automatically deposited sample of caffeine. There are slight differences in the intensities of the absorption bands, but the relative intensities are consistent. These differences are likely attributed to a lack of thickness of the sample deposit onto the IRE element active site. Figures 6 and 7 show comparison spectra between manual and semi-automated deposits of caffeine and sodium benzoate, respectively.

When compared spectrally, the manual and semi-automatic deposits are nearly identical. There are slight differences in the intensities of the absorption bands, but the relative intensities are consistent. These differences are likely due to incomplete coverage of the depth of penetration of the infrared reflection element active site. Figures 6 and 7 show comparison spectra between manual and semi-automated deposits of caffeine and sodium benzoate, respectively.

To determine the reproducibility of deposit size, a series of deposits onto CaF_2 was made and measured. Aqueous samples were measured to determine a standard deviation from deposit to deposit. As mentioned above, one of the problems with manual deposition is consistent deposit size. One of the main goals of the new

Figure 4.3 Manual deposit of caffeine on CaF_2 crystal

Manual Deposit of Caffeine

Figure 4.4 ~1000 μm manual deposit made on CaF_2

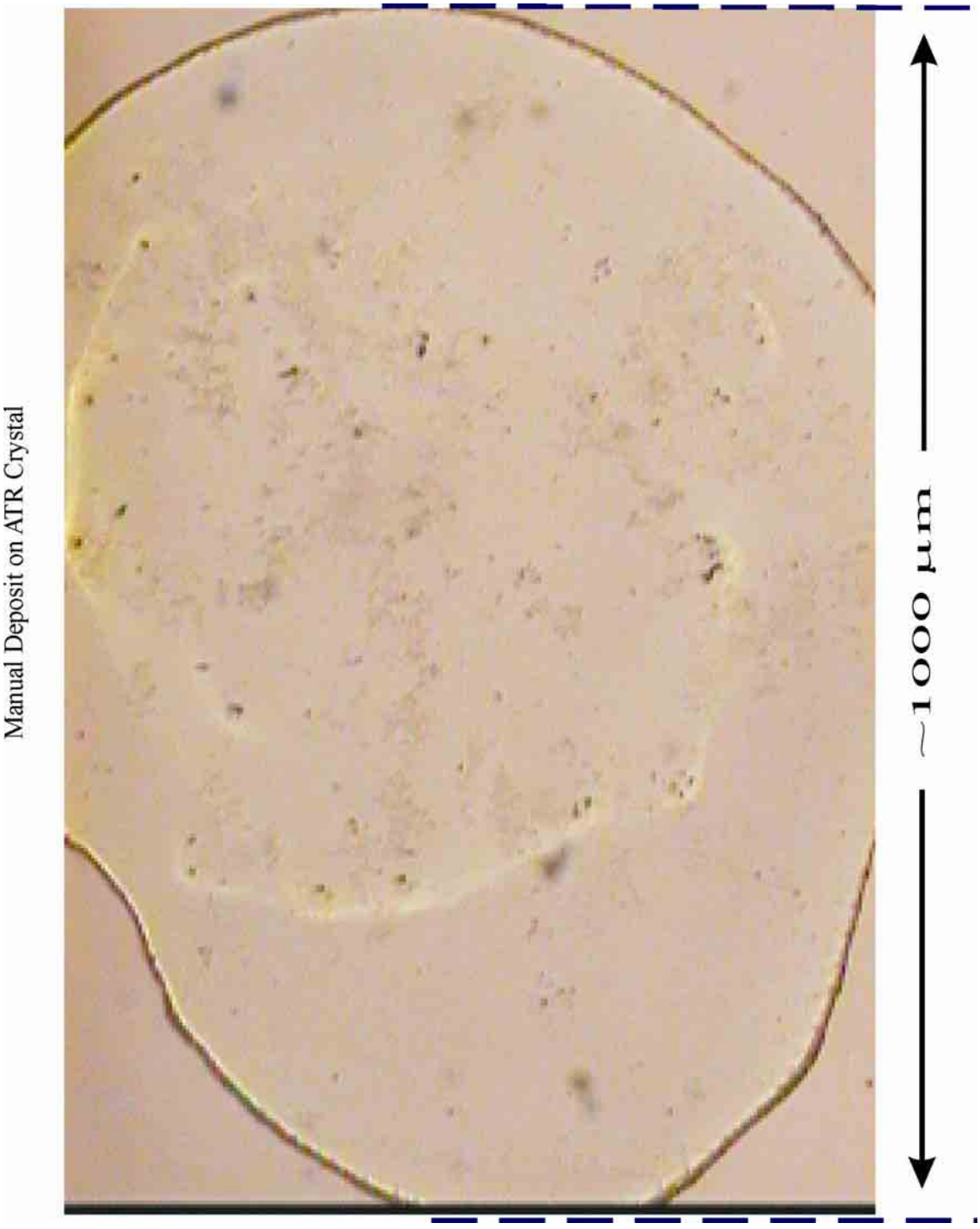
Manual Deposit on ATR Crystal
~1000 µm

Figure 4.5 ~300 μm semi-automated sample depositor deposit of caffeine

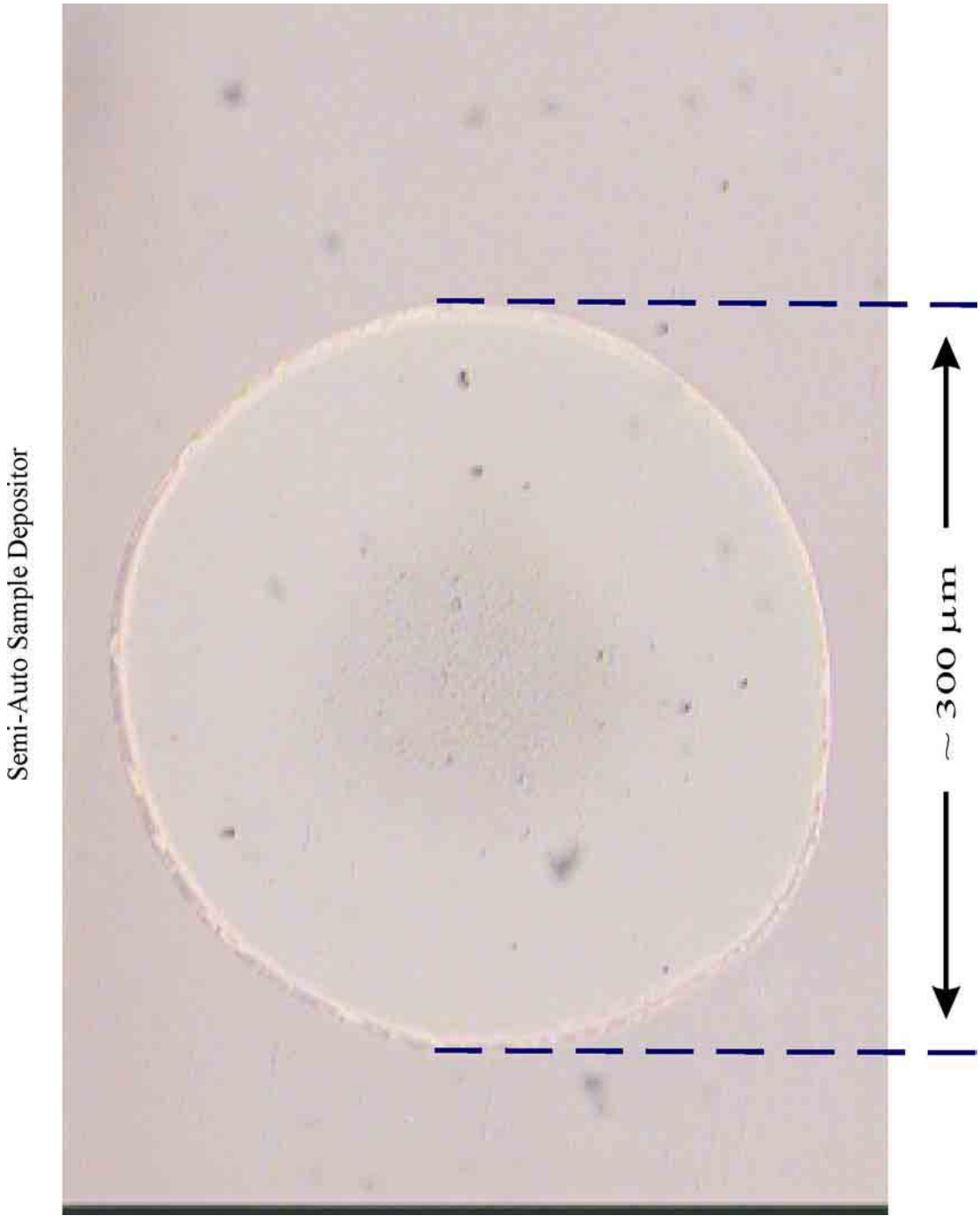
Semi-Auto Sample Depositor
~ 300 µm

Figure 4.6 Manual deposit versus a semi-automated sample deposit of a solution of 5.0×10^{-3} M Caffeine. 1000 scans each at 4 cm^{-1} resolution

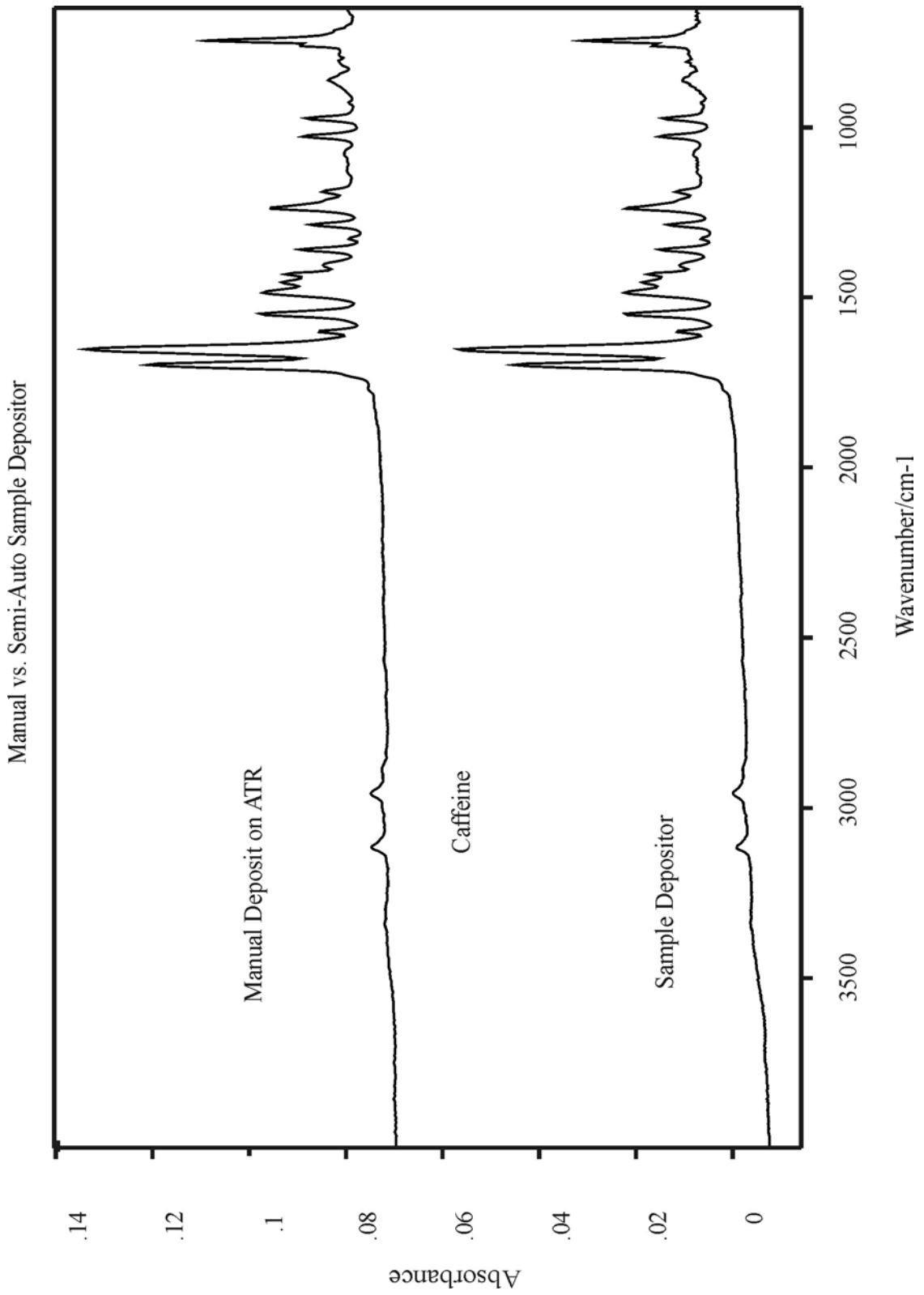
Manual vs. Semi-Auto Sample Depositor
Manual Deposit on ATR
Caffeine
Sample Depositor
Absorbance
.14
.12
.1
.08
.06
.04
.02
0
3500
3000
2500
2000
1500
1000
Wavenumber/cm-1

Figure 4.7 Manual Deposit versus a semi-automated sample deposit of a solution of 5.0×10^{-3} M of sodium benzoate. 1000 scans each at 4 cm^{-1} resolution

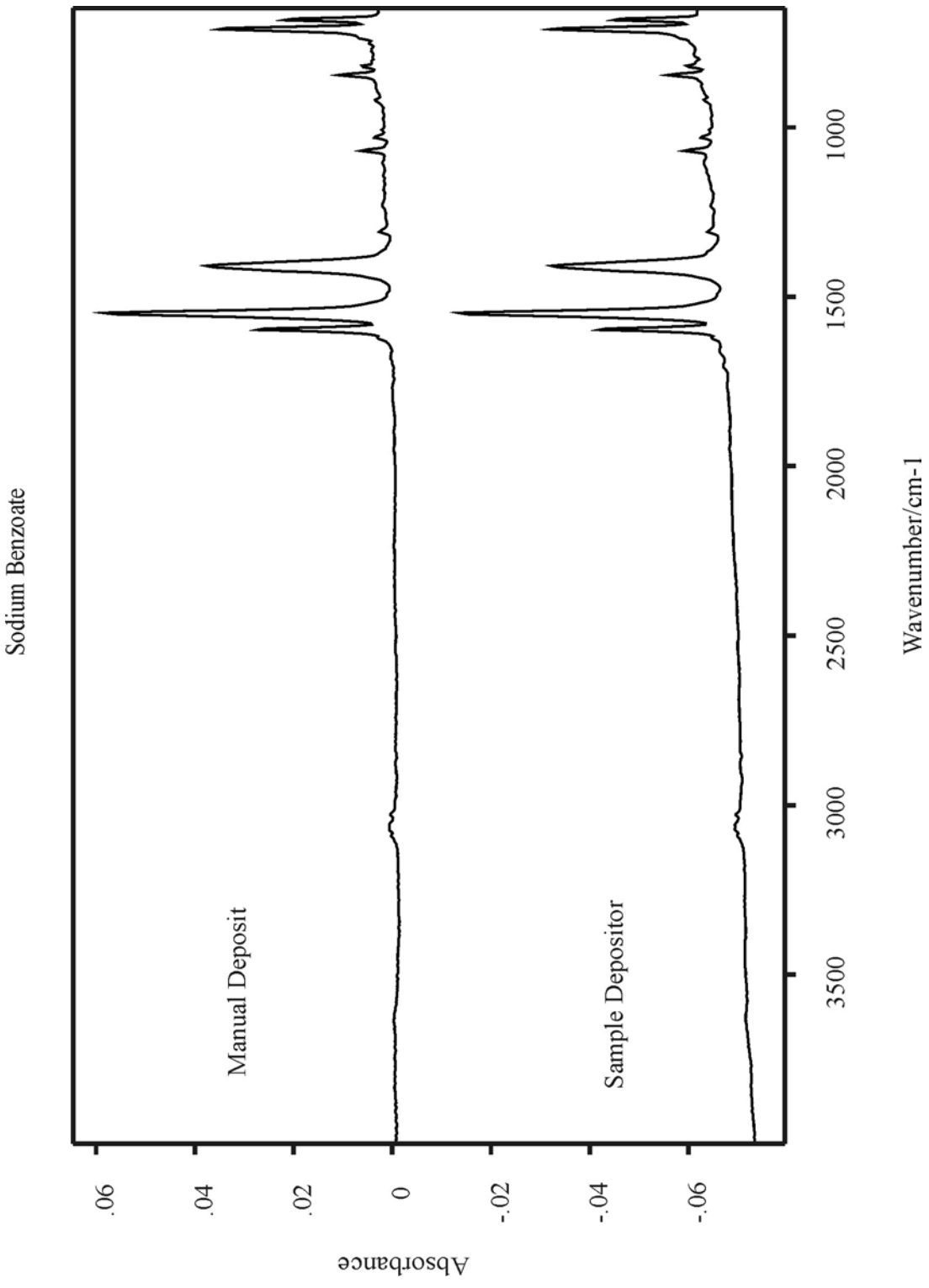
Sodium Benzoate
Manual Deposit
Sample Depositor
Absorbance
.06
.04
.02
0
-.02
-.04
-.06
3500
3000
2500
2000
1500
1000
Wavenumber/cm-1

deposition method was control of the deposition size. Table 1 lists the average size of the deposits using the semi-automated sample depositor for aqueous samples. The aqueous deposits had an average size of 535 μm in the x direction to 509 μm in the y direction, which produced a standard deviation of less than 27%. It should be noted that the size of the deposit is greatly dependent on the amount of solution that is loaded into the semi-automated depositor. The greater the amount of sample the larger the deposit, thus it is very important to control the amount of sample loaded. This is done by loading the sample to a certain height within the inner capillary of the depositor. From this value the amount of sample being deposited can be calculated. If a 0.005 M sample is loading into the depositor to a height of 1 mm, roughly 39 ng of sample is deposited onto the surface for analysis.

Another major concern when using the new sample deposition method is the reproducibility of the deposition placement. While this is not a problem when deposits are placed onto CaF_2 crystals for analysis using a FT-IR spectrometric microscope system, placement becomes crucial when the ATR/FT-IR spectrometric system is used. As stated above the Harrick SplitPea™ has an active site that measures roughly 250 μm in diameter. Deposition onto this very small area is very difficult to do reproducibly using manual methods. To determine the placement precision, a series of deposits were made as close as possible to the center of a target. The distance from the center of the deposit to the center of the target area was then measured. The average variation in deposit location is reported in Table 1. On average the deviation from the center of the target area varied by 250 μm. The standard deviation for this measurement is reported at 33 %. It should be note that these measurements were made by placing a CaF_2 window under the depositor and aligning the bottom with crosshairs on the windows visually. The alignment of the depositor over the active site of the SplitPea™ proved to easier, however visual measurements of this were difficult. The semi-automated sample

Table 4.1 The average deposit size of the aqueous samples in the X and Y directions, the standard deviation of the deposits' sizes, the average distance from the center of the crosshairs for aqueous deposits, and the standard deviation of the distance

Table 4.1

	X Axis	Y Axis
Average Deposit Size (μm)	535	509
Standard Deviation	132	150

	Z
Distance from Center (μm)	249.5
Standard Deviation	82.6

deposition system was determined to be a superior method when compared to manual deposition methods previously employed.

Conclusions

The sample deposition system described above is a significant improvement over manual deposition systems. The sample placement, size, and geometry are more reproducible and therefore better suited for single-bounce ATR analyses. The active area of the IRE is uniformly covered by the deposited sample, which eliminates noise and other interference on the signal. Spectral analyses of manual and semi-automated deposits are nearly identical. Furthermore, the time required for semi-automatic deposition is less than or equivalent to the manual deposit. Because the same depositor can be used for a variety of sample types and for a nearly infinite number of samples, supply costs are reduced. Furthermore, because deposit size is directly dependent on the amount of sample loaded into the depositor, the load amount can be regulated for highly reproducible results. In order to achieve this, the syringe used should be tightly fitted with the fused silica needle and should not be changed between samples. Once assembled, the depositor is a single piece of simple laboratory equipment that can help to eliminate a number of tedious steps between sample runs. Technical expertise, therefore, is not essential for quality analyses. Future developments of the deposition system will only increase its usability, cost-effectiveness, and high throughput characteristics.

Numerous improvements on the semi-automated sample deposit system are already in progress. The depositor is being redesigned as a single piece of glassware to simplify the sample loading and washing procedure and to help increase the effect of the vacuum on sample shape and solvent evaporation. Figure 8 shows a diagram of the redesigned semi-automated sample deposition system. The wash line has been removed from the side of the depositor and has been moved to the top. This removes the

Figure 4.8 Redesigned semi-automated sample deposition system

Redesigned Semi-Automated Sample Depositor

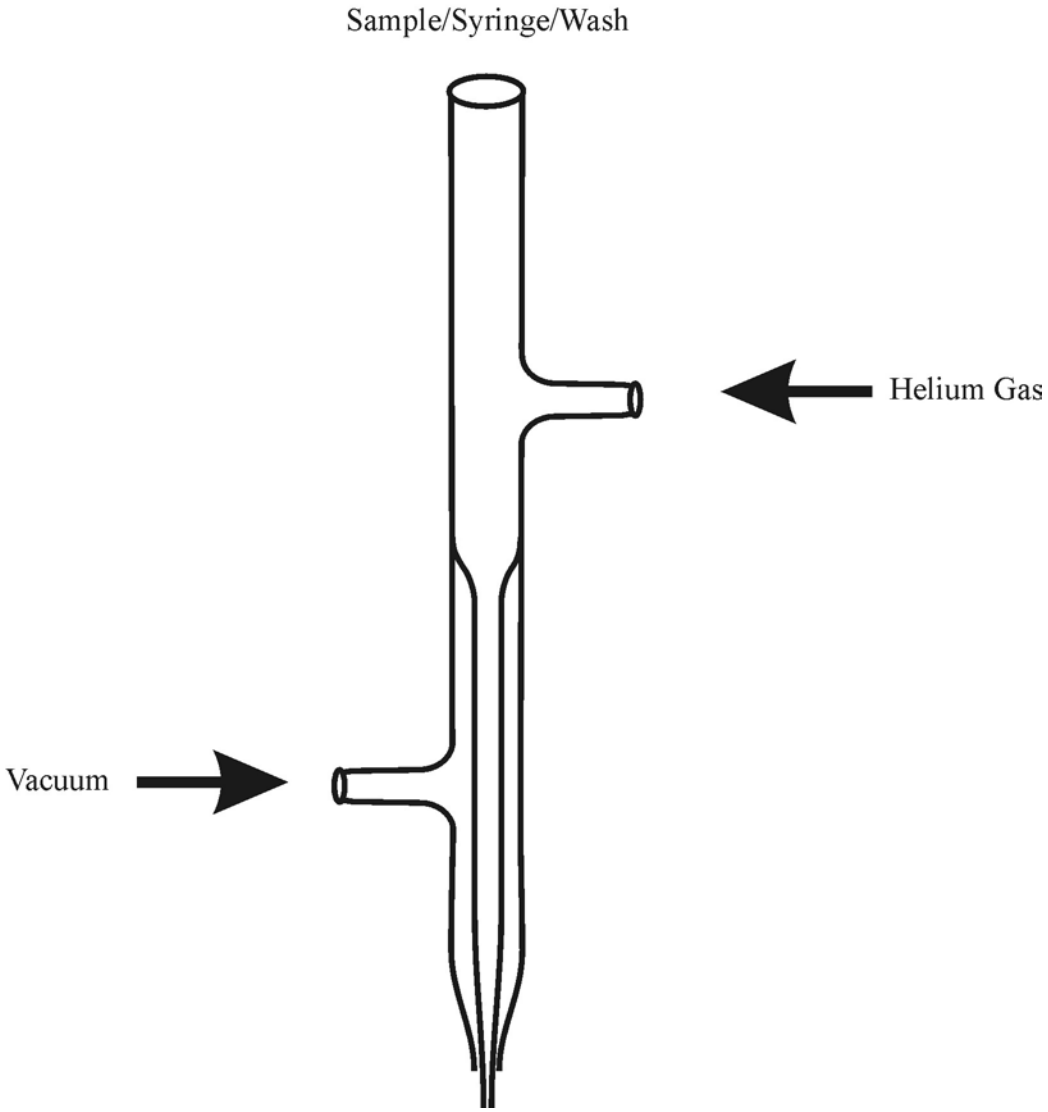

possibility of the wash solution remaining in the depositor. The helium flow will be regulated in a more precise manner to allow for optimization of deposit size and thickness. In addition, the depositor will be kinematically mounted over the spectrometer to ensure exact sample placement and therefore reduce sample volume requirements. A device similar to a holding well will be placed just on top the IRE crystal to minimize sample spreading and to increase sample thickness after deposition which also allows small sample volumes to be used.

Acknowledgements

The authors thank the National Institutes of Health (grant number 2P41-RR-05351) for financial support in the form of a National Center for Research Resources. We would also like to thank the Harrick Scientific Corporation for the donation of a SplitPea™ accessory which was used for data collection. We would like to thank Lindell Ward, Billy Flowers, and Dr. John Stickney for the use of their stereomicroscope and digital camera, and we would also like to thank Dr. Lasse Kalervo for the inspiration in the development of the semi-automated sample deposition system.

References

1. F. Deblase, N. Harrick, and M. Milosevic, J. Appl. Polym. Sci. **34,** 2047 (1987).

2. N. Harrick, Phys. Rev. Lett. **4,** 226 (1960).

3. N. Harrick, Phys. Rev. **125,** 1165 (1962).

4. N. Harrick, Annals of the New York Academy of Sciences **101,** 928 (1963).

5. R. Levitt and N. Harrick, J. Opt. Soc. Am. **56,** 557 (1966).

6. N. Winograd and N. Harrick, Appl. Spectrosc. **25,** 143 (1971).

7. H. Cheung, J. Cui, and S. Sun, Microbiology UK **145,** 1043 (1999).

8. P. Poston, D. Rivera, R. Uibel, and J. Harris, Appl. Spectrosc. **52,** 1391 (1998).

9. Y. Lu, J. Drelich, and J. Miller, J. Colloid Interface Sci. **202,** 462 (1998).

10. K. Oberg and A. Fink, Anal. Biochem. **256,** 92 (1998).

11. M. Gunde, Informacije Midem-Journal of Microelectronics Electronic Components and Materials **27,** 120 (1997).

12. S. Widayati, S. Stephens, and R. Dluhy, Mikrochim. Acta **14,** 679 (1997).

13. B. Johnson and K. Doblhofer, Electrochim Acta **38,** 695 (1993).

14. J. Jeon, R. Sperline, and S. Raghavan, Appl. Spectrosc. **46,** 1644 (1992).

15. L. Liebmann, J. Robinson, and K. Mann, Rev. Sci. Instrum. **62,** 2083 (1991).

16. B. Molochnikov, I. Vasileva, and N. Gubel, Sov. J. Opt. Tech. **46,** 661 (1979).

17. N. Harrick *Internal Reflection Spectroscopy* (Harrick Scientific Corp., Ossining, New York, 1987).

18. N. Harrick, M. Milosevic, and S. Berets, Am. Lab. **24,** 50 (1992).

19. N. Harrick, M. Milosevic, and S. Berets, Am. Lab. **24,** 29 (1992).

20. N. Harrick, M. Milosevic, and S. Betets, Appl. Spectrosc. **45,** 944 (1991).

21. G. Powell, M. Milosevic, J. Lucania, and N. Harrick, Appl. Spectrosc. **46,** 125 (1992).

22. A. Sommer and M. Hardgrove, Vib. Spectrosc. **24,** 100 (2000).

23. J. Coates, Spectroscopy **12,** 16 (1997).

24. R. Robertson, J. Dehaseth, and R. Browner, Mikrochim. Acta **2,** 199 (1988).

25. R. Robertson, J. Dehaseth, J. Kirk, and R. Browner, Appl. Spectrosc. **42,** 1365 (1988).

26. J. de haseth and R. Robertson, Microchem. J. **40,** 77 (1989).

27. R. Robertson, J. de haseth, and R. Browner, Appl. Spectrosc. **44,** 8 (1990).

28. V. Turula and J. de haseth, Appl. Spectrosc. **48,** 1255 (1994).

29. R. Bishop, V. Turula, and J. de Haseth, Anal. Chem. **68,** 4006 (1996).

30. V. Turula and J. de Haseth, Anal. Chem. **68,** 629 (1996).

31. R. Bishop and J. de Haseth, Mikrochim. Acta **14,** 721 (1997).

32. J. de Haseth and V. Turula, Mikrochim. Acta **14,** 109 (1997).

33. V. Turula, R. Bishop, R. Ricker, and J. de Haseth, J. Chromatogr. A **763,** 91 (1997).

34. T. Venkateshwaran, J. Stewart, R. Bishop, J. de Haseth, and M. Bartlett, J. Pharm. Biomed. Anal. **17,** 57 (1998).

35. T. Venkateshwaran, J. Stewart, J. de Haseth, and M. Bartlett, J. Pharm. Biomed. Anal. **19,** 709 (1999).

36. Personal communications with Dr. Lasse Kalervo

CHAPTER 5

FUTURE STUDIES

The main goal of this dissertation was to use Fourier transform infrared spectroscopy and capillary electrophoresis for the analysis of monosaccharides, oligosaccharides, and carbohydrates. To facilitate the analysis of these compounds two different CE/FT-IR spectrometric interfaces were developed and proved to be successful. The two interfaces were based on low flow rate LC/FT-IR spectrometric interfaces[1] and the electrospray design developed in CE/MS.[2] The latter of the two interfaces was designed with a silver-coated capillary column placed within the glass concentric nebulizer. This allows for the low flow rate effluent from the CE column to be deposited on to an infrared transparent window for spectrometric analysis. Future studies that involve the CE/FT-IR spectrometric interface will include the use of other volatile buffer systems, automated sample collection, capillary electrochromatography (CEC), attenuated total reflection (ATR), as well as continued improvement to the interface design.

The current CE/FT-IR spectrometric interface employs off-line sample collection for the spectrometric analysis. The method of moving the infrared crystal in and out of the nebulization stream involves a great deal of practice for the operator to perfect. To try to remove the possibility of sample contamination due to the manual operation, a programmable stage could be used. The stage would be set to move at a constant velocity under the nebulizer and collect the analytes. The window that holds the samples could then be taken to the FT-IR microscope and analyzed. Although the use of a stage is still an off-line method, this removes one of the largest sources of error in this technique

In order to make this interface a true on-line method, it may be possible to use a single bounce attenuated total reflection accessory. This method would allow the effluent to be deposited directly onto the internal reflection element and analyzed in real time. This would make the CE/FT-IR interface a truly automated separation and detection method. The use of ATR offers high sensitivity, spectral collection of small sample quantities, and no need for normalization with respect to spectra collected with the FT-IR microscope system.

Even though capillary electrophoresis provides rapid separation and high resolution, there are some problems involved in the use of volatile buffer systems to separate carbohydrates. Most carbohydrates are neutral in solution and are not easily ionized without the use of a borate buffer system. To help with the separation of these compounds, capillary electrochromatography (CEC) may be used. CEC not only provides electrophoretic separation, but it adds partitioning to increase the resolving power of the method. This technique uses a packed capillary column that has the same dimensions as a normal CE column, which should allow for easy attachment to the FT-IR spectrometric interface.

The CE/FT-IR spectrometric interface provides very small, uniform, and concentric deposits for spectrometric analysis, regardless, improvements to the interface could be made. The end of the inner glass capillary could be made smaller or only extended to the end of the outer glass capillary tip. A smaller deposit, on the order of 100 μm in diameter, should be attainable if the inner glass capillary was made smaller. Ideally the deposits should be ~50 μm in diameter. This deposit would match the image of the limiting aperture and provide the highest spectrometric sensitivity for this technique.

The other focus of this research was to develop a semi-automated sample deposition method for single bounce attenuated total reflection that would provide a number of advantages over manual deposition methods. To this end a semi-automated

sample depositor was successfully designed. The depositor helped to remove the problem of run-to-run sample placement, decreased the amount of sample waste, and decreased the size of the sample deposit so that it matched the active internal reflection element (IRE).

Future improvements would be to redesign the depositor so that all the valves and fittings are incorporated into a single glass piece. This would remove some of the chance of sample contamination and wash liquid that remains in the depositor. The helium flow also needs to be optimized and regulated as not to blow the sample from the tip with too much force that it misses the IRE. The use of a fused silica capillary sample delivery system could be changed to a steel needle, which would improve sample loading. The volume of sample delivered into the depositor is dependent on the syringe volume and could be regulated better. These improvements would allow the depositor to be loaded with a large amount of sample and a number of deposits made without the need to cleaning the depositor after each deposit. The last improvement would be to investigate the use of different materials in the construction of the depositor. It is well known that certain biological compounds adhere strongly to glass surfaces. It may be necessary to modify the glass surface to eliminate this problem. Any and all of these improvements would allow the semi-automated sample depositor to be used for a wider variety of applications.

References

1. A. J. Lange, P. R. Griffiths, and D. J. J. Fraser, Anal. Chem. **63,** 782 (1991).

2. J. Wahl, D. Gale, and R. Smith, J. Chromatogr. a **659,** 222 (1994).